博士論文番号: 1381011

High-resolution analysis of DNA binding property of VND7, the master transcription factor for vessel cell differentiation

Taizo Tamura

Nara Institute of Science and Technology Graduate School of Biological Sciences, Laboratory of Plant Metabolic Regulation

(Taku Demura)

November 22, 2016

Table of contents

1. Introduction

1.1 Transcription factors controlling xylem vessel differentiation

The xylem of plant vascular systems is an important tissue that conducts water and minerals throughout the plant body and supports the entire plant via mechanical strength of thick secondary cell walls. Acquisition of lignified secondary cell walls during plant evolution enabled the colonization of plants on land. The major constituent cells of the xylem are vessel elements and fibers, the differentiation processes of which involve secondary cell wall (SCW) deposition and programmed cell death (PCD) (Oh *et al*., 2003; Turner *et al*., 2007; Fukuda, 2004).

Recent research revealed that the differentiation of xylem vessel elements in *Arabidopsis* is regulated by transcription factors of the *VNS* gene family, which are part of the large NAC (NO APICAL MERISTEM, NAM; ARABIDOPSIS TRANSCRIPTION ACTIVATION FACTOR, ATAF1/2; and CUP-SHAPED COTYLEDON2, CUC2) transcription factor family. The vascular-specific VNS subfamily was named for several of the well-characterized family members: VASCULAR-RELATED NAC-DOMAIN (VND)/ NAC SECONDARY WALL THICKENING PROMOTING FACTOR (NST)/ SOMBRERO (SMB) transcription factors. This subfamily is composed of 13 NAC domain transcription factors.

VND1 to VND7 are important for vessel differentiation, turning on both SCW deposition and PCD (Kubo *et al*., 2005; Zhou *et al*., 2014; Endo *et al*., 2015). NST1 and NST3/SECONDARY WALL-ASSOCIATED NAC DOMAIN PROTEIN1 (SND1) are required for interfascicular and xylary fiber development, in which SCW deposition is activated (Mitsuda *et al*., 2007; Zhong *et al*., 2006). Although all the *VNS* genes have an ability to induce ectopic SCW deposition with the up-regulated expression of SCW-related genes including *CELLULOSE SYNTHASE1* (*CesA4*)/*IRREGULAR XYLEM* (*IRX5*), *CesA7*/*IRX3*, *CesA8*/*IRX1*, and *MYB46* upon overexpression, only *VND1* to *VND7* genes can strongly induce the expression of PCD-related genes such as *XYLEM CYSTEINE PEPTIDASE1* (*XCP1*), *XCP2*, and *Arabidopsis thaliana METACASPASE 9* (*ATMC9*), suggesting distinct functions of *VND* subgroup genes (Yamaguchi *et al*., 2011). Among the *VND* genes, *VND7* gene has been functionally investigated extensively because it has the strongest activity to induce xylem vessel cell differentiation and is expressed all types of primary xylem vessel cells. The expression of the dominant negative C-terminus-truncated VND7

protein, under the control of the native VND7 promoter, inhibited the normal differentiation of vessels in whole plant body (Yamaguchi *et al*., 2008).

1.2 Gene regulatory network for xylem vessel cell differentiation

The extensive investigation of *VND7* function, including the microarray gene expression profiling after the artificial induction/activation of *VND7* gene by the estrogen/glucocorticoid receptor-mediated system (Zhong *et al*., 2010; Yamaguchi *et al*., 2011), has revealed a gene regulatory network (GRN) initiated by *VND7* gene (Figure 1; reviewed in Yamaguchi and Demura, 2010; Schuetz *et al*., 2012; Hussey *et al*., 2013; Nakano *et al*., 2015). The GRN includes a number of genes possibly regulated directly by *VND7* gene, some of which are closely related to SCW formation, such as cellulose synthase genes (*CesA4*/*IRX5*, *CesA8*/*IRX1)* and *MYB46 (*Zhong *et al*., 2010; Yamaguchi *et al*., 2011; Kim *et al*., 2012, 2013; Ko *et al*., 2009), and to PCD, such as *XCP1* and *XCP2* (Funk *et al*., 2002; Avci *et al*., 2008). Further analysis revealed that the promoter regions of these possible direct target genes of VND7 includes cis-sequences that respond to VND7.

Among various candidate genes directly regulated by VND7, the PCD-related peptidase, *XCP1,* can be considered as one of the direct target genes specific to *VND* genes but not to *NST*/*SND* genes (Yamaguchi *et al*., 2011). This reflects the importance of PCD in to form a hollow tube required for water and nutrient transport as the final step in VND7-driven vessel cell differentiation. A detailed promoter analysis of *XCP1* was performed using a transient reporter assay with the deletion series of *XCP1* promoter sequences fused to *LUCIFERASE* reporter gene, which was co-expressed with *VND7* driven by the strong constitutive cauliflower mosaic virus (CaMV) *35S* promoter. The assay identified the specific region (from -211 to -96 bp) as required for VND7 dependent activation of *XCP1*. An electrophoretic mobility shift assay (EMSA) of the poly-His-tagged N-terminal region of VND7, which contains the whole NAC domain, and a 138-bp *XCP1* promoter sequence (from -233 to -96 bp) resulted in the identification of two *XCP1* promoter fragments, 53-bp X1E1 (from -148 to -96 bp) and 85-bp X1E2 (from -233 to -149 bp), for the direct binding by VND7 (Yamaguchi *et al*., 2011). Moreover, VND7 was shown to bind to promoter regions of other *VND7* direct target genes, *XCP2*, *CesA4*/*IRX5*, and *MYB83* (Yamaguchi *et al*., 2011).

It was also shown by EMSA that the promoter of *MYB46*, one of the direct

target genes of *VND7*, contains multiple regions (MYB46-P1 to P3, P5, and P6) that bind to NST3/SND1 (Zhong *et al*., 2007). Of them, MYB46-P2 and P6 were shown to contain 24-bp sequences, designated as secondary wall NAC binding element1 (SNBE1) and SNBE2, respectively, exhibiting strong binding by NST3/SND1 that is critical for the NST3/SND1-mediated activation of *MYB46* expression (Zhong *et al*., 2010). Further analysis of the SNBE1 and SNBE2 by using mutated sequences coupled with EMSA indicated that nine nucleotides in a 19-bp sequence of the 24-bp SNBE1 are critical for NST3/SND1 binding, leading to the identification of a 19-bp consensus sequence, designated as SNBE, (T/A)NN(C/T)(T/C/G) TNNNNNNNA(A/C)GN(A/C/T)(A/T), in the promoters of NST3/SND1 target genes (Zhong *et al*., 2010). Importantly, Zhong *et al*. (2010) showed that not only NST3/SND1, but also VND6 and VND7, have the ability to bind to the SNBE sequences found in their target genes including *MYB46* and *XCP1*. Moreover, McCarthy *et al*. (2011) used GUS reporter constructs to compare the *in planta* expression patterns of SNBE sequences from xylem vessel-specific genes (*XCP1* and *Ribonuclease 3*, *RNS3*), with SNBE sequences from genes whose expression is found in all SCW-forming cells (*MYB46* and *KNAT7*). Vessel-specific SNBE sequences (from *XCP1* and *RNS3*) directed xylem-specific (but not xylem vessel-specific) GUS expression, while those from genes whose expression is found in all SCW-forming cells (*MYB46* and *KNAT7*) directed GUS expression in both xylem cells and interfascicular fibers. This suggested the hypothesis that the SNBE sequences from xylem vessel cell-specific genes contain certain sequences that specifically bind to xylem-vessel specific VNS transcription factors, VND1 to VND7. It should be noted that the *XCP1* SNBE motif is included in the X1E1 region described above (from -130 to -112 bp: TGTCTTTGCTTCAAAGCCA), suggesting that the *XCP1* SNBE is indeed responsible for the xylem-vessel specific expression of *XCP1*.

In addition to the identification of cis-sequences for VND7 described above, a 11-bp cis-element (CTTGAAAGCAA) that confers the xylem vessel cell-specific expression of the *Zinnia Cysteine Protease 4* (*ZCP4*) gene, the ortholog of *Arabidopsis XCP1* in *Zinnia elegans*, was found in the promoter region of *ZCP4* by GUS reporter assay with deletion and mutation series of *ZCP4* promoter (Demura *et al*., 2002; Pyo *et al*., 2004, 2007). By comparing the *Zinnia ZCP4* 11-bp cis-element with promoters of genes whose transcripts strongly accumulate during differentiation of vessel cells in an *Arabidopsis* cell culture system (Kubo *et al*., 2005), Pyo *et al*. (2007) identified a 11-bp consensus sequence, designated as the

tracheary-element-regulating cis-element (TERE) (CT[C/T]NAA[A/C]GCN[A/T]). Many known xylem vessel-related genes contained the TERE, including *XCP1*, *XCP2*, and *Xylem Serine Protease 1* (*XSP1*) (At4g35350, At1g20850, and At4g00230 respectively: Funk *et al*., 2002; Zhao *et al*., 2000), a xylanase gene (At1g08610; Kubo *et al*., 2005; Sawa *et al*., 2005), a peroxidase gene (At5g51890; Sato *et al*., 2006), an alpha-L-arabinofuranosidase gene (*ARAF1*) (At3g10740), and *Arabidopsis fasciclin-like arabinogalactan-protein 11* (*ATFLA11*) (At5g03170) (Pyo *et al*., 2007). When five tandem copies of the TERE from each of these genes was fused to GUS, high levels of GUS activity in differentiating vessel cells was observed in the transgenic *Arabidopsis* plants (Pyo *et al*., 2007).

There are two conflicting results on the binding between the TERE and the VNS transcription factors (Ohashi-Ito *et al*., 2010; Zhong *et al*., 2010). Based on data showing that a 24-bp *XCP1* promoter sequence containing the TERE sequence could not competitively inhibit binding between a 216-bp *XCP1* promoter sequence and the VNS transcription factors, Zhong *et al*. (2010) suggested that VND6, VND7 and NST3/SND1 do not directly bind to TERE. On the other hand, Ohashi-Ito *et al*. (2010) used EMSA to demonstrate VND6 binding to TERE sequences from *XCP1*, *CesA4*/*IRX8*, *POLYGARACTULONASE* (*PG*) (At1g70500), *ATMC9*, and *ARABIDOPSIS THALIANA SUBTILASE 1.1* (*ATSBT1.1*). Furthermore, it should be mentioned that the *XCP1* TERE (CTTCAAAGCCA) is a part of *XCP1* SNBE (TGTCTTTGCTTCAAAGCCA) in the *XCP1* X1E1 sequence. These results strongly suggest, in spite of the negative data by Zhong *et al*. (2010), that the specific binding between the *XCP1* X1E1 sequence and VND7 could contribute to the strict regulation of xylem vessel cell-specific expression of *XCP1* gene *in planta*. However, the detailed mechanisms underlying the specific binding between *XCP1* X1E1 and VND7, which would be responsible for the xylem vessel cell-specific *XCP1* expression directed by VND7, are still largely unknown.

1.3 Methods for quantitative analysis of binding between transcription factors and cis-sequences

It is important to identify the specific cis-sequences binding to transcription factors of interest for understanding the mechanisms underlying regulation of gene expression. So far, various kinds of methods for identifying cis-sequences were established (summarized in Helwa and Hoheisel, 2010; Dey *et al*., 2012; Gonzalez,

2015). Each method has advantages as well as drawbacks, therefore their application depends on the specific purpose of each research objective. *In vivo* techniques have been developed, such as chromatin immunoprecipitation-chip and -sequencing (ChIP-chip and ChIP-seq), yeast one-hybrid assay, transient reporter expression assays, and DNA adenine methyltransferase identification (DamID). *In vitro* techniques are also important, such as DNA footprinting, EMSA, systematic evolution of ligands by exponential enrichment (SELEX), protein binding microarray, southwestern blotting, surface plasmon resonance (SPR), fluorescence resonance energy transfer (FRET; Furey *et al*., 1998), and DNA affinity purification-sequencing (DAP-seq; O'Malley *et al*., 2016).

In this thesis, I employed a powerful *in vitro* technique called fluorescence correlation spectroscopy (FCS, which was developed by Kobayashi *et al*., 2004) to characterize the binding specificity between VND7 and the promoter sequence of *XCP1* in detail. FCS was chosen to investigate VND7 binding to the *XCP1* promoter at the single nucleotide level, it is a reliable, simple, fast, and quantitative method for characterizing the interaction between transcription factors and DNA fragments (Kobayashi *et al*., 2004; Harada *et al*., 2013; Tsutsumi *et al*., 2016).

1.4 Principle of Fluorescence Correlation Spectroscopy (FCS) for the analysis of the molecular interaction between DNA and transcription factors

FCS is considered to be an efficient tool for quantitative analysis of interaction between DNA and transcription factors (Kinjo *et al*., 1995; Octobre *et al*., 2005; Kobayashi *et al*., 2004; Harada *et al*., 2013). FCS monitors temporal changes in the intensity of the fluorescence signal caused by Brownian motion of fluorescent-labeled molecules within a femtoliter-scale observation volume. By calculation of the correlation of the fluorescence intensity changing with time (autocorrelation), FCS allows us to determine the diffusion time and the number of fluorescently labeled molecules that pass through the observation volume. As the diffusion time of the labeled-molecule depends on its molecular weight, interactions between the labeled molecules and other molecules can be evaluated in accordance with the changes in diffusion time. For instance, when DNA molecules are labeled with fluorescence, the degree of interaction with DNA-binding proteins such as transcription factors can be shown by FCS as the changes in diffusion time caused by changed velocity of the complex of fluorescently labeled-DNA and DNA-binding

proteins. Therefore, FCS has successfully and sensitively quantified the degree of molecular interaction between DNA and protein (Kinjo *et al*., 1995; Octobre *et al*., 2005; Kobayashi *et al*., 2004; Harada *et al*., 2013).

Moreover, it has been demonstrated that FCS can be used for competition assay using unlabeled-DNA molecules as competitors (Kobayashi *et al*., 2004; Harada *et al*., 2013). This is analogous to the competition assays with unlabeled-DNA molecules that are often employed in EMSA experiments. Also, FCS can measure the "binding fraction α" that denotes the ratio of the labeled-DNA molecules bound with the proteins to total labeled-DNA molecules in the solution. The values of "binding fraction α" obtained with the different concentrations of proteins can be used in kinetic analysis for the calculation of the binding affinity, Kd (Kobayashi *et al*., 2004). Thus, FCS assay is an excellent biophysical system for evaluation of the precise molecular interaction between DNA and protein.

1.5 Aim of this research

Based on the conflicting evidence about the nature of VND7 binding, the goal of this research is to understand the molecular mechanisms by which VND7 recognizes its direct target genes specifically, as this is critical to xylem vessel differentiation, from the perspective of protein-DNA interaction.

In this study, I first established a method for FCS assay to analyze binding between VND7 and the promoter sequence of *XCP1* with competitor DNAs, which allowed me to narrow down the cis-sequence responsible for the binding. Next I developed the FCS kinetic assay for calculation of Ki value of each competitor to determine nucleotides responsible for the specific binding between VND7 and *XCP1* promoter. In order to validate my findings with another experimental approach, I conducted SELEX analysis for VND7 to elucidate the cis-sequence of VND7 further. These lines of evidence, with previously described consensus sequences, TERE and SNBE, indicate that VND7 binds to the *XCP1* promoter at an 18-bp incomplete palindromic cis-sequence "CTTNNCTTNNAAGNNAAT", which I designated as the "*XCP1* X1E1 core structure", to emphasize that the FCS approach was important in its identification. The "*XCP1* X1E1 core structure" includes 4 important nucleotides "T, T, A, and A" named "core-nucleotides" (CTTNNCTTNNAAGNNAAT; underlined). The importance of the "core-nucleotides" was further evaluated *in planta*: transient reporter assay in plant cells and GUS

reporter analysis in roots and leaves were carried out, confirming the importance of the “core-nucleotides” *in planta*. I further analyzed the binding specificity of the “*XCP1* X1E1 core structure” and the “core-nucleotides” for VND7 by transient assays in *Arabidopsis* protoplasts with other VNS family members (VND6 and NST3/SND1), compared with VND7, resulted in the indication of the binding specificity of VND7 to the “*XCP1* X1E1 core structure” and the “core-nucleotides”. In addition, I identified promoter sequences responsible for the binding by VND7 with the FCS assay from several other genes that have been found to be direct targets of VND7 and characterized a motif, CTTNNNNNNNA, which important for binding between VND7 and the promoters of VND7 direct target genes. Finally, I searched the “*XCP1* X1E1 core structure”-like sequences in the promoter of *XCP1*/*XCP2* homologous genes in *Physcomitrella patens*, to consider the conservation of binding specificity during plant evolution.

2. Materials and Methods

2.1 Vector construction

For expression and purification of the MBP-tagged recombinant proteins, the coding sequences (CDSs) encoding the NAC domain of VND6, VND7 and SND1/NST3 (VND6$^{1-159}$, VND7$^{1-161}$ and SND1/NST3$^{1-180}$) were subcloned into an entry vector, pENTR/D-TOPO (Thermo Fisher, https://www.thermofisher.com), and then integrated into a Gateway destination vector, pMAL-GWRFC (Yamaguchi *et al*. 2010b) using LR Clonase (Thermo Fisher). For dual LUC transient assay, the amplified full length CDSs of *VND6*, *VND7* and *SND1*/*NST3*, and promoter region of *XCP1* were subcloned into the entry vector and then integrated into Gateway destination vectors, pA35G and pAGL, respectively (Endo *et al*. 2015). The primer information is described in Table 4. The nucleotide sequence of the multicloning site (MCS) 5′-CACCTAGTGGATCCCCCGGGCTGCAGGAATTCGATATCAAGCTTATCGATACCGTCGACCTCGTGATG-3′, which includes a stop codon at the 5′ end and a start codon at the 3′ end, was used as an effector control (Yamaguchi *et al*. 2008). The entry vectors containing the *XCP1* promoters were integrated into a Gateway destination vector, pBGGUS (Kubo *et al*., 2005) for GUS reporter expression assay.

2.2 Expression and purification of recombinant proteins

The MBP-VND6$^{1-159}$, MBP-VND7$^{1-161}$ and MBP-SND1/NST3$^{1-180}$ were expressed into *Escherichia coli*, BL21trxB (DE3) in the presence of isopropyl ß-D-thiogalactoside and purified with amylose resin (New England Biolabs, https://www.neb.com). The protein concentration was determined using relative quantification methods based on the immunoblot with anti-MBP protein antibody (New England Biolab)

2.3 Preparation of DNA fragments

Double-strand DNA (dsDNA) fragments longer than 100-bp were synthesized by PCR amplification. To prepare dsDNA fragments less than 100-bp,

complementary pairs of oligonucleotides were incubated in an annealing buffer [125 mM Tris-HCL (pH7.5), 43.75 mM EDTA, 100.05 mM NaCl], at 95°C for 5 minutes and then at 70°C, 60°C, 50°C, 40°C, 30°C, and 20°C for 10 minutes each. The dsDNA fragments were purified with Exonuclease I (TAKARA BIO INC, http://www.takara-bio.com), which specifically degrades single-strand DNA fragments, and then MERmaid SPIN kit (MP Biomedicals, http://www.mpbio.com). TAMRA-labeled primers were ordered from Hokkaido System Science Co., Ltd (http://www.hssnet.co.jp/index_e.htm). The list of the primer sequences used for preparation of dsDNA was shown in table 5.

2.4 Analysis of molecular interaction by Fluorescence Correlation Spectroscopy (FCS)

Fluorescence correlation spectroscopy (FCS) analysis was operated by a single molecule fluorescence detection system, FluoroPoint-Light (Olympus, Tokyo, Japan; http://www.olympus-global.com/en/). The detection of fluorescence was performed by a 100 μW, 543 nm laser, measuring time set for 10 seconds for each sample and repeated 10 times. TAMRA (MF-D543PX-2, Olympus Corporation Tokyo, Japan, http://www.olympus-lifescience.com) was used as standard to determine the structure parameter. For preparing the sample of the FCS analysis, 5 nM TAMRA-labeled DNA was incubated in a 30 μl binding buffer [50 mM Tris–HCl (pH 7.5), 70 mM KCl, 0.1 μM EDTA, 0.007% 2-Mercaptoethanol, 0.2 mg/ml BSA, 4% glycerol] with or without MBP-VND7$^{1\text{-}161}$ protein and unlabeled DNA fragment as a competitor at room temperature for 20 minutes, and then applied to a 384-well glass-bottomed microplate (Olympus, 384well/plate MP0384120, N1971100).

2.5 Kinetic analysis of protein-DNA interaction by FCS

i. Measurement of binding affinity between TAMRA-labeled DNA fragment and protein (Kd)

The dissociation constant between TAMRA-labeled DNA fragments and MBP-tagged proteins (Kd value) was calculated from Hill equation (Hill, 1910, 1913). “Binding fraction α” that denotes the ratio of the labeled-DNA molecules binding to the proteins to the total labeled-DNA molecules was automatically

calculated by the FluoroPoint-Light based on the parameters of the fluorescence intensity and diffusion time (Harada *et al.*, 2013). A fixed concentration (5 nM) of TAMRA-labeled DNA was incubated with different concentrations (from 0.01 to 0.161 μM) of the MBP-tagged proteins, and then the "binding fraction α" at each protein concentration was obtained. The rations of binding fraction α in each protein concentration divided by the maximum values of binding fraction α are plotted against the concentrations of proteins (refer Figure 28), which were fitted according to the Hill equation shown as below by the method of least squares.

$$y / y_0 = n([E]^n/(Kd + [E]^n)$$

where y and y_0 are the values of binding fraction α in each protein concentration and a maximum value of the binding fraction α, respectively. [E] is a protein concentration, and *n* is Hill coefficient, which describes the degree of the cooperativity between DNA and protein: indicating the number of protein binding sites on DNA fragment.

ii. Measurement of binding affinity between competitor DNA fragment and MBP-VND7$^{1\text{-}161}$ protein (Ki)

The dissociation constant between competitor DNA fragments and MBP-VND7$^{1\text{-}161}$ protein (Ki value) was calculated based on Cheng and Prusoff equation (Cheng and Prusoff, 1973). A fixed concentration of the TAMRA-labeled DNA (5 nM) and MBP-VND7$^{1\text{-}161}$ protein (0.22 μM) was incubated with the different concentrations (from 0.025 μM to 1.5 μM) of competitor DNA fragment, and then the "binding fraction α" at each competitor DNA concentration was obtained. values of "binding fraction α" in the presence of unlabeled competitor fragments divided by the "binding fraction α" in the absence of unlabeled competitor fragment are plotted against the concentrations of competitor DNA fragments (refer Figure 14), which were fitted with the fitting curve generated from the Cheng and Prusoff equation shown below by the method of least squares.

$$y = y_0/1 + (IC_{50} / [I])^{-n}$$
$$Ki = IC_{50}/1 + [L]/Kd$$

where y and y_0 are the values of binding fraction α in the presence and in the absence of unlabeled competitor fragments, respectively. IC_{50} is competitor fragment that reduced y_0 by 50%, *n* is Hill coefficient, [I] is competitor concentration, and [L] is TAMRA-labeled DNA fragment. Kd is dissociation constant between the MBP-VND7$^{1-161}$ protein and the TAMRA-labeled DNA fragment.

2.6 Electrophoretic mobility shifts assay (EMSA)

EMSA was carried out according to Yamaguchi *et al*. (2011). The DNA fragments were labeled with biotin using the Biotin 3' End DNA Labelling Kit (Thermo Fisher), and then purified with the MERmaid SPIN kit (MP Biomedicals). The biotin-labeled DNA fragments were incubated for 30 minutes at 4 ˚C with or without MBP-VND7$^{1-161}$ protein and an excess amount of unlabeled DNA fragment as a competitor, and then separated by polyacrylamide gel electrophoresis. The DNA was electroblotted onto nitrocellulose membrane (Biodyne Plus; Pall, http://www.pall.com) and detected using the LightShift Chemiluminescent EMSA Kit (Thermo Fisher) according to the manufacturer's instructions.

2.7 Systematic evolution of ligands by exponential enrichment (SELEX)

The random DNA oligo nucleotide fragments contain 26 random sequences between a forward and a reverse primer binding sites (5'-agcatcactgattcaagagcatagNNNNNNNNNNNNNNNNNNNNNNNNNNttcaccttcagaactgatgtactc-3'; Table 4). One hundred ng of double-strand random oligo pool was incubated in 100 μl buffer [15 mM HEPES・KOH, 6% glycerol, 75 mM KCl, 2 mM DTT, 0.05 μg/μl poly (dI・dC), 0.25 mM EDTA, 0.1% TritonX-100] for 30 minutes at 22 ˚C with 12.5 pmol MBP-VND7$^{1-161}$ protein. The DNA fragments binding to the MBP-VND7$^{1-161}$ protein was immobilized with the amylose resin (New England Biolabs), and then amplified by PCR. The PCR products were purified and used for the next round of selection. After 5 selections, DNA fragments were ligated into the HincII site of pUC118 (TAKARA BIO INC), and the DNA sequences were confirmed. The consensus motif was detected by MEME (http://meme-suite.org).

2.8 Transient reporter assay

We used a reference construct containing *Renilla reniformis* Luciferase (Ohta *et al*., 2000). The reporter, effector and reference constructs were inserted into 3-day-old *Arabidopsis* T87 cultured cells by polyethylene glycol (Axelos *et al*., 1992; Kovtun *et al*., 2000). After 20 hours incubation, protein fraction was extracted from the cultured cells. Luciferase activities were detected by the Dual-Luciferase Reporter Assay System (Promega, http://www.promega.com) using a TriStar LB941 reader (Berthold Technologies, http://www.berthold.com).

2.9 Microscopy analysis of the transgenic plants expressing GUS

The plasmid construct containing the GUS reporter gene under the control of *XCP1* promoter (-148 to +9 bp) or the four core-mutated *XCP1* promoter (Table 5) was electroporated into *Agrobacterium tumefaciens* strain *GV3101/pMP90*, which was used to transform into wild-type *Arabidopsis thaliana* Col-0 plants. The transgenic seedlings were selected on germination medium (Kubo *et al*., 2005) supplemented with 10 μg/ml bialaphos under continuous light conditions for 2 weeks. Then, the selected plants were transferred to an antibiotic-free medium for additional 3 days. For GUS staining, the seedlings were soaked in 90% (v/v) acetone at -20 ˚C. After rinse with 0.1 M sodium phosphate buffer (pH 7.0), the seedlings were incubated in a GUS staining solution [50 μM $NaHPO_4$, 0.1% Triton X-100, 1 mM $K_3[Fe(CN)_6]$, 1 mM $K_4[Fe(CN)_6]$ and 1 mM 5-Bromo-4-chloro-3-indolyl β-D-galactopyranoside] at 37 ˚C for 24 hours, then fixed in FAA solution (45% ethanol, 2.5% acetic acid and 2.5% formalin). Observation was made with a microscope (BX51, Olympus; http://www.olympus-global. com/).

3. RESULTS

3.1 Optimization of fluorescence correlation spectroscopy and interaction assay between VND7 and *XCP1* promoter sequences

XCP1 encodes a cysteine protease related to PCD during xylem vessel cell differentiation, and it is a direct target gene of VND7 (Yamaguchi *et al*., 2011). Previous research using transient reporter assay and electrophoresis mobility shift assay (EMSA) showed that VND7 binds to the 53-bp X1E1 sequence on the *XCP1* promoter (from -148 to -96 bp; Yamaguchi *et al*., 2011; Figure 2). In this study, I first aimed to define which nucleotides within the X1E1 sequence are critical for binding by VND7, using fluorescence correlation spectroscopy (FCS) that determines the status of interaction between DNA and proteins quantitatively (Kinjo *et al*., 1995; Octobre *et al*., 2005; Kobayashi *et al*., 2004; Harada *et al*., 2013). For the FCS, I prepared a maltose-binding protein (MBP)-tagged C-terminally truncated VND7 protein containing the whole NAC domain (amino acid residues 1 to 161; MBP-VND7$^{1\text{-}161}$) with a molecular weight of 62.3 kDa (Yamaguchi *et al*., 2008, 2010b; Endo *et al*., 2015) and the 138-bp promoter fragment of *XCP1* (from -233 to -96 bp) labeled with a fluorescent dye 5(6)-Carboxytetramethylrhodamine (TAMRA) at the 5'-end (TAMRA-*XCP1*pro) (Figure 2). The FCS assay was carried out using the single-molecule fluorescence detection system, FluoroPoint-Light MF20 (Olympus). When TAMRA-*XCP1*pro was added in the reaction at the final concentration of 5 nM, the diffusion time was 1,400 μsec (Figure 3).

To optimize the amount of proteins added to the reactions, MBP-VND7$^{1\text{-}161}$ proteins at several different concentrations (final from 0.03 to 1.77 μM) were tested with 5 nM TAMRA-*XCP1*pro (Figure 3). Although the control MBP did not affect the diffusion time, addition of MBP-VND7$^{1\text{-}161}$ proteins increased the diffusion time in a dose-dependent manner with almost maximum (up to around 2,200 μsec) at the concentration of 0.22 μM (Figure 3), which determined the concentration of MBP-VND7$^{1\text{-}161}$ protein that I used in further FCS assays to be 0.22 μM. Next, I confirmed whether the TAMRA-*XCP1*pro specifically binds to MBP-VND7$^{1\text{-}161}$ or not by a competition assay using unlabeled 138-bp *XCP1*pro as a competitor together with TAMRA-*XCP1*pro and MBP-VND7$^{1\text{-}161}$. As shown in Figure 4, the unlabeled *XCP1*pro were blocked the complex formation of VND7 and TAMRA-*XCP1*pro and decreased the diffusion time (Figure 4). From this result, I could confirm the specific

interaction between TAMRA-*XCP1*pro and MBP-VND7$^{1-161}$ by the FCS assay. In addition, I further examined the specificity of the binding between TAMRA-*XCP1*pro and MBP-VND7$^{1-161}$ with unlabeled 53-pb *XCP1* X1E1 sequence, which also decrease in the increased diffusion time as same level of unlabeled *XCP1*pro (Figure 4), providing another independent line of evidence, along with the transient assays and EMSA (Yamaguchi *et al*., 2011) that the *XCP1* X1E1 sequence in *XCP1*pro contributes to the specific binding between TAMRA-*XCP1*pro and MBP-VND7$^{1-161}$. However, there is still a possibility that the 85-bp 5'-half of *XCP1*pro sequence (from -233 to -149 bp; referred as *XCP1* X1E2 in Yamaguchi *et al*., 2011) can contribute to the binding TAMRA-*XCP1*pro and MBP-VND7$^{1-161}$. In this case, the binding between *XCP1* X1E2 and MBP-VND7$^{1-161}$ might be much weaker than that between *XCP1* X1E1 and MBP-VND7$^{1-161}$.

3.2 Detailed characterization of binding between VND7 and *XCP1* X1E1

Data shown Figure 2 to 4 suggest that *XCP1* X1E1 strongly interacts with MBP-VND7$^{1-161}$. Therefore, I prepared TAMRA labeled-X1E1 sequence (TAMRA-X1E1) and tested it with different concentrations of MBP-VND7$^{1-161}$, as performed above for the full *XCP1*pro. With TAMRA-X1E1 and at various concentration of MBP-VND7$^{1-161}$, the binding between *XCP1* X1E1 and VND7$^{1-161}$ was evaluated by the FCS assay. The MBP-VND7$^{1-161}$ at 0.03 μM showed significantly increased diffusion time, which was further increased with much higher concentration of MBP-VND7$^{1-161}$ and almost maximized with 0.22 μM of MBP-VND7$^{1-161}$ (about 1,250 μsec), indicating that X1E1 binds to VND7$^{1-161}$ in FCS assay (Figure 5). Based on this data I decided to use MBP-VND7$^{1-161}$ at the concentration of 0.22 μM for following FCS experiments.

3.3 Validation of FCS assay data with EMSA

I carried out EMSA to validate the observation by FCS assays (Figure 5). When 20 fmol of biotin-labeled *XCP1* X1E1 (Biotin-X1E1) was incubated with various amounts of MBP-VND7$^{1-161}$ (from 0.2 to 3.5 pmol), two shifted bands appeared (Figure 6, lane 3 to 13), while they were not observed with MBP (Figure 6, lane 2). The intensity of the upper band increased with the increasing concentrations of MBP-VND7$^{1-161}$ up to 2.1 pmol (Figure 6, lane 8). Next, using 2.1 pmol of

MBP-VND7$^{1-161}$, a competition assay was carried out with 2 to 30 pmol of unlabeled X1E1 (x100 to x1,500) (Figure 7), showing that 2 pmol (x100) of unlabeled X1E1 could abolish the upper band (Figure 7, lane 4) and that 20 pmol (x1,000) of unlabeled X1E1 is needed to completely remove the lower band (Figure 7, lane 12). These EMSA data suggest that biotin-X1E1 specifically binds to MBP-VND7$^{1-161}$ in the EMSA assay, validating the FCS assay data showing that X1E1 binds to VND7$^{1-161}$ (Figure 4).

3.4 Determination of region that responsible for VND7 binding in *XCP1* X1E1 sequence

A deletion series of unlabeled *XCP1* X1E1 with progressive deletions from the 5′ or 3′ terminus (X1E1-a to X1E1-r; Figure 8) was prepared to use as competitors in a competition assay. In the controls, MBP did not change the diffusion time compared with the reaction without MBP, and as seen in earlier experiments, MBP-VND7$^{1-161}$ prolonged the diffusion time significantly (Figure 9 to 11). This binding was cancelled by excess amounts (1 μM, x200) of unlabeled X1E1 sequence (Figure 9 to 11), suggesting again the specificity between TAMRA-X1E1 and MBP-VND7$^{1-161}$.

When the competitor fragment series with deletions from 5'-end (X1E1-a to X1E1-i) was mixed with TAMRA-X1E1 and MBP-VND7$^{1-161}$, diffusion time with X1E1-a (-143 to -96 bp) to X1E1-f (-127 to -96 bp) was equivalent to that with full-length *XCP1* X1E1 (Figure 9). When the competitors X1E1-g (-126 to -96 bp) to X1E1-i (-123 to -96 bp) were used, diffusion time was increased gradually up to that without any competitors (about 1,500 μsec) (Figure 9). Similarly, when the competitor series with deletion from 3'-end (X1E1-j to X1E1-r) was used, X1E1-j (-148 to -101 bp) to X1E1-m (-148 to -110 bp), diffusion time was equivalent to that with *XCP1* X1E1. X1E1-n (-148 to -112 bp) to X1E1-r (-148 to -96 bp) revealed the gradually increased diffusion time (up to about 1,300 μsec) (Figure 10). These results define an 18-bp sequence in *XCP1* promoter from -127 to -110 bp (CTTTGCTTCAAAGCCAAT; designated as X1E1-18bp; Figure 8, box nucleotide sequence) that is important for binding between TAMRA-X1E1 and MBP-VND7$^{1-161}$. It is notable that this sequence has an imperfect palindromic structure (C<u>TTT</u>G<u>CTT</u>CA<u>AAGC</u>C<u>AA</u>T; palindromic sequences are underlined).

To investigate the importance of the X1E1-18bp for the binding further, I used

an unlabeled X1E1-18bp as a competitor together with TAMRA-*XCP1* X1E1 and MBP-VND7$^{1-161}$ in the FCS assay (Figure 11). However, unexpectedly, X1E1-18bp did not work as a competitor, showing no significant change in diffusion time compared with the no competitors control (Figure 11), suggesting that the X1E1-18bp is not sufficient as a competitor for binding of VND7 to the *XCP1* X1E1. To find sequences sufficient for competition toward binding of VND7 to the *XCP1* X1E1, I prepared unlabeled competitors with additional bases on both 5' and 3' ends of X1E1-18bp for the competition assay (Figure 8 and 11), resulted in the finding that a 28-bp sequence with 5 additional bases each on both ends of X1E1-18bp is need for a complete competition to *XCP1* X1E1 sequence (Figure 8 and 11). I designated this sequence X1E1-28bp (from -132 to -105 bp; ATTGTCTTTGCTTCAAAGCCAATCCTAT; palindromic sequences are underlined), which again has an imperfect palindromic structure,

Next I confirmed the data obtained by the above deletion analysis, I conducted an EMSA with excess amount of unlabeled X1E1-28bp as a competitor. The upper band completely disappeared with unlabeled X1E1 as shown in Figure 7 and the unlabeled X1E1-28bp was effective in competing for binding between X1E1 and VND7$^{1-161}$ (Figure 12, lane 5). By contrast, unlabeled X1E1-18bp did not alter the pattern of the shifted bands (Figure 12, lane 6), confirming that X1E1-18bp is not enough to compete to the binding between X1E1 and VND7$^{1-161}$ and that X1E1-28bp can act as an effective competitor that strongly abolishes the binding.

3.5 Identification of nucleotides and nucleotide positions that are pivotal for VND7 binding to X1E1-28bp at single nucleotide resolution

I investigate the contribution of each nucleotide in X1E1-28bp for binding by VND7 by an equilibrium experiments using a competitor series of X1E1-28bp with single mutations (Table 5), which allowed me to determine the inhibitory constant (Ki) value of each competitor sequence. I first determined the concentration of MBP-VND7$^{1-161}$ to be used in the equilibrium experiments (Figure 13), and found that 0.22 μM of MBP-VND7$^{1-161}$ is enough for binding between X1E1 and VND7$^{1-161}$ (Figure 13). The competitors were added in the reaction at the concentration of 0.025 to 1.5 μM to measure diffusion time. Next, the diffusion time was used to calculate the ratio of fluorescent-labeled DNA fragments (TAMRA-X1E1-28bp) that bind to the protein (MBP-VND7$^{1-161}$) in total fluorescent-labeled DNA fragments (defined as

binding fraction α) and then Ki value of each competitor was calculated (Figure 14). Figures 14B shows an example of the calculated values of binding fraction α for a mutation at the nucleotide position +3 of X1E1-28bp where T was substituted with G (Table 5). When original X1E1-28bp was used for a competitor, binding fraction α was decreased drastically even with lower concentration of original X1E1-28bp as a competitor, showing that the original X1E1-28bp at 0.5 μM is enough to abolish the binding between TAMRA-X1E1-28bp and MBP-VND7$^{1\text{-}161}$, while the mutated competitor showed about half value of binding fraction α even if using much higher concentration (1.5 μM) (Figure 14B). To estimate the difference in the binding specificity of VND7 protein to competitor DNA from the plot data, the plot data was fitted according to the Cheng and Prusoff equation (Cheng and Prusoff, 1973) for the dissociation constant of competitor (Ki value) and Hill equation (Hill, 1910, 1913) for the dissociation constant between TAMRA-labeled DNA and VND7 protein (Kd value) which is necessary to calculate the Ki value. The Hill equation was originally formulated to create the fitting curve for molecular interaction between O_2 and hemoglobin and to calculate the binding specificity (Hill, 1910, 1913). This equation was aimed at the allosteric binding model in which multiple proteins coordinately bind to their target. The degree of cooperativity of the molecular interaction was described as Hill coefficient. The Cheng and Prusoff equation and Hill equation can be used for the calculation of the binding affinity between transcription factors and DNA sequences, which are applied to FCS-based binding assays (Anderson *et al.*,2008; Wölcke *et al.*, 2003; Wohland *et al.*, 1999). Figure 14C described an example of the calculated Ki values of original X1E1-28bp competitor and mutated X1E1-28bp competitor, from which the relative Ki value of the mutated competitor was calculated to around 120 (compared with the original competitor, X1E1-28bp). The higher the Ki value means the low binding affinity, indicating that the molecular interaction between the competitor DNA and the protein became unstable by the nucleotide substitutions.

Figure 15 and Table 1 show the calculated values of Ki for all the competitors with single substitutions on X1E1-28pb. None of nucleotide substitutions at the first 5-bases of X1E1-28bp (Figure 15, -5 to -1 bp) showed any significant changes in relative Ki values, suggesting that sequence specificity in this 5-bp sequence is not a matter of the binding of X1E1-28bp to VND7 (Figure 15). Similarly, nucleotide substitutions at the last 5-bases did not significantly increase relative Ki value, rather some substitutions reduced relative Ki values (e.g. A to G at +4 and T to A at

+3) (Figure 15). In contrast, some of the nucleotide substitutions in X1E1-18bp region (from -127 to -110 bp) significantly increased the Ki values (Figure 15). Especially, the substitutions at position 3, 6 to 8, and 16 (T, C, T, T, and A, respectively into any other nucleotides) increased the relative Ki values more than 5-fold (Figure 15), suggesting that these nucleotides make higher contributions to the binding between *XCP1* X1E1 and VND7. It should be noted that the substitution of A at position 17 into C and that of T at position 18 into G significantly reduced the relative Ki values (Figure 15), showing that the original nucleotides at position 17 and 18 are not optimal for binding between *XCP1* X1E1 and VND7. Also, it might be noteworthy that the substitution from T to G at position 18 leads a much more perfect palindromic structure (CTTTGCTTCAAAGCCAAG) compared with the original *XCP1* X1E1-18bp sequence (CTTTGCTTCAAAGCCAAT).

3.6 Further characterization of nucleotides that have a significant effect on the specificity for binding VND7 to X1E1-18bp

The competition assay using competitors with single substitutions in X1E1-18bp region showed that several nucleotides have significant impact on binding between *XCP1* X1E1 and VND7 (Figure 15). However, as shown in Figure 16, which provides the details of the competition assay from which the Ki values in Figure 15 were calculated, the diffusion time of each competitor with single substitutions was still shorter than the diffusion time without any competitors even when these competitors were used at a higher concentration (1 μM, Figure 16; e.g. from original T into G at position 3, Figure 16B), suggesting that additional and combinational substitutions might reveal the nucleotide specificity required for the binding between *XCP1* X1E1 and VND7 much more clearly. Therefore, I created another competitor series with second nucleotide substitutions in addition to the first substitution (shown in Table 5, Figure 15). The first substitution used in this series was from original T into G at position 3, which showed the strongest effect among the single substitution series. I performed a competition assay using the double-mutation DNA fragments and calculated relative Ki values (Figure 17). The second substitution from A to G at position 16 had a strongest effect as an increased relative Ki value. Also, some other second substitutions including those at position 4 to 12 led to increased relative Ki values, while and second substitution at position 18 produced a reduced relative Ki value (Figure 17). The second substitution from A to

G at position 16 had a strongest effect as an increased relative Ki value. Also, some other second substitutions including those at position 4 to 12 led to increased relative Ki values, while and second substitution at position 18 produced a reduced relative Ki value (Figure 17). Taken together with a consideration of the palindromic structure (CTTTGCTTCAAAGCCAAT), these data show that 1) VND7 has a high binding affinity to CTT/AAG sequence, of which the third base-pair, T/A, is most important for the binding between *XCP1* X1E1 and VND7, and that 2) the configuration of three CTT/AAG sequences (position 1 to 3, 6 to 9, and 12 to 14) and one CTT/AAG-like sequence (ATT/AAT; position 16 to 18) with 2-base-pair intervals in 18-bp *XCP1* X1E1 (CTTNNCTTNNAAGNNAAT) could be important for the binding. Therefore, I defined the sequence structure, CTTNNCTTNNAAGNNAAT, as "*XCP1* X1E1 core structure" of *XCP1* X1E1 for further analysis.

3.7 Systematic Evolution of Ligands by Exponential Enrichment (SELEX)

To investigate the binding sequence specific for VND7 further, I employed the Systematic Evolution of Ligands by Exponential Enrichment (SELEX) technique, which can enrich the oligo-DNA with ability to bind to target proteins from pools of random oligo-DNA, allowing us to determine the consensus sequence for binding between target protein and DNA (Tuerk *et al*., 1990; Shimada *et al*., 2005; Slattery *et al*., 2011). Using MBP-VND7$^{1\text{-}161}$ and a pool of oligo-DNA containing 26-bp random oligo-DNA with the 24-bp adaptors at 5' and 3'ends ((24-bp-forward adaptor)-(26-bp random oligo-DNA)-(24-bp reverse adaptor); Table 5), SELEX was performed to find consensus sequence(s) for VND7. From this work, 35 sequences that bind to VND7$^{1\text{-}161}$ (but not MBP) were identified (Table 2), and analyzed using Multiple Em for Motif Elicitation (MEME; http://meme-suite.org). The MEME program highlighted an 18-bp consensus sequence C(G/T)TNNNNNTNA(C/A)GNNNNN (defined with nucleotides with more than 0.8 bits) (Figure 18). This SELEX consensus sequence is clearly matched with the sequence of the core structure of *XCP1* X1E1 (CTT at position 1 to 3 and AAG at position 11 to 13) (Figure 18, boxed and underlined nucleotides). As the substitution of nucleotide T at position 18 into G was shown to effective to enhance the binding of VND7 (Figure 15 and 17), it is plausible that the SELEX consensus sequence is also closely related to the sequence, CTT and AAT (position 6 to 8 and 16 to 18) in the core structure (Figure 18, box and

underlined nucleotides).

3.8 Sequence alignment of *XCP1* X1E1-28bp, *XCP1* X1E1 core structure, SELEX consensus sequence, TERE, and SNBE

Previously, TERE and SNBE were designed with the sequences of *XCP1* promoter from -122 to -112 bp (position 6 to16 in *XCP1* X1E1-28bp) and from -130 to -112 bp (position -3 to16 in *XCP1* X1E1-28bp), respectively (Figure 19; Pyo *et al*., 2004; Zhong *et al*., 2010). When these consensus sequences were aligned with *XCP1* X1E1-28bp, *XCP1* X1E1 core structure, and SELEX consensus sequence, with a consideration of the single and double substitution data, I could define the "ideal core structure" as "CTTNNCTTNNAAGNNAAG" with more palindromic structure as compared with the FCS core structure (Figure 19).

To investigate whether the ideal core structure is included in promoter regions of some other putative VND7 direct target genes, I compared the promoter sequences of putative VND7 direct target genes with the ideal core structure. It was experimentally shown that VND7 binds to promoter sequences of several putative direct target genes for VND7, including *XCP2*, *CesA4*, *MYB46*, and *MYB83* (Zhong *et al*., 2010; Yamaguchi *et al*., 2011) (Figure 20). In addition, a number of genes that have TERE-like motifs in their promoter regions were speculated to be the direct targets of VND7 (Yamaguchi *et al*., 2011), including *POLYGALACTURONASE* (*PG*, At1G70500) and *METACASPASE 9* (*ATMC9*, At5G04200) (Figure 20). Among these promoter sequences, I found that some of the promoters include at least one pair of the palindromic structure, CTTNNNNNNAAG, if some restricted substitutions and one-base gaps are allowed. In addition, with a consideration of the single and double substitution data, it is supposed that T, T, A, and A at position 3, 8, 11, and 16, respectively, in X1E1-18bp are important for the binding between *XCP1* X1E1 and VND7, thus I designated these as "core-nucleotides".

3.9 Detailed analysis of the "*XCP1* X1E1 core structure" in X1E1-28bp for binding between *XCP1* X1E1 and VND7

Next, I probed whether the *XCP1* X1E1 core structure is significant for binding between *XCP1* X1E1 and VND7, guided by the results of the analysis above. Several competitors were prepared from original *XCP1* X1E1-28bp with two or four

substitutions in the core-nucleotides into G (Figure 21), with which further FCS competition assays were conducted (Figure 22). Figure 23A shows values of diffusion times in FCS analysis with the competitors at the concentration of 1 μM, indicating that any changes in the core-nucleotides significantly increase the diffusion time (Figure 22A). When relative Ki values were calculated from the competition assay, all the competitors increased the relative Ki values, and interestingly, the competitor with substitutions in all the core-nucleotides showed the highest relative Ki value (Figure 22B). These targeted assays show that core-nucleotides within the *XCP1* X1E1 core structure greatly contribute to the binding between *XCP1* X1E1 and VND7.

3.10 Contribution of the *XCP1* "core-nucleotides" for transcriptional regulation activity

To investigate whether the core-nucleotides are responsible for transcriptional regulation by VND7 in plant cells, a transient reporter assay was conducted with dual luciferase (LUC) transient expression system (Mitsuda *et al*., 2005; Yamaguchi *et al*., 2010b; Endo *et al*., 2015). I prepared reporter constructs containing the firefly *LUC* gene driven by a series of *XPC1* promoter variants of which the core-nucleotides of *XCP1* X1E1-18bp region were modified as shown in Figure 23 and Table 5. The *XCP1*pro:Luc (*XCP1* promoter from -148 to +9 bp translationally fused with *LUC* reporter gene) showed extremely high relative LUC activity with the *35S*:VND7 effector (VND7 driven by CaMV *35S* promoter) (Figure 23). Single substitutions in position 10 and 14 (*XCP1*pro-sm.5 and 6:Luc), which did not affect the diffusion time (Figure 16B, X1E1-ls_51 and 54) and relative Ki values (Figure 15, position 10 and 14) in the FSC assay, exhibited high relative LUC activity that is statistically equivalent to that with *XCP1* pro:Luc (Figure 24A). Single substitutions in each of the core-nucleotides (*XCP1*pro-sm.1 to 4:Luc) could still induce LUC activity compared with the control effector (*35S*:MCS), but the levels of relative LUC activity were statistically lower than that with *XCP1*pro:Luc (Figure 24A). In contrast, all 6 combination of double substitutions in the core-nucleotides (*XCP1*pro-dm.1 to 6:Luc) and quadruple substitution in all the core-nucleotides (*XCP1*pro-core-mu:Luc) mostly showed very low relative LUC activity (Figure 24B), clearly suggesting the importance of the core-nucleotides for transcriptional regulation by VND7 *in vivo*. It is noteworthy that the double substitutions in the

core-nucleotides at position “3 and 11” (*XCP1*pro-dm.2:Luc), at position “3 and 16” (*XCP1*pro-dm.3:Luc), and at position “8 and 16” (*XCP1*pro-dm.4:Luc) exhibited very slight changes in the LUC activity relative to the MCS control, but statistically significant strongly reduced LUC activity compared to the positive control wild-type *XCP1*pro (Figure 24B). Competitors with corresponding double substitutions in the FCS assay (X1E1-core-dm.2 to 4) showed statistically significant reduction in diffusion time and increased relative Ki values, so some binding between these competitors and VND7 can still be expected (Figure 21 and 22). Comparing the *in vivo* and *in vitro* data suggests that the regulation of gene expression *in planta* can be much more sensitively affected by the binding status between transcription factors and cis-sequences of the target genes.

3.11 Importance of the *XCP1* core-nucleotides for vessel-specific expression of *XCP1 in planta*

In order to examine further the importance of the core-nucleotides in the “*XCP1* X1E1 core structure” of the *XCP1* promoter, I prepared transgenic plants harbouring the *ß-glucuronidase* (*GUS*) gene driven by an original *XCP1* promoter (from -148 to +9 bp) or a mutated *XCP1* promoter with nucleotide substitutions in all the core-nucleotides (Figure 25A). In agreement with a previous study showing that the *XCP1* promoter (from -704 to +9 bp) is enough for specific expression in differentiating xylem vessel cells of *Arabidopsis* roots and leaves (Yamaguchi *et al*., 2011), I observed the GUS signal in roots and leaves of 17-day-old T1 plants (Figure 25, Table 3). The 157-bp *XCP1* promoter showed expression in protoxylem pole (in 24/39 T1 plant lines) and in root caps (in 6/39 T1 lines) in meristematic zone (Figure 25B and 25C, Table 3) and differentiating xylem vessel cells of protoxylem (in 24/39 lines) and metaxylem (in 28/39 lines) of roots (Figure 25E and 25F, Table 3), leaf veins of cotyledons (in 3/39 lines) and true leaves (in 13/39 lines) (Figure 25I and 25J, Table 3). On the other hand, the mutated *XCP1* promoter could not induce any GUS signal in protoxylem pole of the meristematic zone of roots (Figure 25D, Table 3) and in leaf veins of cotyledons and true leaves (Figure 25K and 25L), while the GUS signal was detected in root caps (in 4/52 lines), the pericycle cells (in 9/52 lines), and some other cells in stele of roots (Table 3, Figure 25G and 25H), epidermal and mesophyll cells in cotyledons (in 1/52 lines) and in true leaves (in 6/52 lines), cells at the leaf distal margin (in 13/15 lines), and stomata guard cells in

true leaves (in 1/52 lines) (Table 3). In addition, it should be noted that the 157-bp promoter is not sufficient to confer the expression of *XCP1* restricted in xylem vessel cells that was shown in previous studies by much longer promoter sequences (Funk *et al*., 2002; Yamaguchi *et al*., 2011) as the 157-bp promoter induced the expression in various cell types (Table 3). These results indicate that the core-nucleotides in the *XCP1* promoter contribute to the xylem vessel-specific expression of *XCP1* gene *in planta* and probably the core-nucleotides have function in repressing the expression in some cells such as pericycle cells and mesophyll cells. Alternatively, the nucleotide substitutions may have produced unexpected cis-sequence(s) on the promoter.

3.12 Binding of VND6 and NST3/SND1 with *XCP1* X1E1-28bp

It was shown that not only VND7 but VND6 and NST3/SND1 have ability to induce the expression of XCP1 and to bind to the *XCP1* promoter sequences which contain at least a part of the core-nucleotides (Ohashi-Ito *et al*., 2010; Zhong *et al*., 2010). Therefore, I investigated whether the core-nucleotides in *XCP1* promoter contribute to the gene expression of *XCP1* by these two transcription factors by using the dual LUC transient assay with a reporter construct with the mutated core-nucleotides (Figure 26). VND6 and NST3/SND1 can significantly induce the LUC activity with the original core-nucleotides (Figure 27A), but almost negligible activity was induced with the mutated core-nucleotides that are substituted into G (Figure 27B), suggesting that the core-nucleotides are responsible for the expression of *XCP1* gene by VND6 and NST3/SND1. However, relative LUC activity by NST3/SND1 was significantly weaker than that of VND7 (Figure 27A), which can be explained by the ability to bind to the *XCP1* promoter and by characteristics of the transcriptional activation domains. Therefore, I prepared two effector constructs with chimeras of VND7 NAC-domain ($VND7^{1-161}$) with NST3/SND1 transactivation (TA)-domain ($NST3/SND1^{181-159}$) and of NST3/SND1 NAC-domain ($NST3/SND1^{1-180}$) with VND7 TA-domain ($VND7^{162-325}$), with which the transactivation activity to *XCP1*pro:LUC reporter was analysed (Figure 27C). As a result, VND7 NAC-domain:NST3/SND1 TA-domain showed high relative LUC activity but NST3/SND1 NAC-domain:VND7 TA-domain exhibited very low activity, indicating that the difference in the relative LUC activity between VND7 and NST3/SND1 is mainly attributed with the NAC-domains.

To understand the binding characteristic of these transcription factors to the *XCP1* promoter, NAC-domain of VND6 and NST3/SND1 were fused with MBP (MBP-VND6$^{1-159}$ and MBP-NST3/SND1$^{1-180}$, respectively) and prepared for the FCS assay. DNA-binding affinity (Kd value) between each transcription factor with X1E1-28bp was calculated from values of diffusion time measured with various concentration of the transcription factors (0.01 to 0.155 μM) (Figure 28A to 28C), showing that VND6 and VND7 have Kd values significantly lower than NST3/SND1 (Figure 28D; VND6, 40.0±13.5 nM; VND7, 37.4±12.3 nM; and NST3/SND1, 78.6±16.3 nM), demonstrating that VND6 and VND7 bind more strongly to the X1E1-28bp than NST3/SND1 does. This is consistent with their biological function indicated by mutant analysis, as VND6 and VND7 promote differentiation in cells with strong and rapid PCD, compared NST3/SND1 which controls development of long-lived fibers.

3.13 Conservation of the ideal core structure among several promoters of VND7 direct target genes

In the promoter sequences of several putative direct target genes for VND7, such as *XCP2*, *CesA4*, *MYB46*, *PG* (At1G70500), *ATMC9* (At5G04200), one or two palindromic structures (CTTNNNNNNNAAG) contained in the ideal core structure (CTTNNCTTNNAAGNNAAG) were found (Figure 20). To confirm that the promoter regions of these genes can bind to VND7 and to narrow down the binding sequences of the promoter regions, I carried out FCS deletion analysis using TAMRA-labelled promoter fragments of these genes and MBP-VND7$^{1-161}$, as well as a deletion series of the promoter fragments of each gene as competitors (Figure 29). The position and length of promoter regions were determined based on previous work (Yamaguchi *et al*., unpublished) carried out in my affiliate laboratory (Saitama University). Using these TAMRA-labeled promoter fragments, MBP-VND7$^{1-161}$, and competitors FCS analysis was carried out and diffusion times were measured (Figure 29B to 29I), which narrowed down the sequences required for the binding by VND7 (Figure 30). Alignment of these sequences using the MEME program emphasized the similarity of these sequences with the "ideal core structure", "CTTNNCTTNNAAGNNAAG" (Figure 30). Moreover, with a consideration of the importance of the "core-nucleotides", I noticed the conservation of a motif "CTTNNNNNNNA" in all the aligned sequences (Figure 30). Since this motif is

highly conserved among SELEX consensus sequence, TERE, and SNBE, it is plausible that this motif is a minimal sequence required for the binding of VND7 to DNAs.

3.14 Comparison the binding affinity of the VND7 direct target gene promoters

In Figure 30, I characterized similar sequences to the identified ideal core structure found in the VND7 direct target gene promoters. In order to compare the binding affinity of VND7 to its direct target gene promoters, I demonstrated the FCS-based binding assay with the TAMRA-labeled *XCP1* X1E1-28bp and the ~40-bp-sequences of these promoter, in which the similar sequences to the identified ideal core structure sequences, as the competitor, to measure Ki value against the *XCP1* X1E1-28bp sequence (Figure 31). In the competitor binding assay, *XCP1* X1E1-28bp showed the lowest Ki value among the tested sequences (Figure 31). The Ki values of the *CesA4*, *MYB46-3* and *MYB83* sequences seemed to be comparative with *XCP1* X1E1-28bp, and the *PG*, *XCP2*, *MYB46-1*, *MYB46-2*, and *ATMC9* sequences demonstrated the statistically-significant increase in the Ki values when compared with *XCP1* X1E1-28bp (Figure 31). Especially, the promoter of *ATMC9* exhibited the highest Ki value, approximately 4 times to the Ki value of *XCP1* X1E1-28bp, suggesting that the tested *ATMC9* sequence has lower affinity for VND7 than *XCP1* X1E1-28bp. However, the ranges of increment in Ki values in the promoter sequences of VND7 direct target gene were lower than those in the core-mutated X1E1 competitors (Figure 22B). Thus, although the core structure sequences are not perfectly conserved in some promoters of VND7 direct target genes (Figure 30), the promoter regions containing similar sequences to the ideal core structure would show high binding affinity to VND7.

3.15 Investigation of molecular evolution of X1E1-28bp in *XCP1* gene

To investigate the evolutionary conservation of the XCP1 ideal core structure, I checked the promoter sequence of XCP1 homologues gene in the moss plant *Physcomitrella patens*. Based on the analysis of *P. patens* VNS proteins (PpVNS1 to PpVNS8), the homologous proteins to Arabidopsis VND7, Xu *et al*. (2014) showed that PpVNS proteins contributes to the water conductive cell differentiation in *P. patens*, and that VNS-based transcriptional network would be basically conserved

between Arabidopsis and *P. patens*. The NAC domains of the *P. patens* VNS proteins show more than 90% sequence identity with the vascular plant orthologs (e.g. PpVNS7 and VND7 has 92.3% amino-acid identity; Xu *et al*., 2014). Overexpression of one of the *PpVNS* genes, *PpVNS7*, induces the expression of 3 genes with sequence similarity to *Arabidopsis XCP1* and *XCP2*, *Pp1s49_32V6*, *Pp1s315_40V6*, and *Pp1s52_60V6*. The genome of *P. patens* has 8 homologues of *XCP*, a phylogenetic tree of which does not tell us about exact phylogenetic relationship because of very low bootstrap values in the trees (Xu *et al*., 2014), suggesting that the *XCP* homologs were diversified very early in plant evolution. However, the strong up-regulation of these *XCP1/XCP2* homologs by *PpVNS7* in *P. patens* evokes a possibility that PpVNS7 binds to promoters of *XCP* homologous genes through the sequences with similarity to the "ideal core structure". When the *XCP1* X1E1-like sequences were used to search the 1-kb upstream of the *XCP* homologs (*Pp1s49_32V6*, *Pp1s315_40V6*, *Pp1s52_60V6*, and *Pp1s199_134V6*; Xu *et al*., 2014), several 18-bp sequences with more than 40% sequence identity (between 44% and 67%) were found in each gene. For up-regulated genes, *Pp1s49_32V6*, *Pp1s315_40V6*, and *Pp1s52_60V6*, there were 3 to 4 sequences, while for down-regulated gene, *Pp1s199_134V6*, there were only two sequences (Figure 32). Among these four genes, *Pp1s49_32V6* has an 18-bp sequence with the highest identity (67%) to X1E1-18bp. It would be important to note that a fold-change in the expression level of this *Pp1s199_134V6* gene induced by PpVNS7 was highest among XCP homologs (around 80-fold; Xu *et al*., 2014). When the sequence identity to the "ideal core structure" is considered, only some sequences have higher sequence identity (more than 60%) to the "ideal core structure" (Figure 32). Also, the "CTTNNNNNNNA" motif is conserved in the *VND7* target genes of *Arabidopsis* (Figure 30). It could be speculated that numbers of the "CTTNNNNNNNA" motifs could be related to the expression level, because *Pp1s49_32V6* with the highest expression has three motifs, while other two genes with up-regulated expression have two motifs but the down-regulated gene has only one motif (Figure 32). Additional experiments are needed to explain why the down-regulated gene has one similar motif. Taken together, these data suggest that 1) promoters of moss *XCP* homologous genes have the "CTTNNNNNNNA" motifs putatively important for the binding by VNS proteins, 2) a mechanism underlying the recognition of direct target genes by VNS transcription factors through the primitive "ideal core structure" had been established in the common ancestors of moss plants and vascular plants, and 3)

the optimization of cis-sequences for the VNS transcription factors occurs during plant evolution.

4. Discussion

4.1 FCS kinetic binding assay is suitable for identifying cis-sequence at the single nucleotide level

Xylem vessel cell differentiation contains two major distinct processes, secondary cell wall (SCW) formation and programmed cell death (PCD) (Oh *et al*., 2003; Turner *et al*., 2007; Fukuda, 2004), and the tight control of the expression of genes related to these processes is regulated by the transcription factor VND7 (Kubo *et al*., 2005; Yamaguchi *et al*., 2011). The recognition of specific DNA sequences (cis-sequences) by transcription factors, in other words the interaction between transcription factors and promoter sequences of the target gene is the first essential step for initiation of gene expression (White *et al*., 2016; Weirauch *et al*., 2014). Therefore, identification and characterization of the cis-sequences for VND7 are essential for understanding the mechanisms of xylem vessel cell differentiation. Previously, a consensus cis-sequence for the expression of vessel-specific genes, TERE, was found (Pyo *et al*., 2007), which can be recognized by VND7 (Ohashi-Ito *et al*., 2010; Yamaguchi *et al*., 2011). Additionally, SNBE, a consensus cis-sequence for SCW-related VNS proteins, NST3/SND1, NST1, NST2, VND6, and VND7, was shown to bind to VND7 (Zhong *et al*., 2010). However, information on the binding specificity between cis-sequences with the VNS transcription factors is still insufficient to fully explain the specific regulation by VND7 and other VNS proteins (McCarthy *et al*., 2011; Yamaguchi *et al*., 2011). Therefore, I optimized biophysical quantitative methods to identify and characterize the cis-sequences for VND7 in detail, verified the results with additional approaches, and relate the new detailed understanding to these earlier studies.

Currently several methods are established as the analytical technique to examine the affinity of specific binding of TF to their target DNA, such as EMSA, protein binding DNA-microarray, surface plasmon resonance (SPR) and FCS, and SPR and FCS are considered as the typical quantitative methods for protein-DNA binding (reviewed in Helwa and Hoheisel, 2010) .In the case of plants, for example, SPR successfully quantitated the interaction between auxin response factors (ARFs) and their target cis-elements, the auxin response DNA element (AuxRE) (Boer *et al*., 2014). However, SPR is suitable for the detailed analysis of limited numbers of

protein and/or DNA samples, because 1) the protein or DNA molecules should be immobilized onto the sensor chips, and 2) the immobilization of molecules can also affect the interaction between TF and DNA, thus the pre-analysis on critical regions of TF and DNA for their interaction is basically required (reviewed in Helwa and Hoheisel, 2010). In contrast, FCS, which is also the quantitative method for the affinity of TF and DNA like SPR, has the advantage of being able to analyse a large number of samples with small scales (Kinjo *et al*., 1995; Octobre *et al*., 2005; Kobayashi *et al*., 2004; Harada *et al*., 2013). Although it is difficult to apply FCS to the molecules slow in motion, since FCS measures the diffusion and dynamics of single fluorescent molecule (Kinjo *et al*., 1995; Octobre *et al*., 2005; Kobayashi *et al*., 2004; Harada *et al*., 2013), the typical experiments to test the interaction between TF and DNA fragments fall within the ranges of FCS application.

In this study, by the binding assay system with FCS, I succeeded in identifying and characterising a cis-sequence named X1E1-18bp located in the promoter of *XCP1* gene, one of direct target genes of VND7. This quantitative examination of the interaction between the VND7 tagged with MBP and the TAMRA-labeled DNA fragments from *XCP1* promoter, with a variety of competitors at different concentrations, demonstrate that the FCS kinetic binding assay system is suitable for analysing DNA-protein interaction at the nucleotide level.

The FCS binding assay employed in this study identified specific pivotal nucleotides in the *XCP1* X1E1-18bp for VND7-regulated expression (Figure 23 to 25). These data were combined with data from SELEX conducted in this study, and with comparison of the TERE and SNBE data to define the “ideal core structure”, CTTTGCTTCAAAGCCAAG (underlined), in the X1E1-18bp of *XCP1* promoter that is responsible for the binding with VND7. With these multiple lines of evidence, especially the mutant analyses combined with FCS, the “core-nucleotides”, CTTTGCTTCAAAGCCAAT (underlined), were shown to be pivotal for binding (Figure 21 and 22).

It is possible to identify important nucleotides for the binding between DNAs and proteins by using semi-quantitative methods such as EMSA. In fact, Zhong *et al*. (2010) carried out EMSA for NST3/SND1 with a number of competitors with single nucleotide substitutions in SNBE, succeeded in the identification of nucleotides that have strong effects on the binding between SNBE and NST3/SND1 based on the changes in the intensity of sifted bands. However, it is not easy to evaluate the difference in the contribution of each nucleotide because of the semi-quantitative

nature of EMSA. In contrast, the FCS assay employed in this study allowed me quantitatively detects small changes in the binding affinity. I consider that the kinetic FCS assay is one of the best methods to quantitatively analyze the binding property between DNA fragments and DNA-binding proteins including transcription factors.

The FCS kinetic competition assay with competitors with nucleotide substitutions revealed that 5-bp non-specific flanking sequences on both 5' and 3' ends of X1E1-18bp are necessary for stable binding (Figure 8 to 12, and 15). It has been reported that such non-specific flanking sequences serve as a scaffold to maintain the binding stability between DNAs and transcription factors, by recruiting the transcription factors to DNAs and by increasing DNA binding specificity in a structure-dependent/specific manner (Slattery *et al*., 2011; Rohs *et al*., 2010; Rohs *et al*., 2009a and 2009b White *et al*., 2016). In the EMSA study by Zhong *et al*. (2010), they reported no binding between VND7 and a 11-bp fragment of the TERE cis-element, which may be because the TERE fragment used lacked stabilizing flanking sequence. Therefore, the FCS assay employed in this study is useful for identifying the flanking sequences for stability of DNA-protein interaction as well as the core sequences/nucleotides pivotal for the specificity of DNA-protein interaction.

4.2 Mode of binding of VND7 with X1E1-18bp

In this study, I proposed that a motif "CTTNNNNNNNA" is the minimal sequence required for the binding by VND7 proteins (Figure 30), based on the careful consideration of data obtained in this study and TERE and SNBE consensus sequences (Pyo *et al*., 2007; Zhong *et al*., 2010). Especially, this idea helps to interpret the data by Pyo *et al*. (2007), showing promoter activity of five tandem repeats of 11-bp TERE from Zinnia *ZCP4* "CTTGAAAGCAA", *XCP1* "CTTCAAAGCCA", and some *Arabidopsis* genes related to SCW formation and PCD of xylem vessel cell differentiation led to the expression of *GUS* reporter gene. The effectiveness of these five tandem repeats for binding with VND7 has been explained by the speculation that the tandem repeats produce artificial binding structures. In fact, tandem repeats of *ZCP4* "CTTGAAAGCAA" produce new imperfect palindromic structure "CTTGAAAGCAACTTGAAAGCAA" with "CTTNNNNNNNACT" which might be functional for biding with VND7 based on

the single nucleotide substitution data showing that “ACT” at the position 16 to 18 in *XCP1* X1E1-18bp caused an increased binding affinity (small Ki value) (Figure 15). In addition, the SELEX data obtained in this study suggests the possibility that the VND7 proteins bind to the “CTTNNNNNNNA” motif, because some SELEX fragments shown in Table 2 do not have any palindromic structure (e.g. fragment number 2, 9, 10, 15, and so on) even if several nucleotide substitutions are accepted. In order to confirm whether the VND7 proteins can bind to these sequences or not, further experimental data might be needed.

The recent publication by O’Malley *et al*. (2016) showed large-scale identification of consensus sequences for plant transcription factors based on the DAP-seq data. Their predicted consensus sequences for some NAC proteins, including the four VNS proteins, VND3, VND4, VND6, and NST1, contain the “CTTNNNNNNNA” motifs. (e.g. CGTNNNNNNNAAG for VND4 includes the motif once). Their analysis did not include VND7, but the analysis of remaining VNS family members suggests that the “CTTNNNNNNNA” motif is widely conserved for the binding of NAC transcription factors.

A previous study using protein binding DNA-microarray showed that VND7 has a distinctive binding specificity for the TACGT core motif, while NST3/SND1 shows a specificity for TTGCGT (Lindemose *et al*., 2014). The SELEX data conducted in this thesis shows that VND7 has a binding preference for C(G/T)TNNNNNTNA(C/A)GNNNN, which is partly matched with the TACGT core motif described by Lindemose *et al*. (2014). Mutant analysis and FCS provides additional information that while “CGT” in the core motif detected in the VND7 SELEX sequence, it is likely that VND7 prefers binding to “CTT”, because “CTT” at position 6 to 8 in *XCP1* X1E1-18bp is sensitive to nucleotide substitution including a substitution from “CTT” into “CGT”, which increases the Ki value significantly (Figure 15). On the other hand, it is still possible that VND7 has a binding preference not only for “CTT” but “CGT” since nucleotide substitutions “from T to G at position 2” and “from A to C at position 12” do not have any statistically significant change in the Ki value, rather the substitution “from AAT to ACT at position 16 to 18” reduced the Ki value significantly (Figure 15). Therefore, although further experimental elucidation is needed to understand the DNA binding preference of VND7, “CTT” or “CGT”, especially *in vivo*, there seems no room for doubt that VND7 binds to “CTT” or “CGT”.

The palindromic sequences are known as binding sequences for dimerized

transcription factors (Boer *et al*., 2014; Welner *et al*., 2012). As it has been reported that VND7 forms homo dimer and hetero dimers with other VND family proteins (Yamaguchi *et al*., 2008), it is plausible that VND7 binds to the palindromic structure as homo-dimerized form. Indeed, it was shown by EMSA assay that homo-dimerized ANAC019 proteins, but not monomer ANAC019 proteins, can bind to the target DNA sequence (Olsen *et al*., 2005). Recently, crystal structure analysis of ANAC019 showed that homo-dimerized ANAC019 (two ANAC019 proteins) bind to one palindromic cis-sequence (Welner *et al*., 2012). Based on my work, I propose a model where two homo-dimerized VND7 proteins bind to two imperfect palindromic structures "CTTNNNNNNNAAG" and "CTTNNNNNNNAAT" included in the *XCP1* X1E1-18bp "CTTTGCTTCAAAGCCAAT" (Figure 33).

Up to now, there are no reports indicating that the VND transcription factor proteins form multiprotein complex for interaction to DNA. Previous studies on the signal transducer and activator of transcription (STAT) transcription factor revealed that two homo-dimerized STAT proteins interact with two nearby binding sites and that the molecular interaction between two STAT dimer proteins increases in the interaction stability between the STAT proteins and DNA (Vinkemeier *et al*., 1996; Horvath, 2000). Vinkemeier *et al*. (1996) measured the binding stability of STAT dimer proteins on DNA by EMSA with competitor DNA fragments, resulted in a conclusion that the stabilization of the two STAT dimer proteins contributes to the increase in the DNA binding affinity. The *XCP1* X1E1-28bp showed higher binding affinity for the VND7 protein, compared with other target gene promoters (Figure 31), suggesting a possibility that molecular interaction between two homo-dimerized VND7 proteins affects the stabilization of DNA interaction and binding affinity. I expect that further analysis will provide us key evidences to understand the molecular mechanisms underlying the specific gene regulation by VND7, particularly gene recognition and expression.

4.3 The molecular mechanisms that regulate the specific target gene recognition and expression by VND7

In this study, I showed that the binding affinity of VND7 to *XCP1* X1E1-28bp is much higher than that of NST3/SND1, the master transcriptional regulator for fiber cell differentiation in *Arabidopsis* (Ko *et al*., 2007; Mitsuda *et al*., 2005, 2007; Zhong *et al*., 2006). Based on the artificial overexpression of NST3/SND1 enhancing

the expression of *XCP1*, and transient reporter assays using VND7 and NST3/SND1 as effectors and *XCP1* promoter as reporters, low but significant levels of NST3/SND1 activity on *XCP1* has been proposed (Ohashi-Ito *et al*., 2010; Zhong *et al*., 2006). This is not consistent with either my detailed binding analysis nor with the expression pattern of *XCP1 in planta* (no expression in fibers), thus it is plausible that *XCP1* is not target gene of NST3/SND1 *in planta*. The higher binding affinity of VND7 (and VND6) to the *XCP1* promoter, as compared with NST3/SND1, may contribute to specific expression of XCP1 in vessels and the promotion of rapid PCD, which is an important feature specific to vessel cells. Additional investigation is needed to confirm this possibility: such as the identification of nucleotides responsible for the difference in the binding affinity between VND7 and NST3/SND1 in *XCP1* promoter (*XCP1* X1E1-18bp) and investigation of promoter sequences of other target genes including common target genes of VND7 and NST3/SND1. My data on the competitor binding assay showed that the promoter regions containing the ideal core structure like sequences of VND7 direct target genes have similar the binding affinity to VND7 (Figure 31). This finding suggested that the ideal core structure found from *XCP1* promoter can be a good indicator to find out the targeting sites of VND7 within promoters of VND7 direct target genes. Similar analysis on the binding affinity to NST3/SND1 will help to obtain additional insights into this question. It would be also important to analyse difference in the binding properties between VND7 and VND6 because these sister proteins have an ability to induce two different types of vessel cells, protoxylem vessel cells with spiral patterned SCW and metaxylem vessel cells with pitted or reticulate SCW, respectively (Kubo *et al*., 2005; Yamaguchi *et al*., 2011).

The transient assay of *XCP1* promoter using chimeric effectors demonstrated the differential transactivation activities in NAC domains of VND7 and NST3/SND1 affect (Figure 27). Crystal structure analysis of the complex of NAC domain of ANAC019 and its binding DNA revealed several important amino acid residues that are involved in the protein dimerization and DNA recognition (Welner *et al*., 2012), showing that the outer ß-sheet structure, ß3-strand (WKATGDK, Figure 34) (Ernst *et al*., 2004), interacts with the DNA major groove and contributes to target recognition (Welner *et al*., 2012). Moreover, Welner *et al*. (2012) identified the amino acid residues that interact with the DNA backbone (R85, R88, K96, K123, K129, and K162 in ANAC019 NAC domain, Figure 34), which contribute to general affinity of interaction with DNA (Figure 34). These residues are conserved in the NAC domains

of VND and NST/SND transcription factors (Figure 34), suggesting that other structural characteristics except above mentioned amino acid residues affect the specificity of VND7 and NST3/SND1 (Figure 27, 28D). When compared with the NAC domains among ANAC019, VND, and NST/SND proteins, NST/SND proteins have additional amino acid sequences between NAC sub domain IV and V (Figure 34; Kubo *et al*., 2005; Olsen *et al*., 2005; Welner *et al*., 2012). In this study, although I could not investigate the importance of the difference in the protein structure for target gene recognition, it will be necessary to conduct a further detail analysis, such as transient assay with domain swapped or mutated VND7 and NST3/SND1 effector proteins, to understand the specific target gene regulation.

4.4 Evolutionary analysis of VNS gene regulatory network

I showed that some homologous genes of *XCP1* in *P. patens* have sequences with similarity to *XCP1* X1E1-18bp in their promoters (Figure 32). As the expression of these genes was up-regulated upon the overexpression of *PpVNS7*, one of the *P. patens* homologs of VNS proteins in vascular plants, it is reasonable that these *XCP1* homologs of *P. patens* are direct targets of PpVNS7. Based on the data, it is suggested that the mechanism for binding between VNS transcription factors and their direct target genes had been established in the common ancestors of moss plants and vascular plants, optimization of which including nucleotide changes in the cis-sequences and changes in the amino acid sequences of VNS transcription factors that occurred during plant evolution. To understand the optimization of VND gene regulatory network, further analysis using several plant species including *Marchantia polymorpha*, *Selaginella moellendorffii*, *Ceratopteris richardii*, and gymnosperm plants such as loblolly pine and white spruce will be valuable.

5. Figures

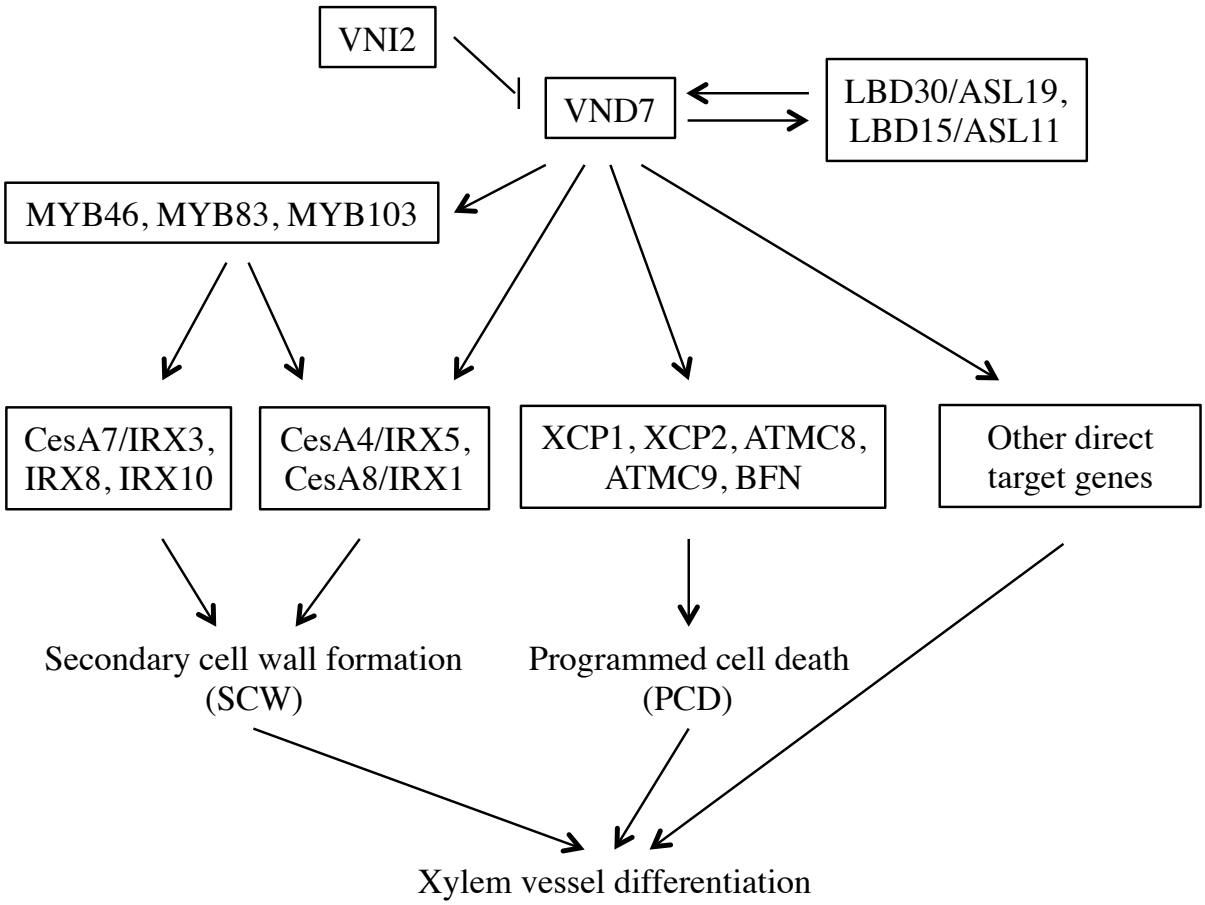

Figure 1.

Schematic diagram of gene network by VND7 during xylem vessel formation.

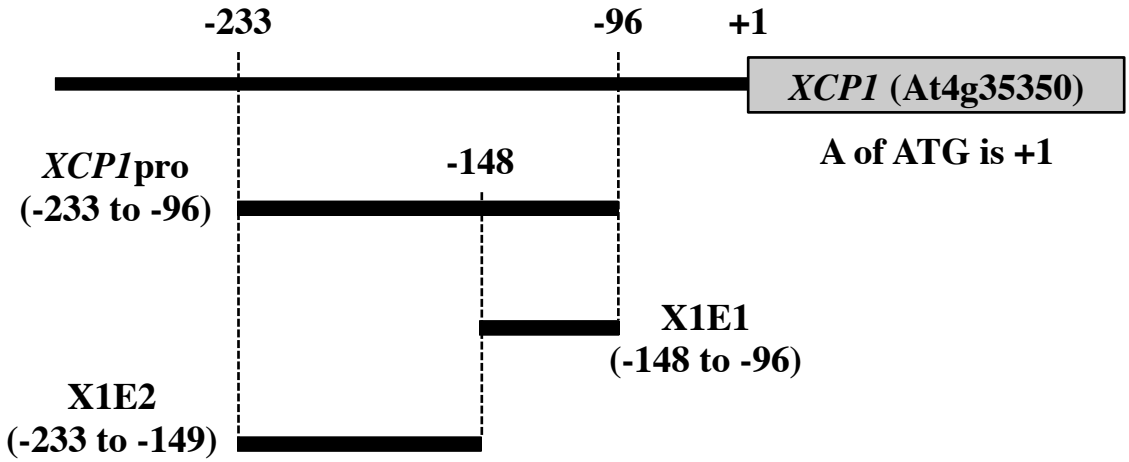

Figure 2.

Schematic diagram of DNA fragments, *XCP1* pro and X1E1 region.

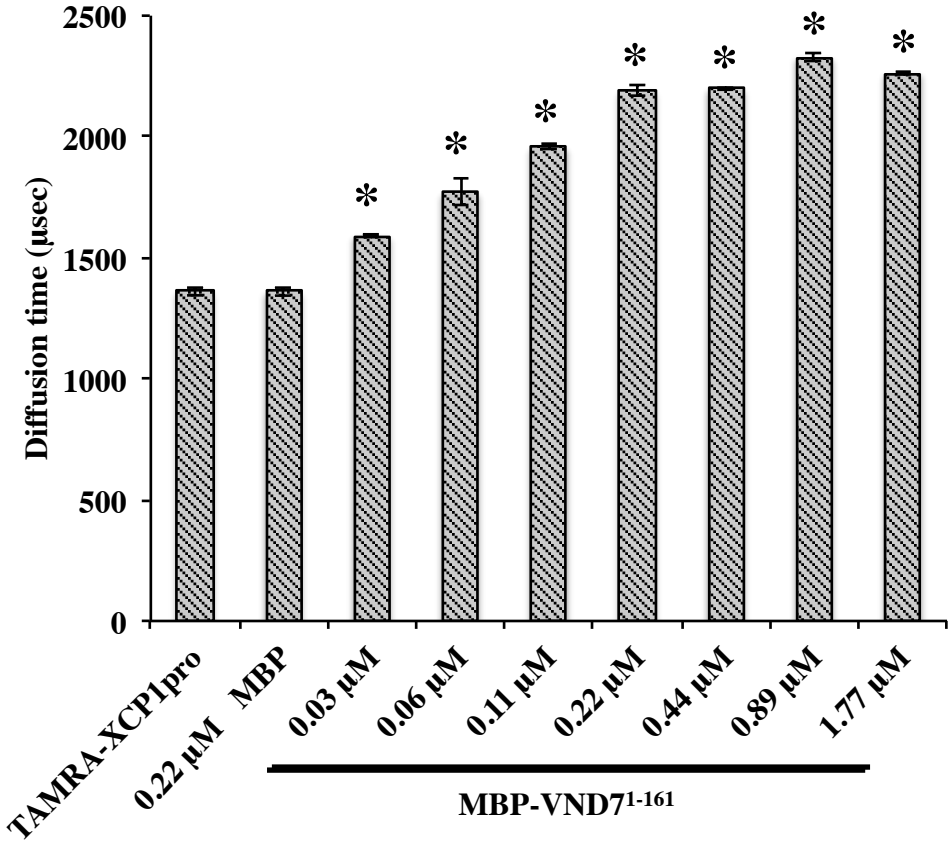

✻ : p < 0.05 (Compared with TAMRA-*XCP1*pro)

Figure 3.

Result of binding assay between TAMRA-labeled *XCP1*pro and MBP-VND71-161 protein by FCS. Y-axis indicate diffusion time of TAMRA-*XCP1*pro. Error bars are S.D. (n=3). Asterisks indicate statistically significant differences (Student and Welch's t-test; $p < 0.05$) from the diffusion time of TAMRA-*XCP1*pro.

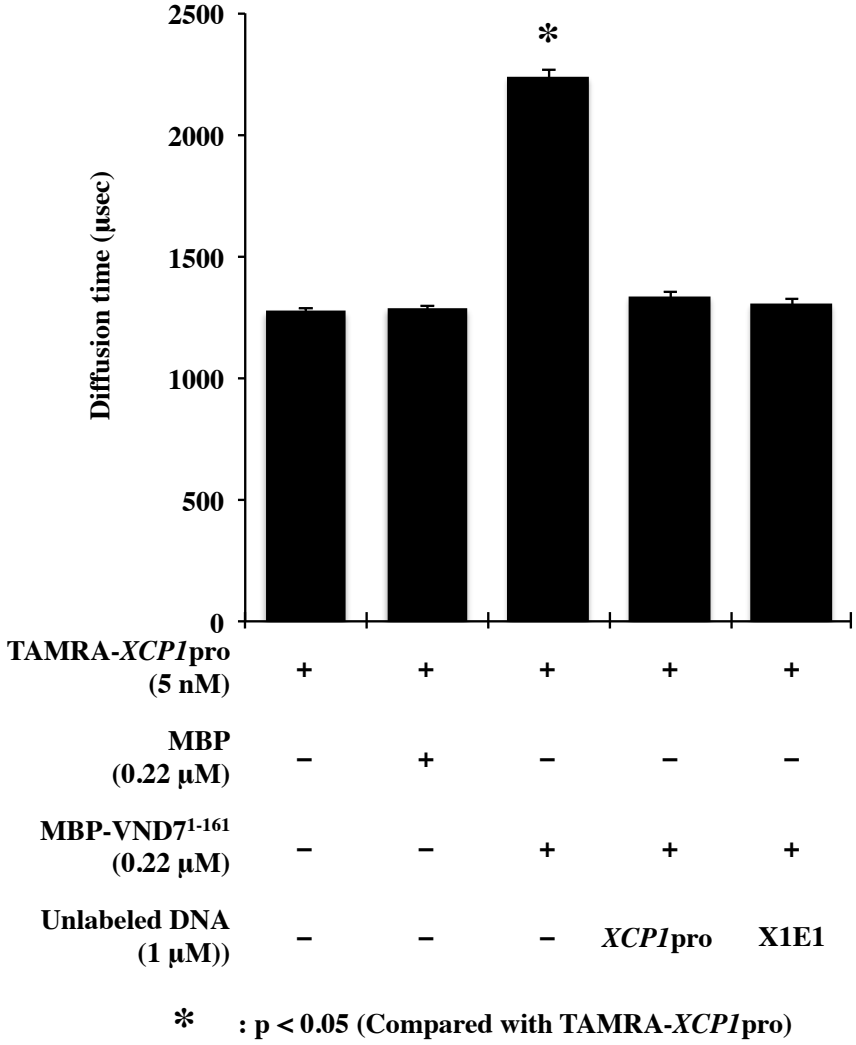

Figure 4.

Result of binding assay of *XCP1* promoter by FCS. X-axis indicates a diffusion time of TAMRA-*XCP1*pro. Error bars are standard deviation (S.D.) (n=3). Asterisks indicate statistically significant differences (Student and Welch's t-test; $p < 0.05$) from the diffusion time of TAMRA-*XCP1*pro.

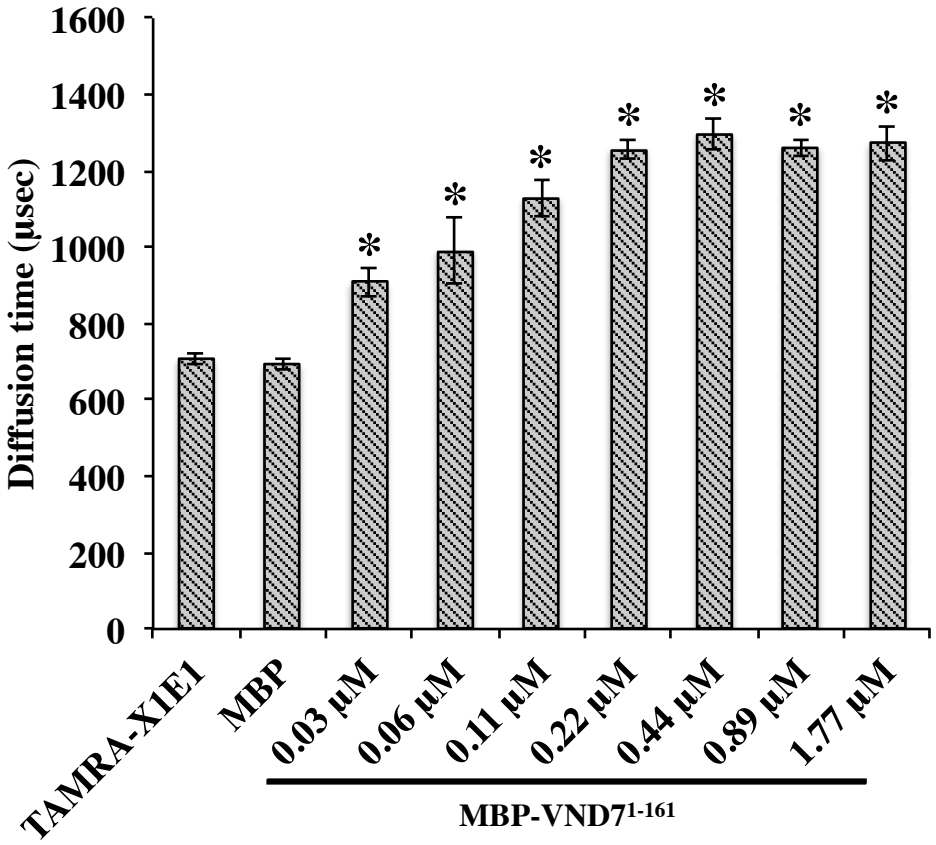

Figure 5.

Result of binding assay between TAMRA-labeled X1E1 and MBP-VND7$^{1-161}$ protein by FCS. Y-axis indicate diffusion time of TAMRA-X1E1. Error bars are S.D. (n=3). Asterisks indicate statistically significant differences (Student and Welch's t-test; $p < 0.05$) from the diffusion time of TAMRA-X1E1.

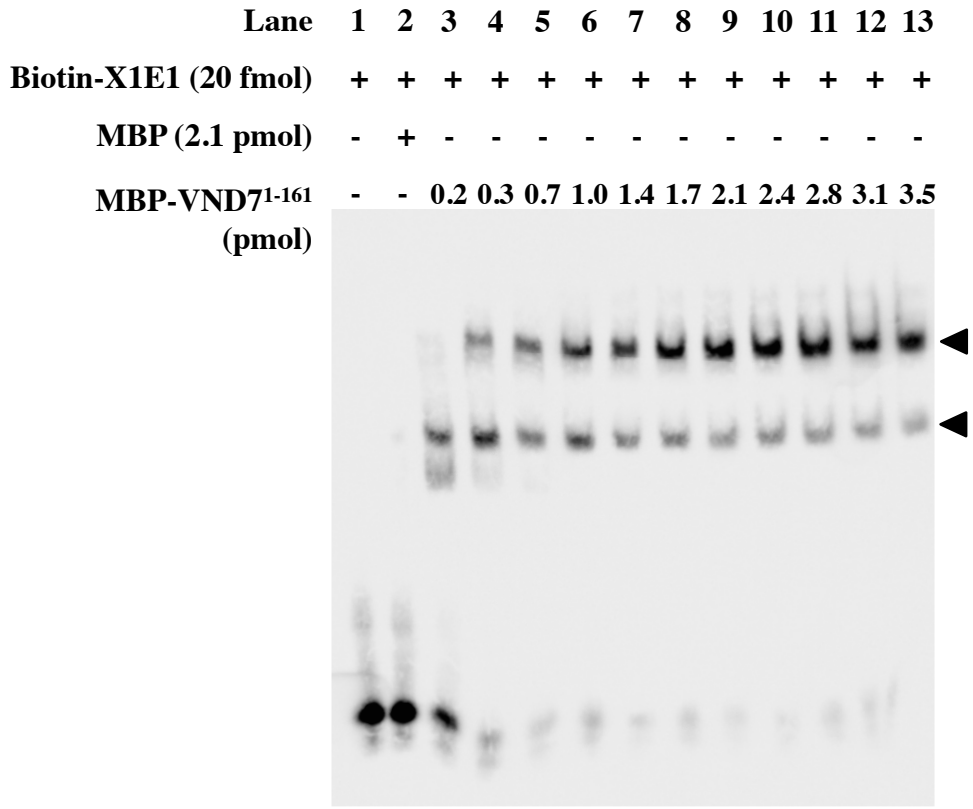

Figure 6.

Binding assay between biotin-labeled X1E1 and MBP-VND7$^{1-161}$ protein by EMSA. The protein concentration is gradually increased from 0.2 to 3.5 pmol. Arrowheads indicate shifted bands position.

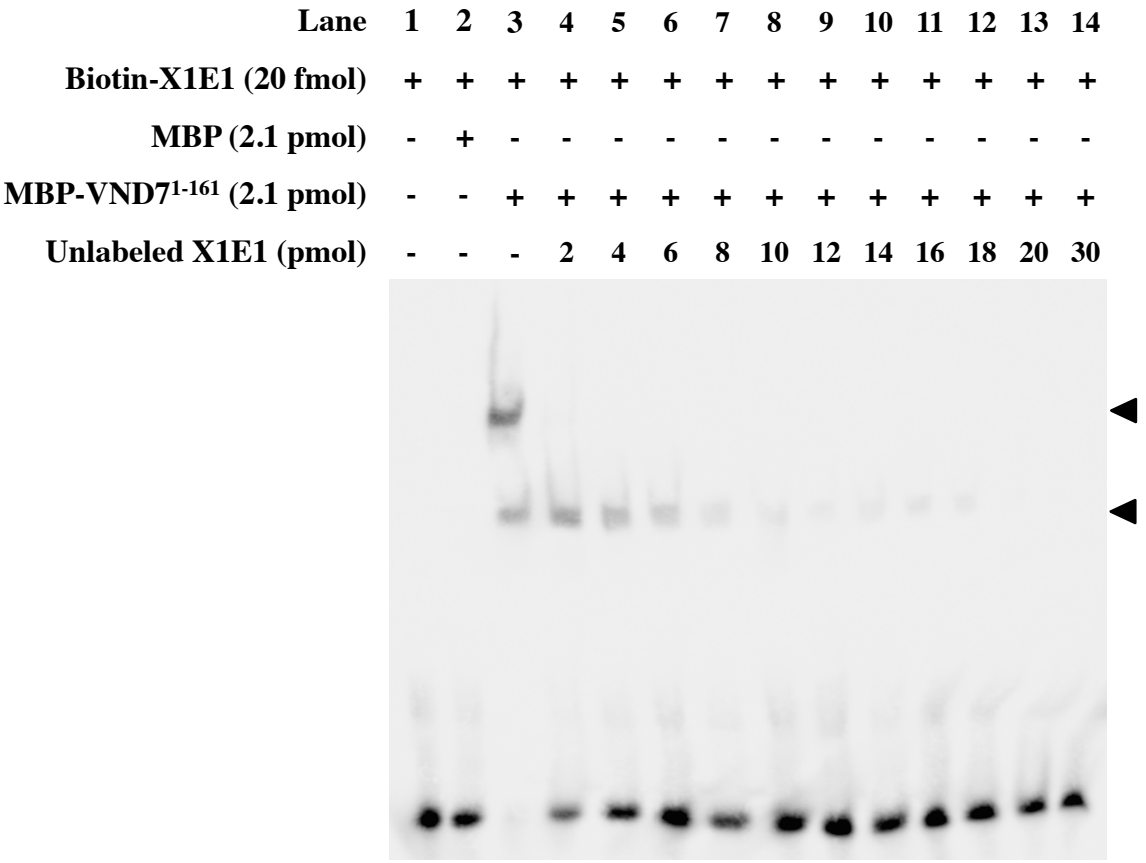

Figure 7.

Competitor binding assay between biotin-labeled X1E1 and MBP-VND7$^{1-161}$ protein by EMSA. The competitor concentration is gradually increased from 2 to 30 pmol (4 pmol; 200 times higher than biotin-X1E1). Arrowheads indicate shifted bands position.

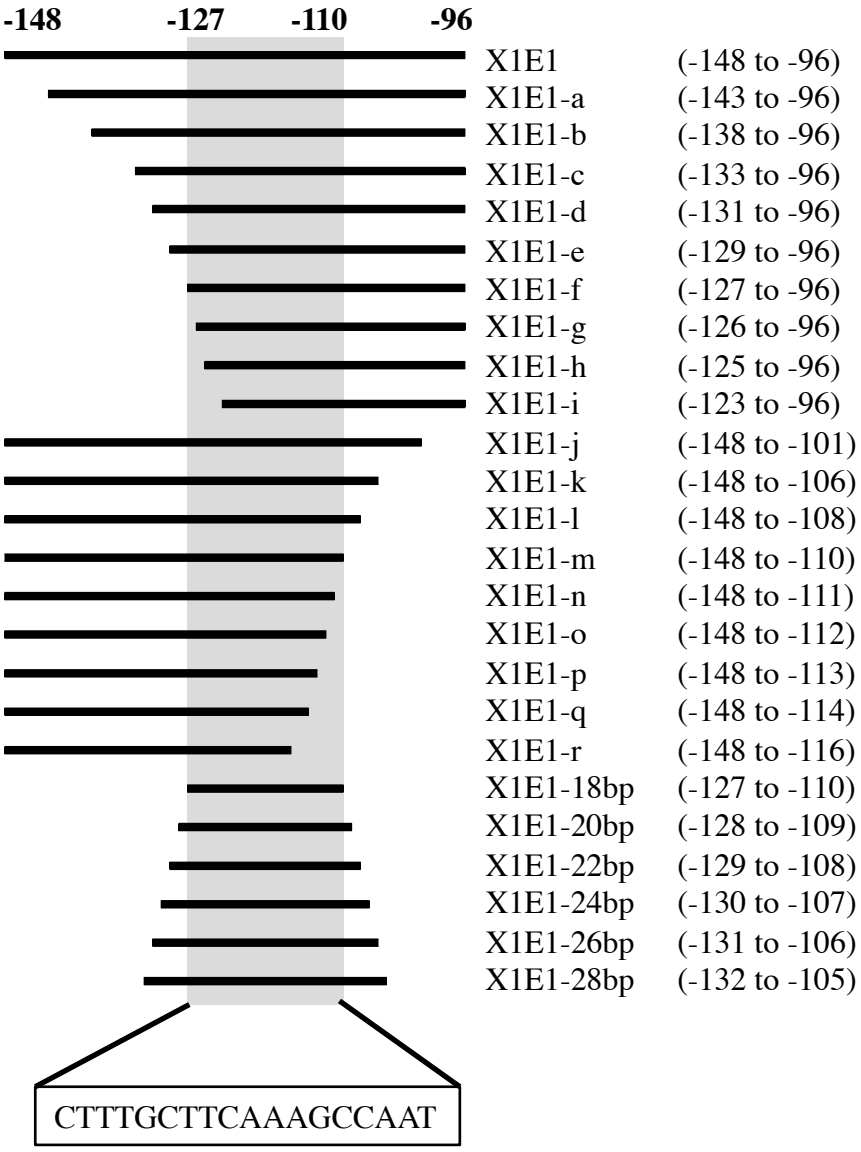

Figure 8.

Schematic diagram of deletion DNA fragments that are progressively deleted X1E1 region from its 5' or 3' terminus. Box indicates X1E1-18bp region.

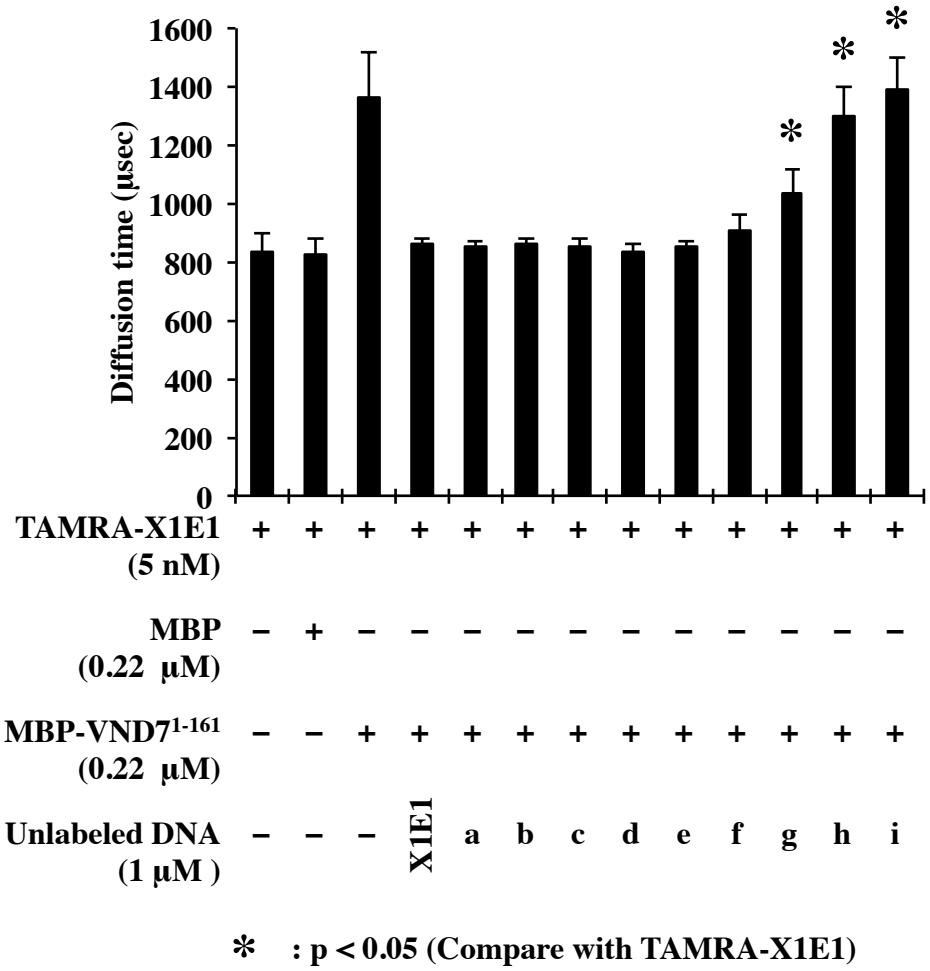

Figure 9.

Result of 5' deletion binging assay by FCS. Y-axis indicates a diffusion time of TAMRA-X1E1, X-axis indicates a competitor fragment name (X1E1, X1E1-a to i) as shown in Figure 8. Error bars are S.D. Asterisks indicate statistically significant differences (Student and Welch's t-test; $p < 0.05$) from the diffusion time of TAMRA-X1E1.

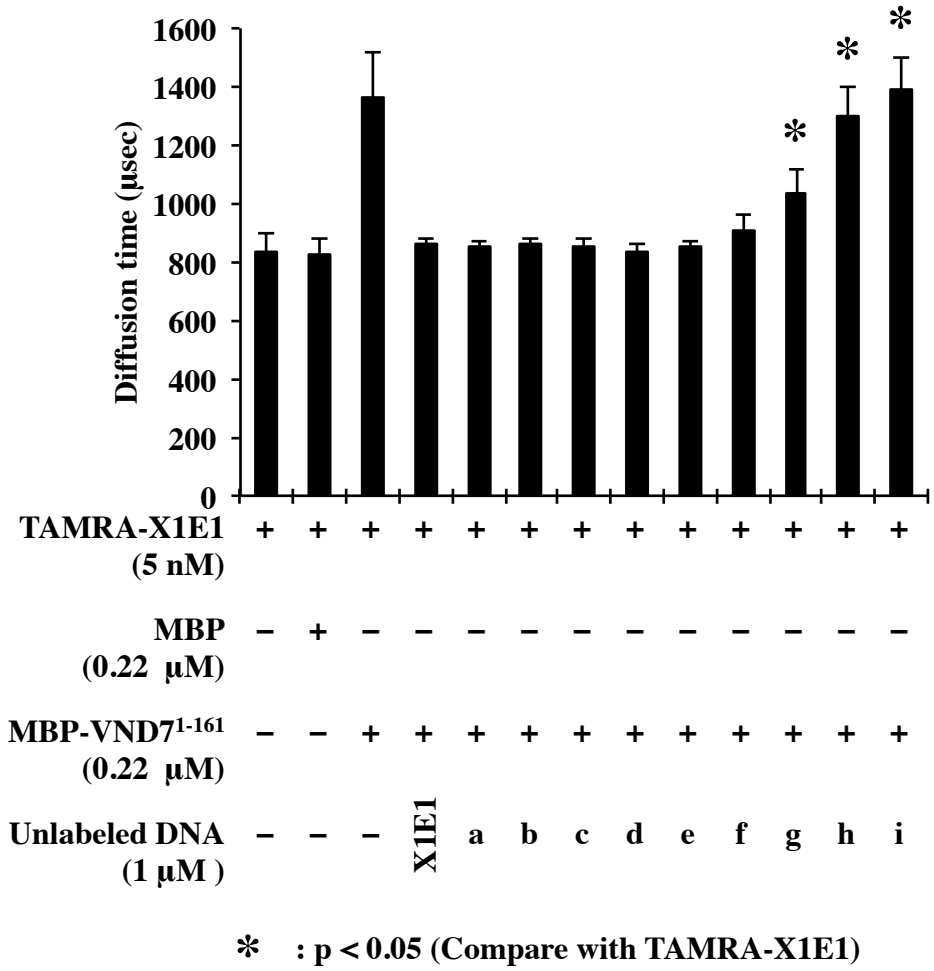

Figure 10.

Result of 3' deletion binging assay by FCS. Y-axis indicates a diffusion time of TAMRA-X1E1, X-axis indicates a competitor fragment name (X1E1, X1E1-a to i) as shown in Figure 8. Error bars are S.D. Asterisks indicate statistically significant differences (Student and Welch's t-test; $p < 0.05$) from the diffusion time of TAMRA-X1E1.

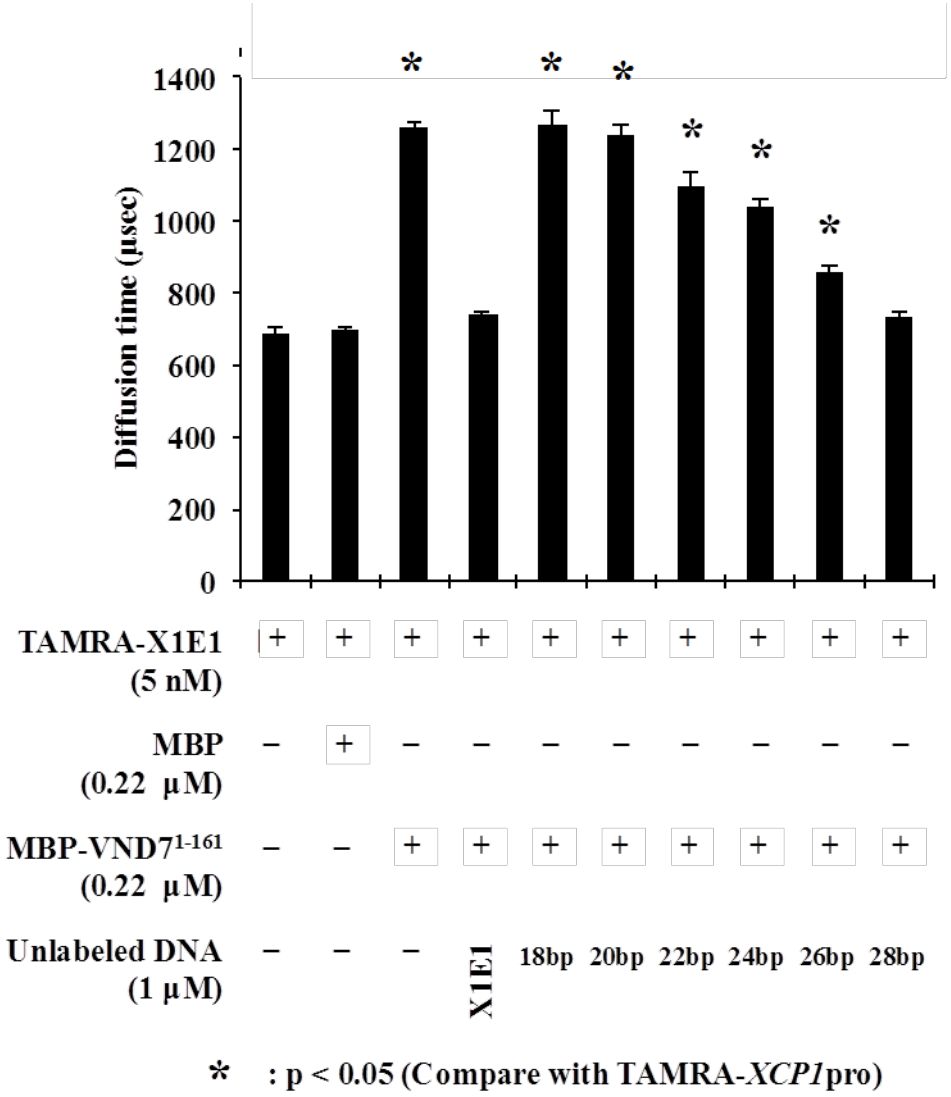

Figure 11.

Result of based binding assay of X1E1-18bp fragment by FCS. Y-axis indicates a diffusion time of TAMRA-X1E1, X-axis indicates a competitor fragment name (X1E1, X1E1-18bp to 28bp) as shown in Figure 8. Error bars are S.D. (n=3). Asterisks indicate statistically significant differences (Student and Welch's t-test; $p < 0.05$) from the diffusion time when used X1E1 as a competitor.

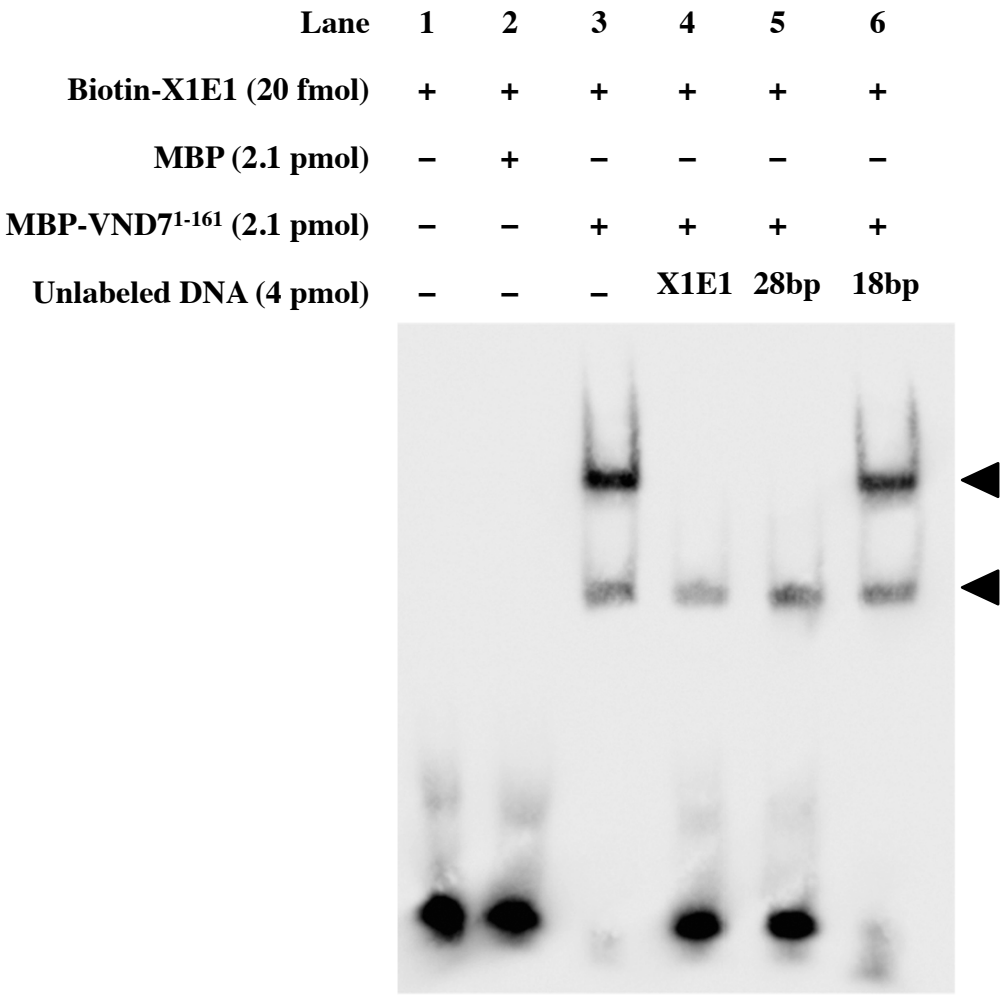

Figure 12.

Result of binding assay between biotin-labeled X1E1 and MBP-VND71-161 protein by EMSA. The concentrations of the competitor DNA fragments (X1E1, X1E1-18bp and X1E1-28bp) were used 200 times higher than Biotin-X1E1 (4 pM). Arrowheads indicate shifted bands position.

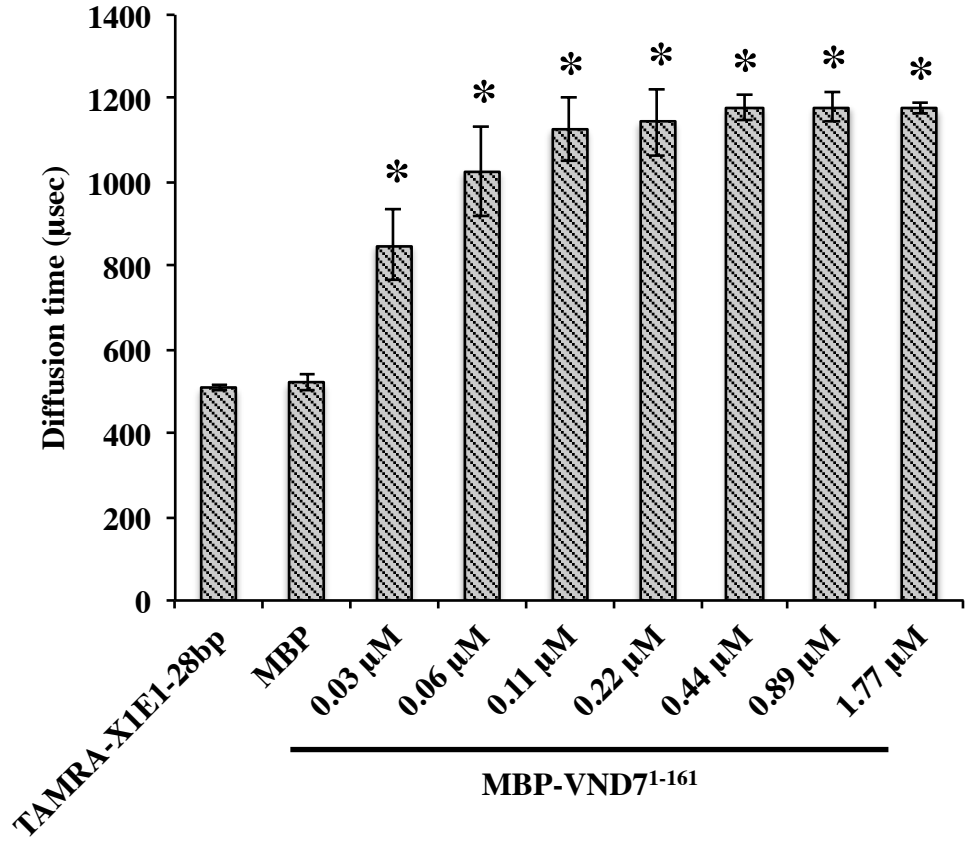

＊ : p < 0.05 (Compared with TAMRA-X1E1-28bp)

Figure 13.

Result of binding assay between TAMRA-labeled X1E1-28bp and MBP-VND71-161 protein by FCS. Y-axis indicate diffusion time of TAMRA-X1E1-28bp. Error bars are S.D. (n=3). Asterisks indicate statistically significant differences (Student and Welch's t-test; $p < 0.05$) from the diffusion time of TAMRA-X1E1-28bp.

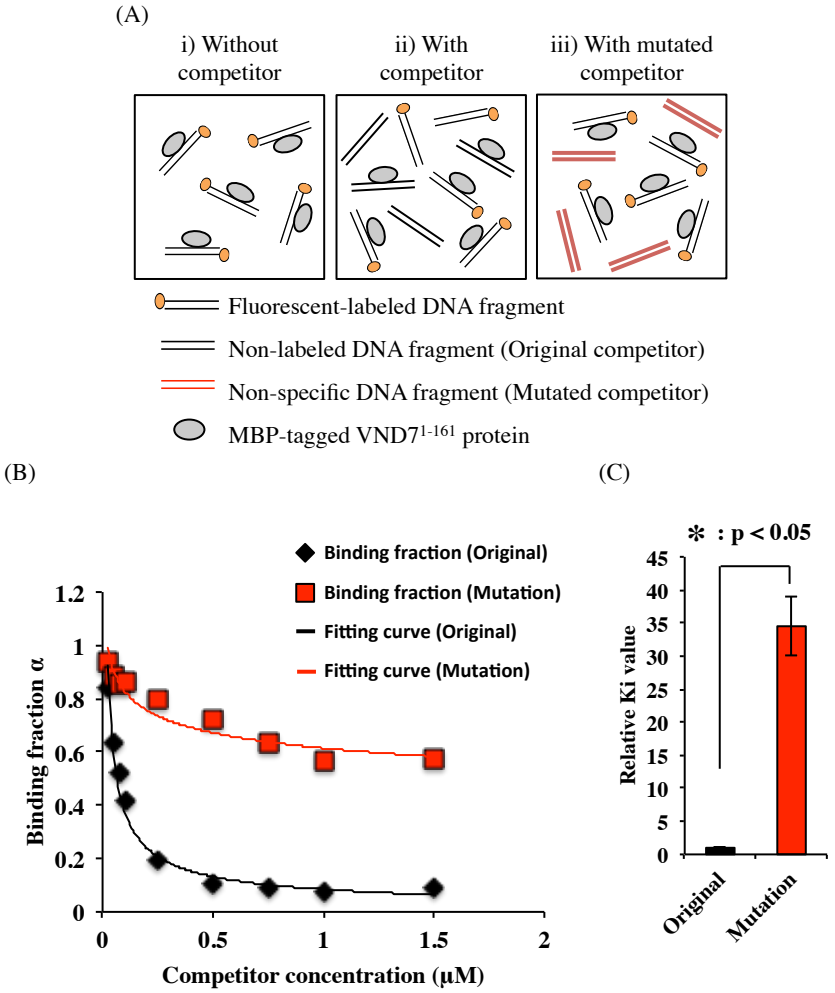

Figure 14.

FCS-based equilibrium binding assay.

(A) Schematic drawing of the competition assay by FCS. (B) The fitting curves which are derived from Cheng and Prusoff equation for the calculation of Ki values (Original; X1E1-28bp, Mutation: X1E1-ls_45: see Table 4). X-axis indicates a concentration of competitor DNA fragments and Y-axis showing binding fraction that is proportion of protein-bound TAMRA-X1E1-28bp fragment. (C) Calculated Ki value calculated from fitting curve of (B). Error bar is S.D. (n=3). Asterisks indicate statistically significant differences (Student and Welch's t-test; $p < 0.05$) from the Ki value of original competitor (X1E1-28bp).

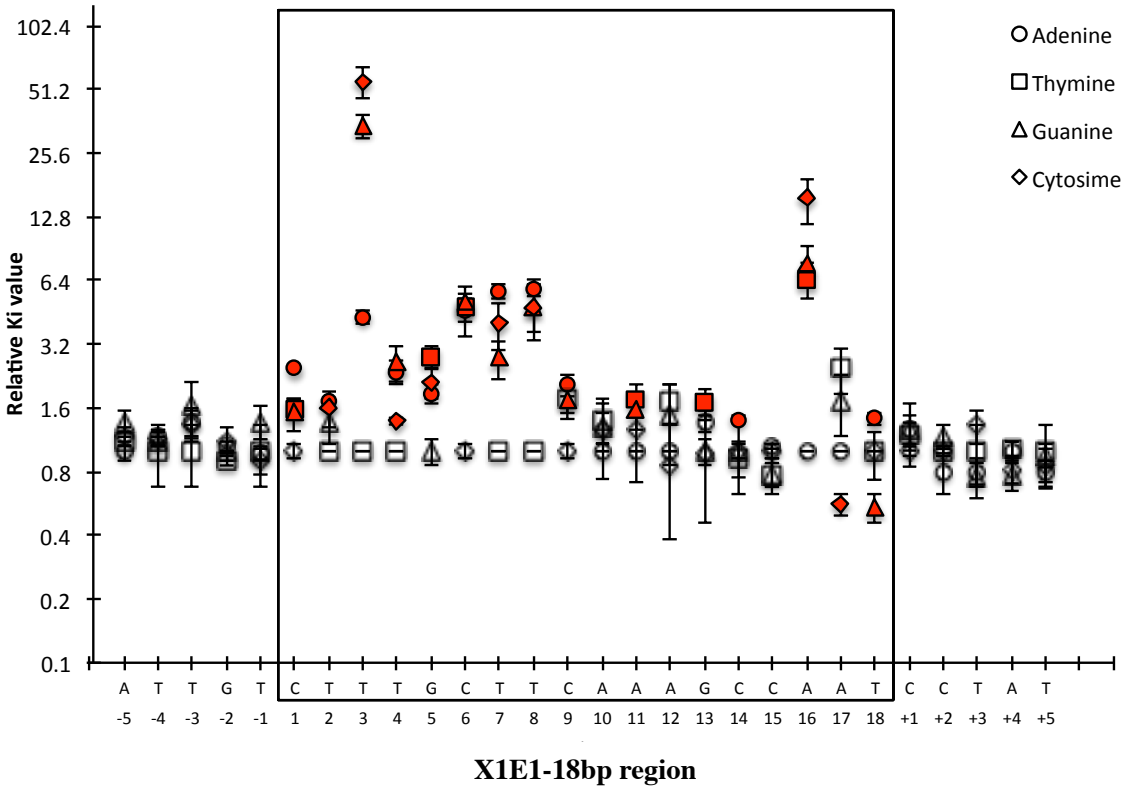

Figure 15.

Result of FCS-based kinetic assay. Y-axis indicates relative Ki value between competitor DNA fragment and MBP-VND7$^{1\text{-}161}$ protein. X-axis indicates a nucleotide sequence of X1E1-28bp, black bar and number represents X1E1-18bp region. Error bars are standard deviation (S.D.) (n=3). Red plots indicate statistically significant differences (Student and Welch's t-test; $p < 0.05$) from the Ki value of X1E1-28bp.

(A)

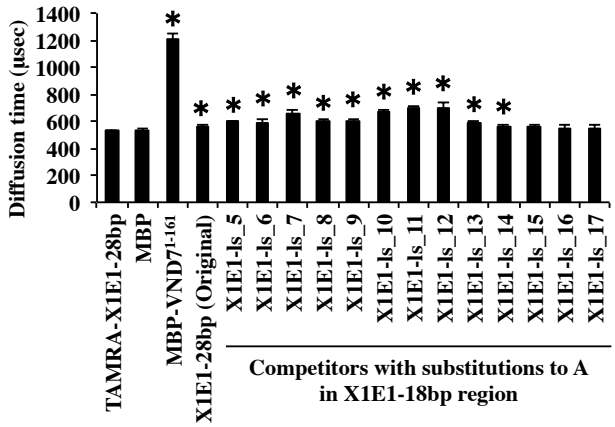
Diffusion time (μsec)
1400
1200
1000
800
600
400
200
0
TAMRA-X1E1-28bp
MBP
MBP-VND7[1-161]
X1E1-28bp (Original)
X1E1-ls_5
X1E1-ls_6
X1E1-ls_7
X1E1-ls_8
X1E1-ls_9
X1E1-ls_10
X1E1-ls_11
X1E1-ls_12
X1E1-ls_13
X1E1-ls_14
X1E1-ls_15
X1E1-ls_16
X1E1-ls_17
Competitors with substitutions to A
in X1E1-18bp region

(B)

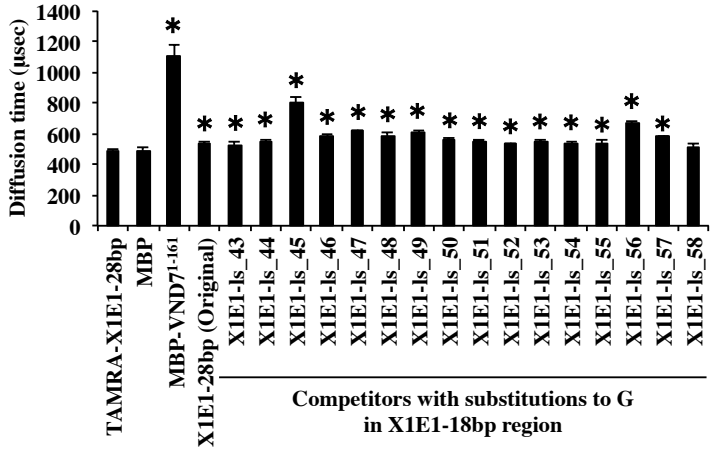
Diffusion time (μsec)
1400
1200
1000
800
600
400
200
0
TAMRA-X1E1-28bp
MBP
MBP-VND7[1-161]
X1E1-28bp (Original)
X1E1-ls_43
X1E1-ls_44
X1E1-ls_45
X1E1-ls_46
X1E1-ls_47
X1E1-ls_48
X1E1-ls_49
X1E1-ls_50
X1E1-ls_51
X1E1-ls_52
X1E1-ls_53
X1E1-ls_54
X1E1-ls_55
X1E1-ls_56
X1E1-ls_57
X1E1-ls_58
Competitors with substitutions to G
in X1E1-18bp region

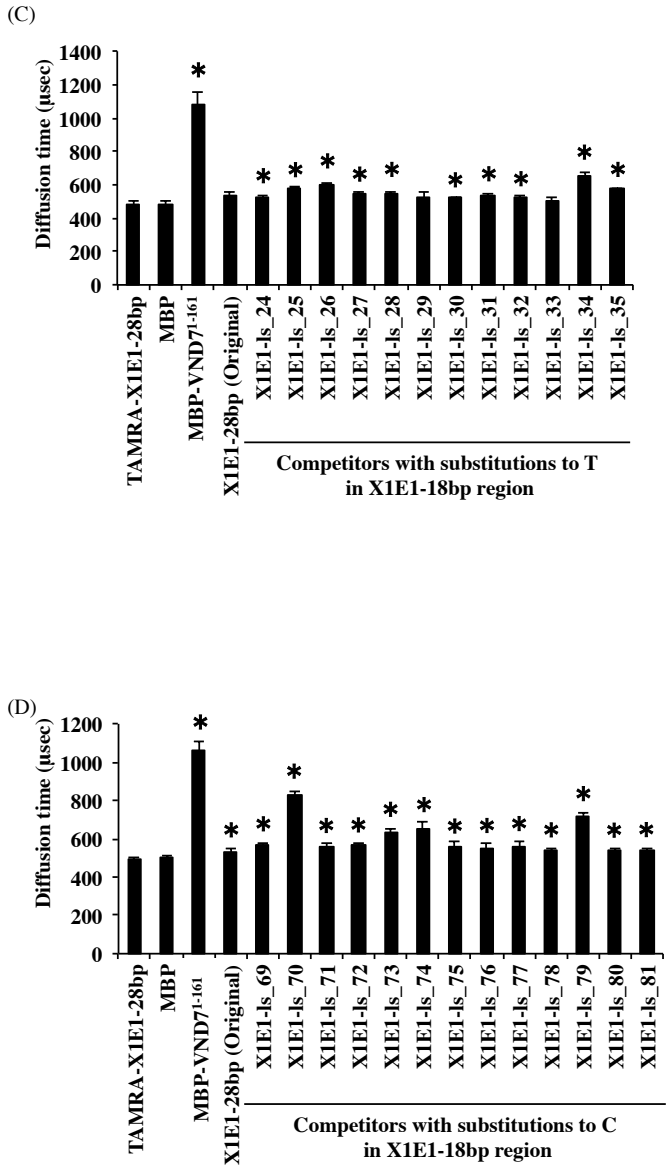

Figure 16.

Competitor binding assay by FCS using linker scan DNA fragments. (A) Result of substitution by adenine, (B) thymine, (C) guanine and (D) cytosine. Y-axis indicates diffusion time of TAMRA-X1E1-28bp. Competitor concentration is 1μM (200 times higher than TAMRA-X1E1-28bp). Error bars are S.D. (n=3). Asterisks indicate statistically significant differences (Student and Welch's t-test; $p < 0.05$) from the fraction of TAMRA-X1E1-28bp.

(A)

	Sequence of double mutated DNA fragment
X1E1-sm_gp.3	ATTGTCTGTGCTTCAAAGCCAATCCTAT
X1E1-dm_gp.1	ATTGTGTGTGCTTCAAAGCCAATCCTAT
X1E1-dm_gp.2	ATTGTCGGTGCTTCAAAGCCAATCCTAT
X1E1-dm_gp.4	ATTGTCTGGGCTTCAAAGCCAATCCTAT
X1E1-dm_gp.6	ATTGTCTGTGGTTCAAAGCCAATCCTAT
X1E1-dm_gp.7	ATTGTCTGTGCGTCAAAGCCAATCCTAT
X1E1-dm_gp.8	ATTGTCTGTGCTGCAAAGCCAATCCTAT
X1E1-dm_gp.9	ATTGTCTGTGCTTGAAAGCCAATCCTAT
X1E1-dm_gp.10	ATTGTCTGTGCTTCGAAGCCAATCCTAT
X1E1-dm_gp.11	ATTGTCTGTGCTTCAGAGCCAATCCTAT
X1E1-dm_gp.12	ATTGTCTGTGCTTCAAGGCCAATCCTAT
X1E1-dm_gp.14	ATTGTCTGTGCTTCAAAGGCAATCCTAT
X1E1-dm_gp 15	ATTGTCTGTGCTTCAAAGCGAATCCTAT
X1E1-dm_gp.16	ATTGTCTGTGCTTCAAAGCCGATCCTAT
X1E1-dm_gp.17	ATTGTCTGTGCTTCAAAGCCAGTCCTAT
X1E1-dm_gp.18	ATTGTCTGTGCTTCAAAGCCAAGCCTAT

(B)

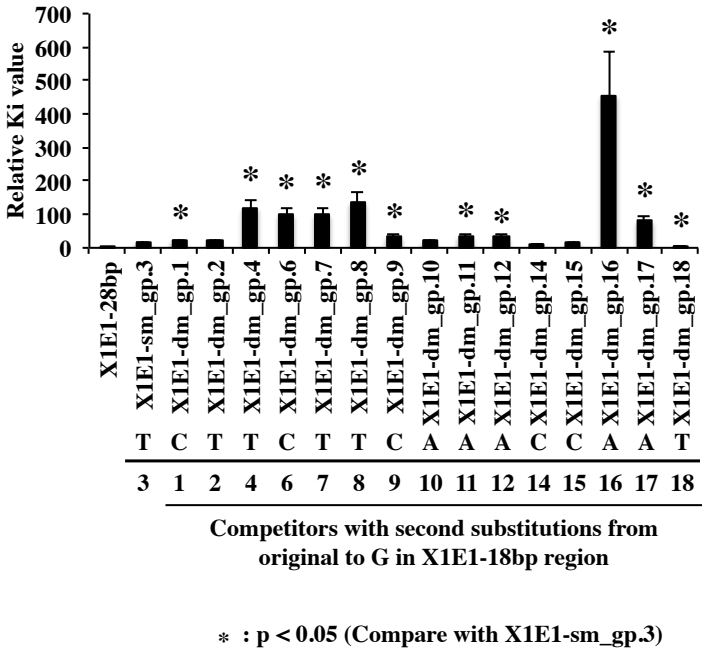

Figure 17.

Schematic diagram of guanine based double mutated X1E1-28bp fragments. Red sequence is indicated X1E1-18bp region. Blue nucleotides are indicated substitution points. (B) Result of kinetic assay using double-mutation DNA fragments by FCS. Y-axis indicates relative Ki value against X1E1-28bp (the Ki value of X1E1-28bp is shown as 1). Error bar indicates S.D. (n=3). Asterisks indicate statistically significant differences (Student and Welch's t-test; $p < 0.05$) from the Ki value of X1E1-sm_gp.3.

SELEX Conserved sequence (bits > 0.8)

C	T	T	T	G	C	T	T	C	A	A	A	G	C	C	A	A	T
1	2	3	4	5	6	7	8	9	10	11	12	13	14	15	16	17	18

***XCP1* X1E1-18bp**

Figure 18.

SELEX-based binding sequence for MBP-VND7$^{1\text{-}161}$. The nucleotide sequence under the logo is conserved sequence that showed bit level more than 0.8 (bits > 0.8). Box and underline indicated the matched sequence between SELEX-based binding sequence and X1E1-18bp region. Selected MBP-VND7$^{1\text{-}161}$ binding sequences are shown in Table 2.

		-1 -2 -3 -4 -5	1 2 3	4 5	6 7 8	9 10	11 12 13	14 15	16 17 18	+1 +2 +3 +4 +5	
XCP1 **X1E1-28bp**		A T T G T	C T T	T G	C T T	C A	A A G	C C	A A T	C C T A T	
XCP1 **X1E1 core structure (This analysis)**			C T T	N N	C T T	N N	A A G	N N	A A T		
SELEX (This analysis)	**Motif 1**		C G/T T	N N	N N N	T N	A C/A G	N N	N N N		
	Motif 2				C G/T T	N N	N N N	T N	A C/A G	N N N N N	
TERE (Pyo et al., 2007)	**-122** in ***XCP1pro***				C T T/C	N A A	A/C G	C N	A/T		**-112** in ***XCP1pro***
SNBE (Zhong et al., 2010)	**-130** in ***XCP1***	T/A N N	C/T T/C/G T	N N	N N N	N N	A A/C G	N	A/C/T A/T		**-112** in ***XCP1pro***
Ideal core structure			C T T		C T T		A A G		A A G		
		-1 -2 -3 -4 -5	1 2 3	4 5	6 7 8	9 10	11 12 13	14 15	16 17 18	+1 +2 +3 +4 +5	

Figure 19.

Comparison of the VND7 binding sequences. The sequences derived from FCS (*XCP1* X1E1 core structure), SELEX analysis and reported motifs, TERE and SNBE, are compared with X1E1-28bp sequence. Red fonts indicate the matched nucleotide sequence with X1E1-28bp.

CesA4 pro	-358	AGAAATACATAATAACTTGAAAGCTACTCTAAGTTATA	-320
PG pro	-142	ATTTTATTGGCTTGGCTTTAAAGTAGATGAAGACAAGC	-179
XCP2 pro	-122	ATTCAGACTACTTTACTCTAAAGCAAAAGAGCGACCT	-85
MYB46 (1) pro	-932	ACAATAATTAGATTTCTTCAAGTATACGTGTTGGTGCG	-895
MYB46 (2) pro	-604	TAATGTATACCTTGTGAATGAAGAAACTAATAGAAATG	-567
MYB46 (3) pro	-254	TATAATATAGTGTTGCTTTGTTTTAAAACATAAAAGAA	-291
MYB83 pro	-615	TTGATTGTGTCGTAAAATGGAAGTTACTTCAAAATAAG	-578
ATMC9 pro	-281	AGGTTTAGTTTCTTGCTTGAAAGCATTAATAAGTCAAG	-244

Figure 20.

Sequences of promoters from putative direct target genes of VND7. Promoter sequences of several putative VND7 direct target genes, *XCP2*, *CesA4*, *MYB46*, *MYB83*, *PG* (At1G70500), and *ATMC9* (At5G04200) are shown. First pairs of palindromic structure found in the sequences are indicated by underline and red-colour, and second pairs by box and blue-colour. “core-nucleotides” are shown by bold letters.

	-5	-4	-3	-2	-1	1	2	3	4	5	6	7	8	9	10	11	12	13	14	15	16	17	18	+1	+2	+3	+4	+5
X1E1-28bp (Original)	A	T	T	G	T	C	T	T	T	G	C	T	T	C	A	A	A	G	C	C	A	A	T	C	C	T	A	T
X1E1-sm_gp.3	A	T	T	G	T	C	T	G	T	G	C	T	T	C	A	A	A	G	C	C	A	A	T	C	C	T	A	T
X1E1-core-dm.1	A	T	T	G	T	C	T	G	T	G	C	T	G	C	A	A	A	G	C	C	A	A	T	C	C	T	A	T
X1E1-core-dm.2	A	T	T	G	T	C	T	G	T	G	C	T	T	C	A	G	A	G	C	C	A	A	T	C	C	T	A	T
X1E1-core-dm.3	A	T	T	G	T	C	T	G	T	G	C	T	T	C	A	A	A	G	C	C	G	A	T	C	C	T	A	T
X1E1-core-dm.4	A	T	T	G	T	C	T	T	T	G	C	T	G	C	A	A	A	G	C	C	G	A	T	C	C	T	A	T
X1E1-core-dm.5	A	T	T	G	T	C	T	T	T	G	C	T	T	C	A	G	A	G	C	C	G	A	T	C	C	T	A	T
X1E1-core-dm.6	A	T	T	G	T	C	T	T	T	G	C	T	G	C	A	G	A	G	C	C	A	A	T	C	C	T	A	T
X1E1 four-core-mu	A	T	T	G	T	C	T	G	T	G	C	T	G	C	A	G	A	G	C	C	G	A	T	C	C	T	A	T
								+					+			+					+							

+ : Core-nucleotide positions

Figure 21.

Schematic diagram of “core-nucleotides” substituted competitor DNA fragments. Red and blue nucleotides indicate X1E1-18bp region and substituted position by guanine, respectively. Shades and pluses indicate “*XCP1* X1E1 core structure” and “core-nucleotides” in X1E1-18bp region, respectively.

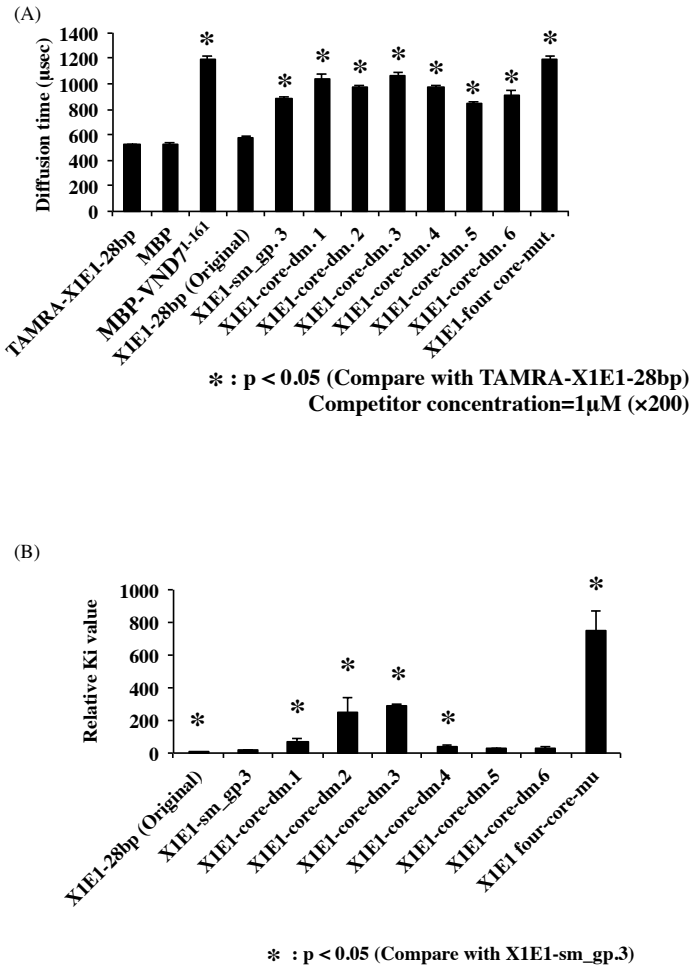

Figure 22.

(A) Competitor binding assay by FCS using core-mutated DNA competitor. Y-axis indicates diffusion time of TAMRA -X1E1-28bp. Competitor concentration is 1μM (200 times higher than TAMRA-X1E1-28bp). Error bars are S.D. (n=3). Asterisks indicates statistically significant differences (Student and Welch's t-test; $p < 0.05$) from the fraction of MBP-VND71-161. (B) Result of binding assay using "core-nucleotides" mutated competitors by FCS. Y-axis indicates a relative Ki value against X1E1-28bp (the Ki value of X1E1-28bp is shown as 1). Error bars are S.D. (n=3). Asterisks indicate statistically significant differences (Student and Welch's t-test; $p < 0.05$) from the Ki value when used X1E1-sm_gp.3 as a competitor.

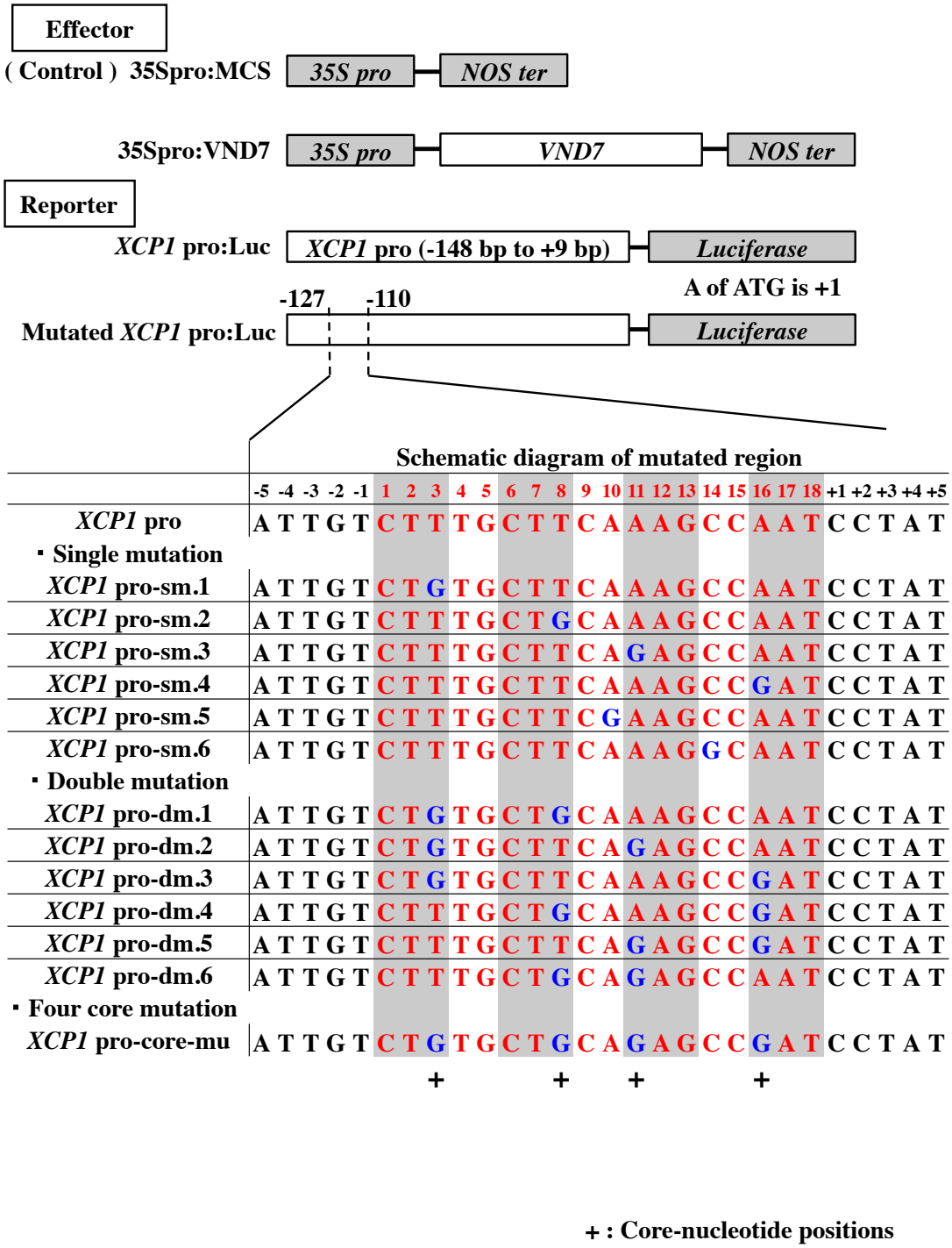

Figure 23.

Schematic diagram of effector and reporter constructs for promoter transient assay of *XCP1* promoter. Red and blue nucleotides indicate X1E1-18bp region and substitution point by guanine, respectively. Shades and pluses indicate "*XCP1* X1E1 core structure" and "core-nucleotides" in X1E1-18bp region, respectively.

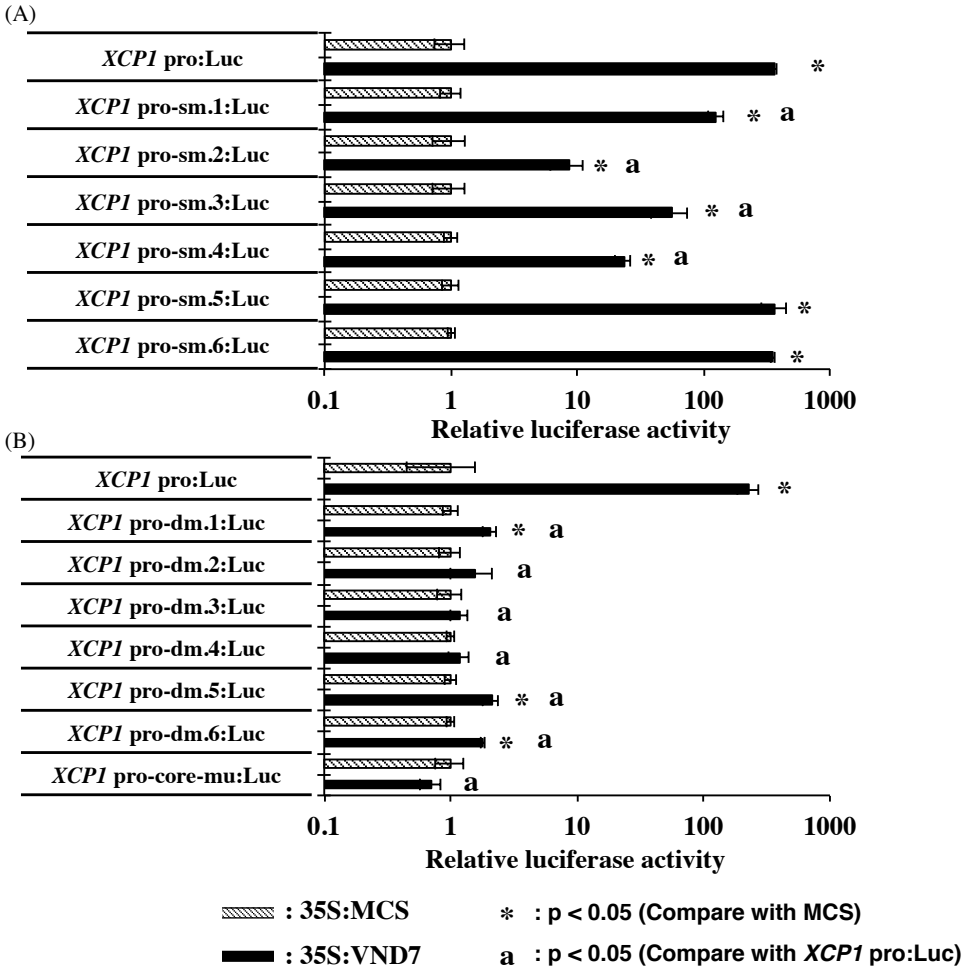

Figure 24.

Result of transient assays. The reporter gene activity was normalized to the activity of *Renilla* luciferase. X-axis indicates relative luciferase activity against the 35S:MCS (control effector; the activity by 35S:MCS is shown as 1). Diagonals and black bars indicate the luciferase activities when use 35S:MCS and 35S:VND7 as an effector, respectively. Error bars are S.D. (n=3). Asterisks indicate statistically significant differences (Student and Welch's t-test; $p < 0.05$) from the values for the control effector (35S:MCS). "a" indicates statistically significant differences (Student and Welch's t-test; $p < 0.05$) from the luciferase activity of *XCP1* pro:Luc (original sequence).

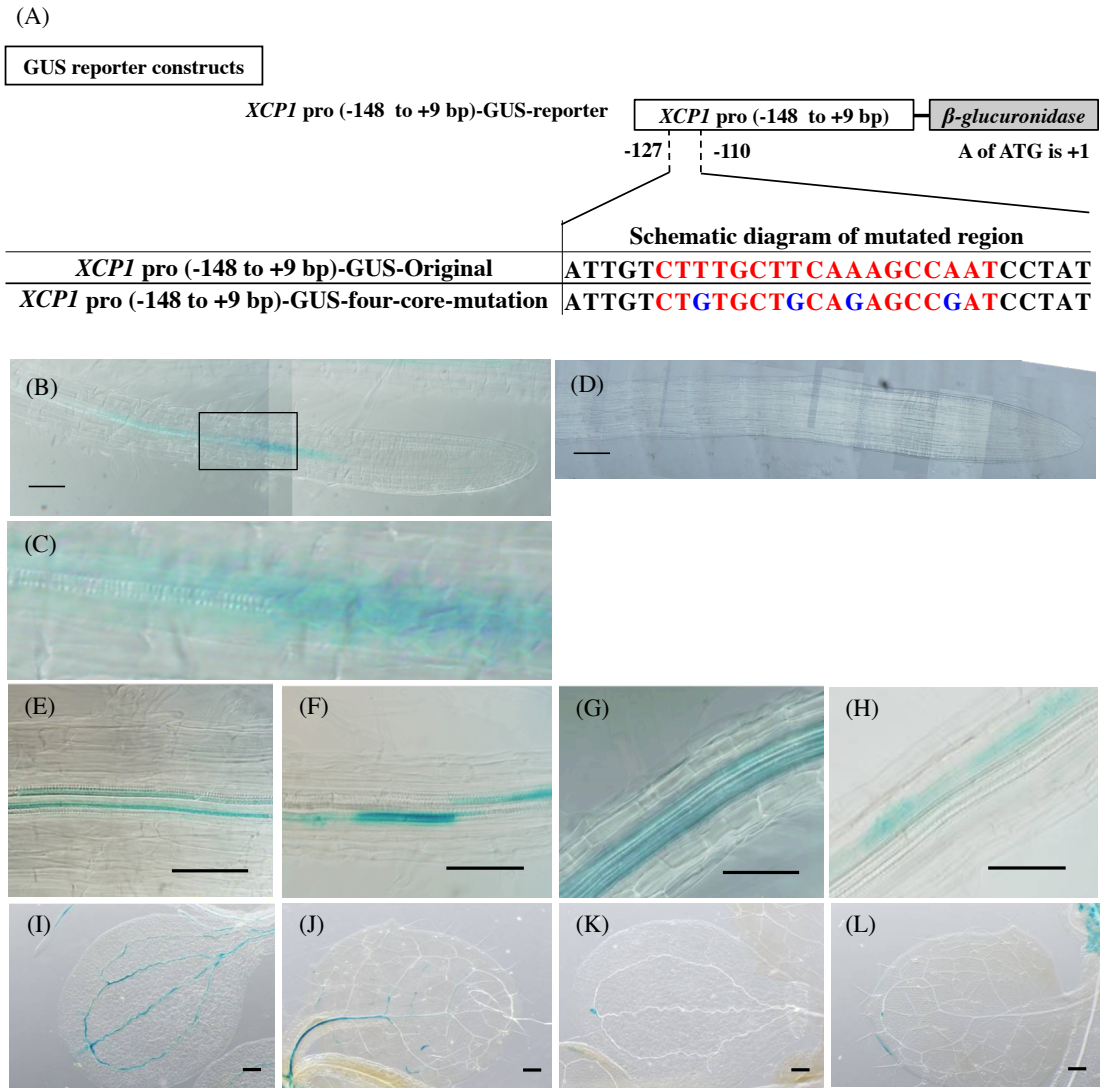

Figure 25.

(A) Schematic diagram of GUS reporter constructs. In the *XCP1*pro (-148 to +9 bp)-GUS-four-core mutation reporter, the four core-nucleotides shown in blue were mutated into G. (B, C, E, F, I, and J) The GUS activities of *XCP1*pro (-148 to +9 bp)-GUS-original reporter. The GUS signals in meristematic zone (B, C), and elongation/differentiation zone (E, F) of roots, in cotyledon (I), and in true leaf (J) were shown. (C) is a magnified view of black box region in (B). (D, G, H, K, and L) The GUS activities of *XCP1*pro (-148 to +9 bp)-GUS-four-core-mutation reporter. The GUS signals in meristematic zone (D), and elongation/differentiation zone (G, H) of roots, in cotyledon (K), and in true leaf (L) were shown. Bars = 100 μm in (B), (D), (I) to (L), and 200 μm in (E) to (H).

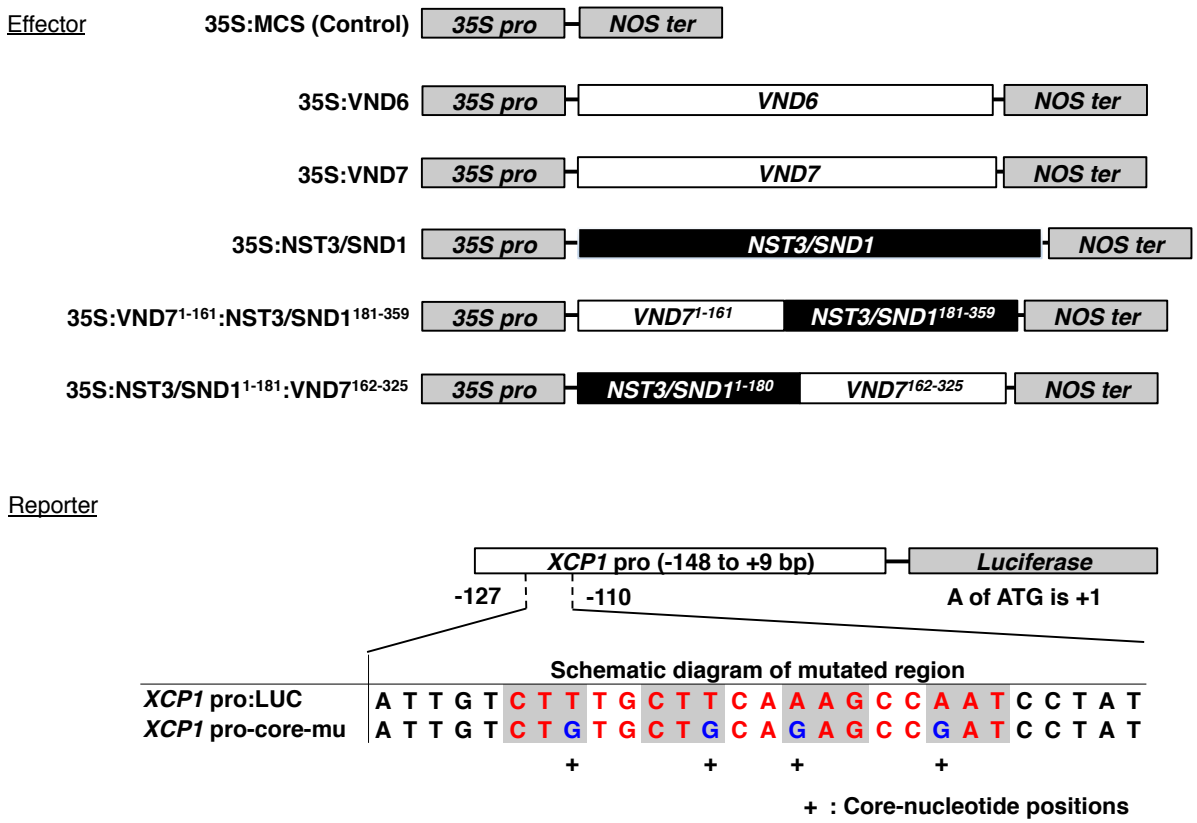

Figure 26.

Schematic diagram of effector and reporter constructs for promoter transient assay of *XCP1* promoter. Red and blue nucleotides indicate X1E1-18bp region and substitution point by guanine, respectively. Shades and pluses indicate "*XCP1* X1E1 core structure" and "core-nucleotides" in X1E1-18bp region, respectively.

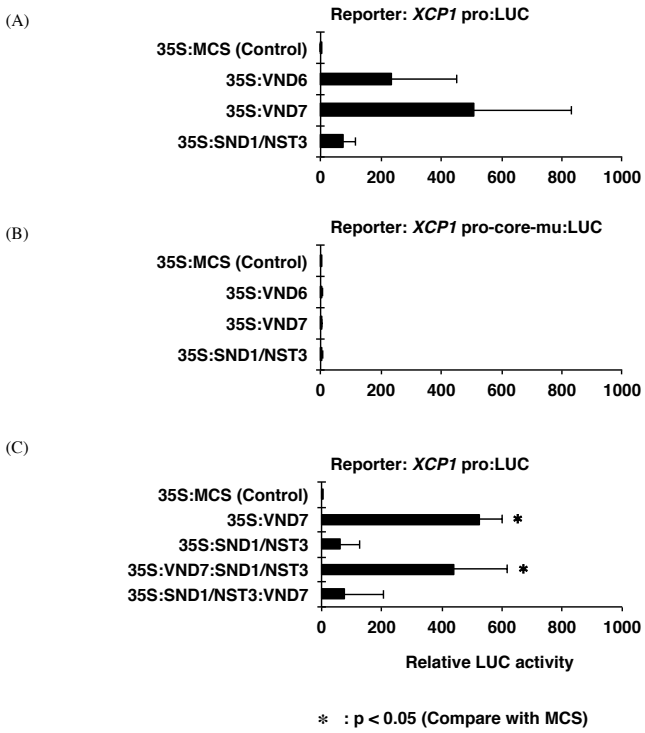

Figure 27.

(A) Result of transient assays of *XCP1* promoter (*XCP1* pro:LUC). The reporter gene activity was normalized to the activity of *Renilla* luciferase. X-axis indicates relative luciferase activity against the 35S:MCS (control effector; the activity by 35S:MCS is shown as 1). Error bars are S.D. (n=3). (B) Result of transient assays of mutated *XCP1* promoter (*XCP1* pro-core-mu:LUC). The reporter gene activity was normalized to the activity of *Renilla* luciferase. X-axis indicates relative luciferase activity against the 35S:MCS (control effector; the activity by 35S:MCS is shown as 1). Error bars are S.D. (n=3). (C) Result of transient assays of *XCP1* promoter (*XCP1* pro:LUC) using chimeric effectors. The reporter gene activity was normalized to the activity of *Renilla* luciferase. X-axis indicates relative luciferase activity against the 35S:MCS (control effector; the activity by 35S:MCS is shown as 1). Error bars are S.D. (n=3). Asterisks indicate statistically significant differences (Student and Welch's t-test; $p < 0.05$) from the values for the control effector (35S:MCS).

(A)

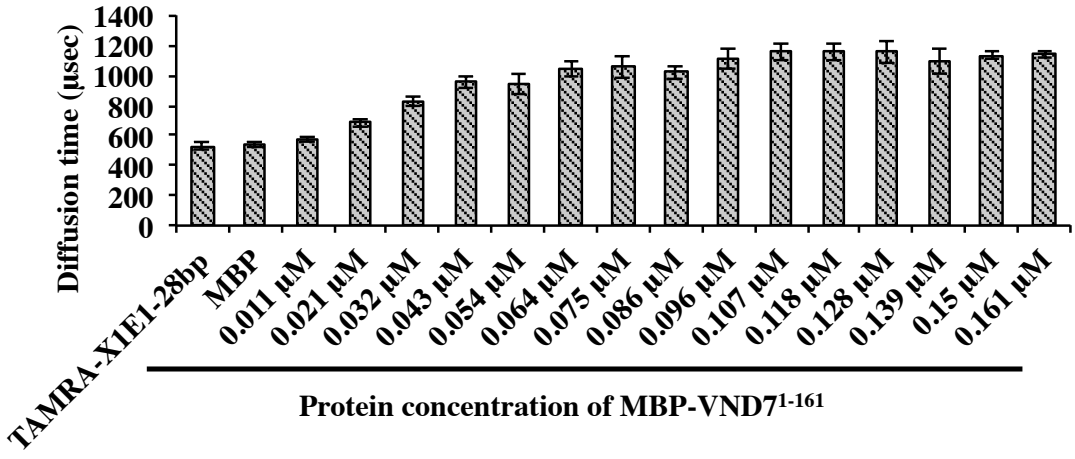

(B)

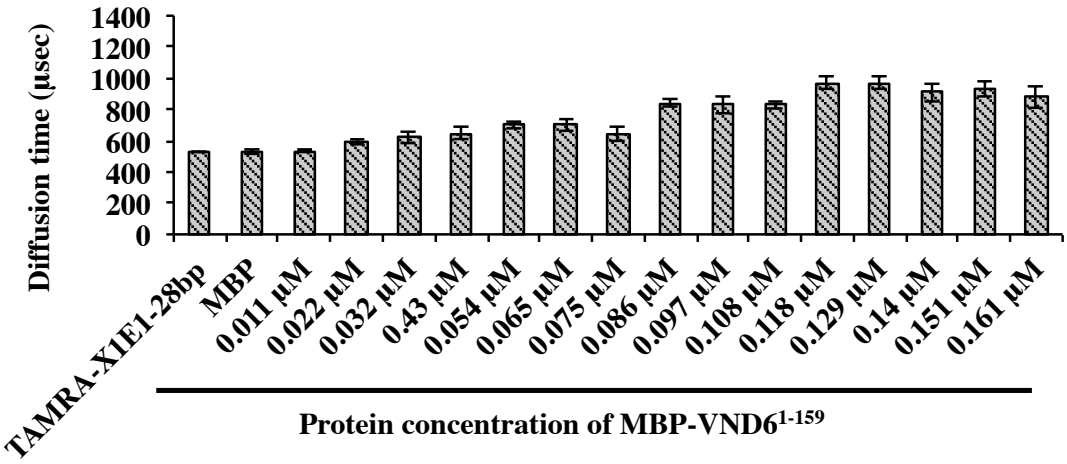

Figure 28.

(A) Result of FCS-based assay between TAMRA-labeled X1E1-28bp and MBP-VND7$^{1-161}$ and protein. Y-axis indicated diffusion time of TAMRA-X1E1-28bp. Error bars are S.D. (B) Result of FCS-based assay between TAMRA-labeled X1E1-28bp and MBP-VND6$^{1-159}$ protein. Y-axis indicated diffusion time of TAMRA-X1E1-28bp. Error bars are S.D.

(C)

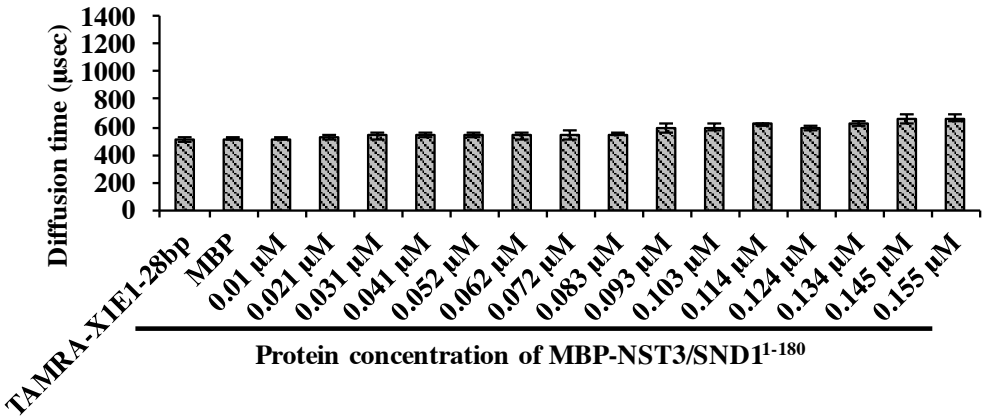

(D)

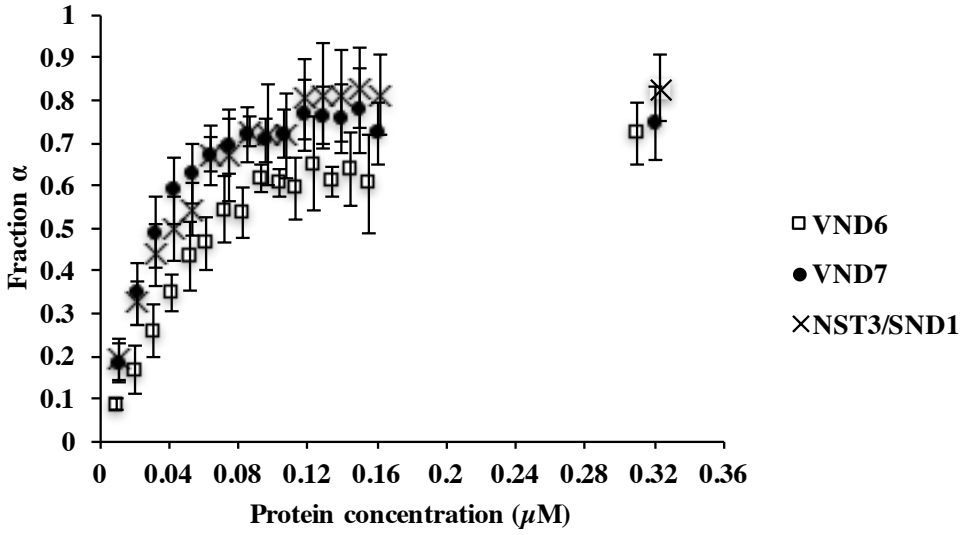

Binding affinity Kd value of VND6, VND7 and NST3 interactions with X1E1-28bp

Transcription factor	Binding affinity (± standard deviation)
	nM
MBP-VND6[1-159]	Kd = 40.0 ± 13.5
MBP-VND7[1-161]	Kd = 37.4 ± 12.3
MBP-NST3/SND1[1-180]	Kd = 78.6 ± 16.3

Figure 28.

(C) Result of FCS-based assay between TAMRA-labeled X1E1-28bp and MBP-VND7$^{1-161}$ and protein. Y-axis indicated diffusion time of TAMRA-X1E1-28bp. Error bars are S.D. (D) Result of FCS-based binding assay between TAMRA-labeled X1E1-28bp and MBP-VND6$^{1-159}$, VND7$^{1-161}$ and NST3/SND1$^{1-180}$ proteins.

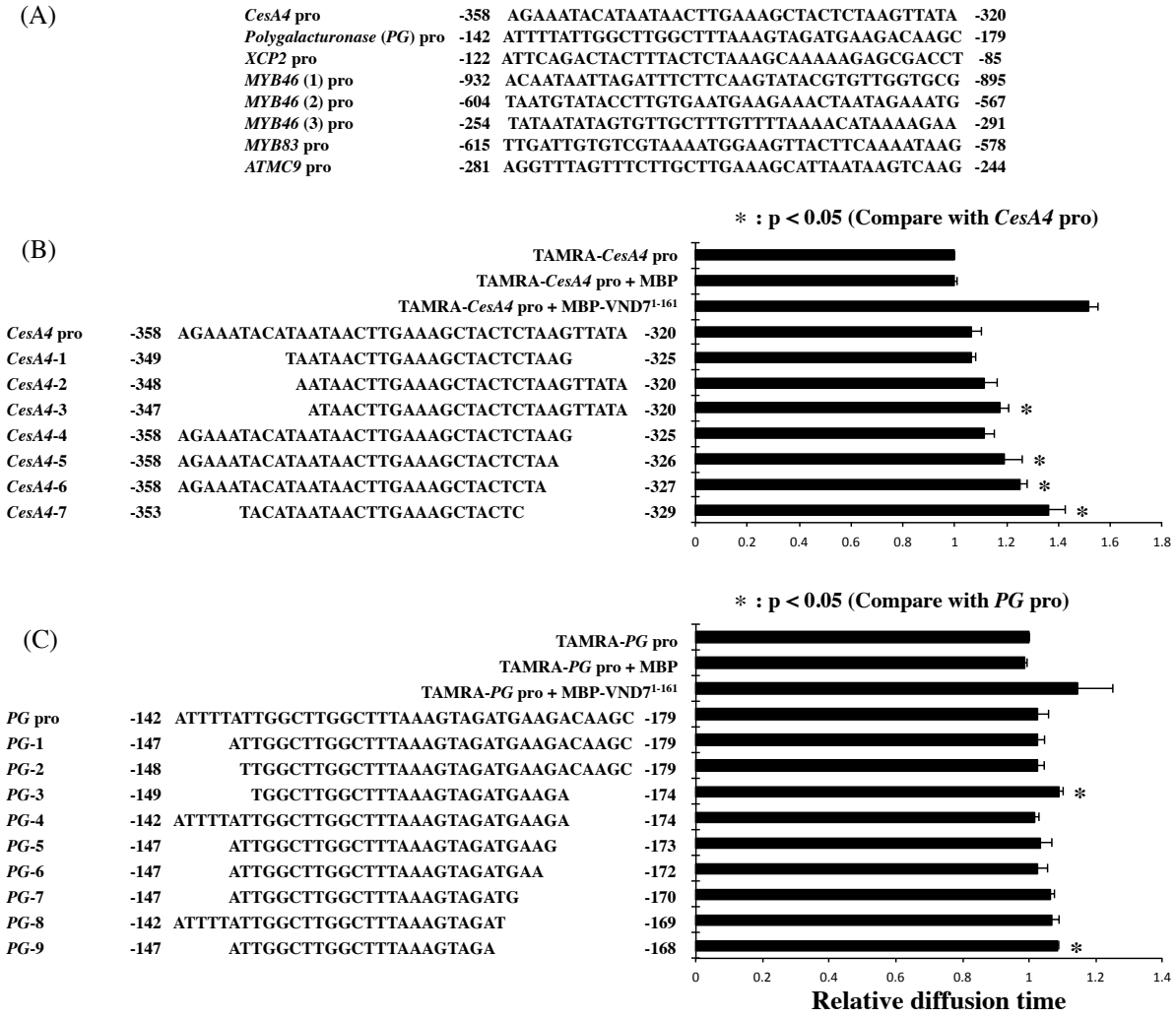

Figure 29.

FCS deletion analysis using TAMRA-labeled promoter fragments of VND7 direct target gene promoters and MBP-VND7$^{1-16}$. (A) Schematic diagram of characterized VND7 binding region by previous study using promoter transient assay. (B) Result of FCS deletion analysis of *CesA4* pro, (C) *PG* pro. Error bars are S.D. (n=3). Asterisks indicate statistically significant differences (Student and Welch's t-test; $p < 0.05$) from the values for diffusion time of TAMRA-labeled DNA.

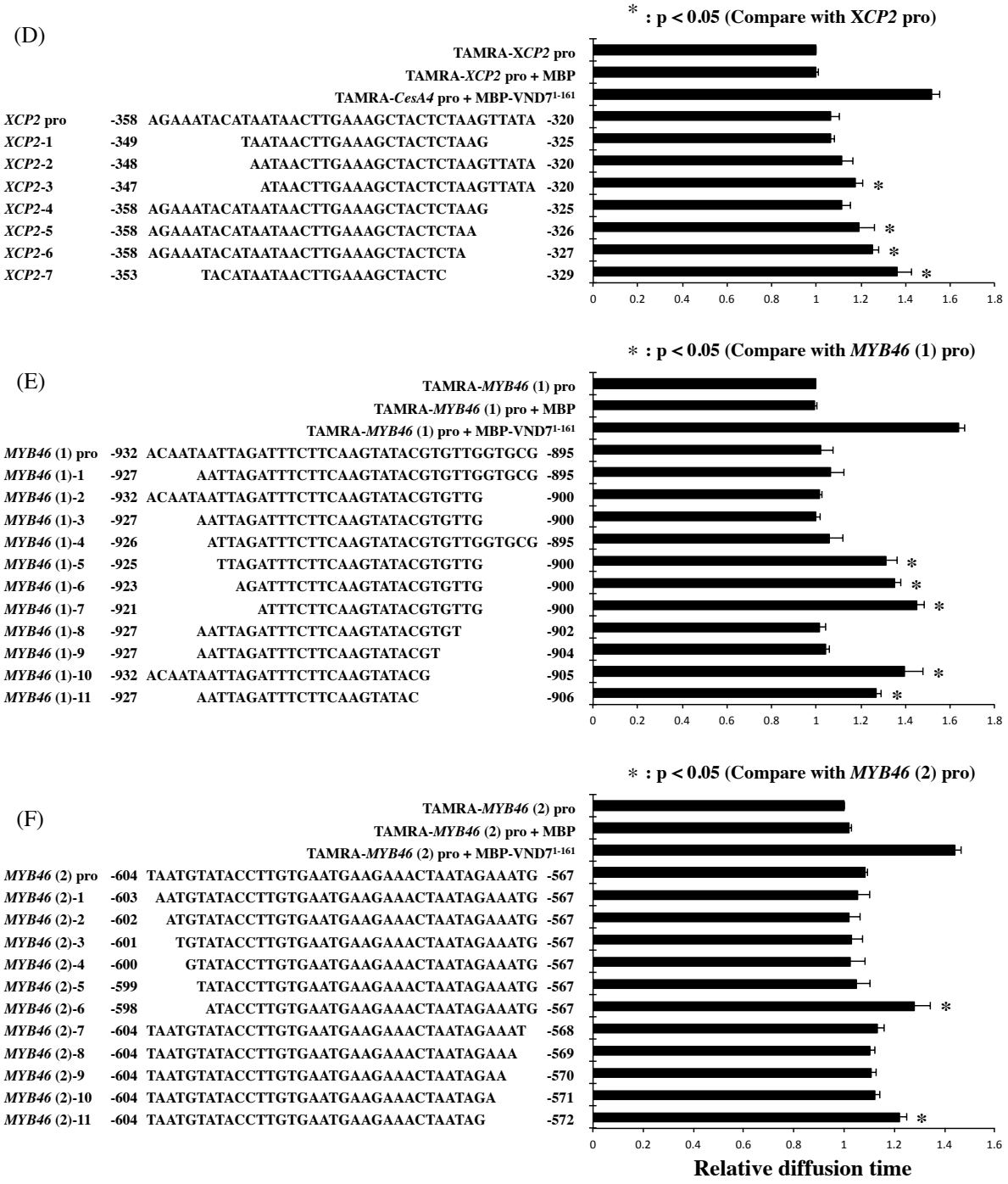

Figure 29.

(D) Result of FCS deletion analysis of *XCP2* pro, (E) *MYB46* (1) pro and (F) *MYB46* (2) pro. Error bars are S.D. (n=3). Asterisks indicate statistically significant differences (Student and Welch's t-test; $p < 0.05$) from the values for diffusion time of TAMRA-labeled DNA.

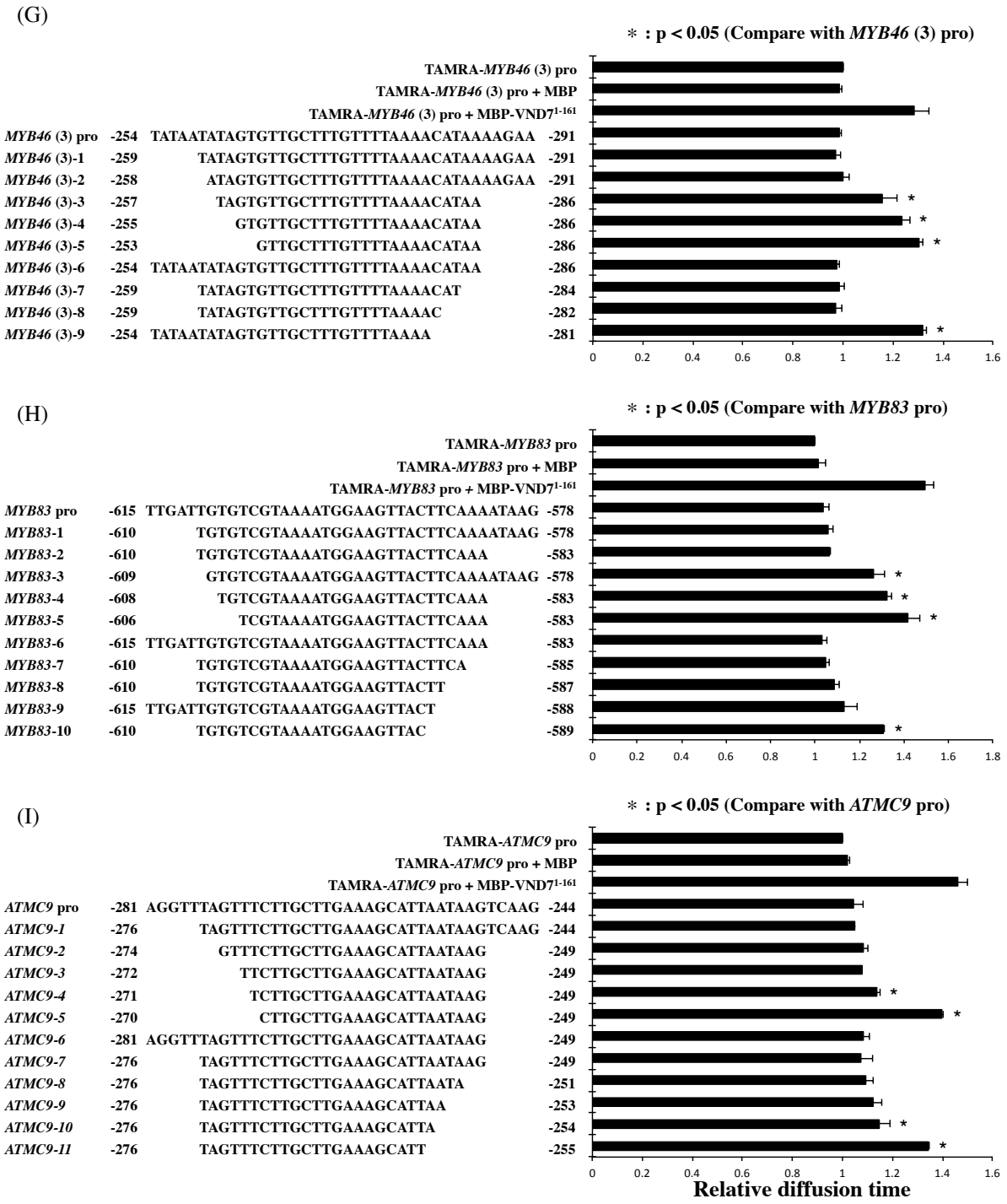

Figure 29.

(G) Result of FCS deletion analysis of *MYB46* (3) pro, (E) *MYB83* pro and (F) *ATMC9* pro. Error bars are S.D. (n=3). Asterisks indicate statistically significant differences (Student and Welch's t-test; $p < 0.05$) from the values for diffusion time of TAMRA-labeled DNA.

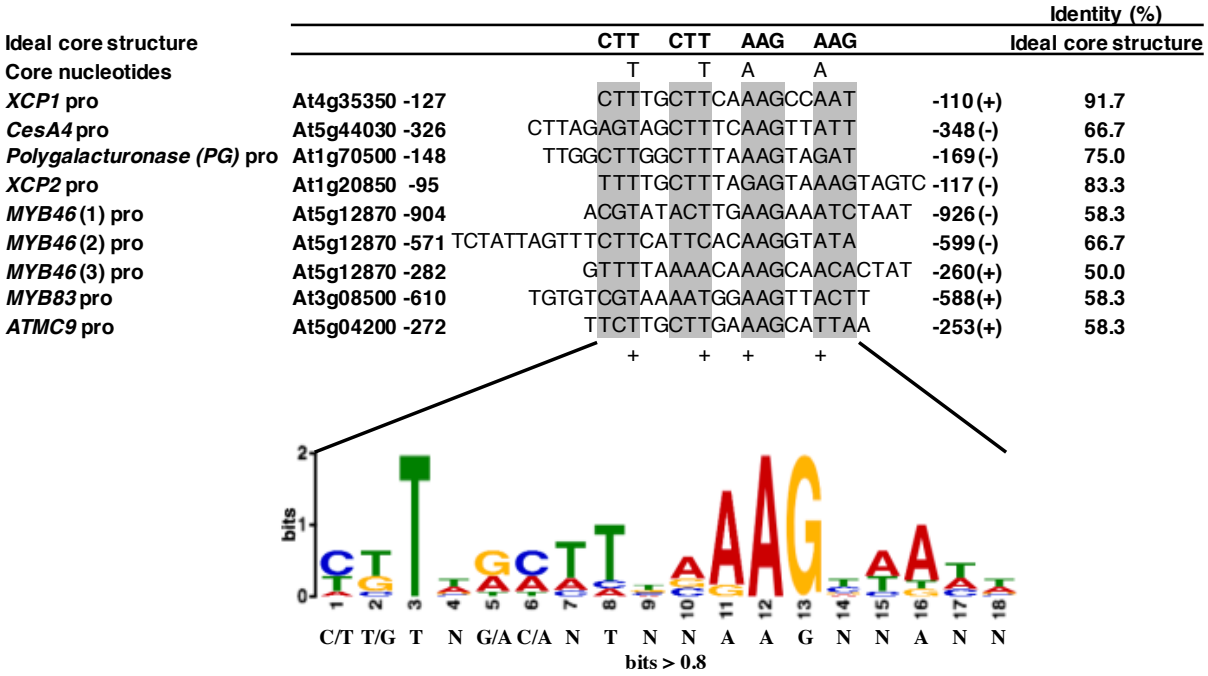

Figure 30.

Comparison of the MBP-VND7$^{1-161}$ binding sequence of several direct target gene promoters. Shades and pluses indicate the matched region with “ideal core structure” in X1E1-18bp. (+) and (-) are indicate sense and antisense strand, respectively. The conserved sequence is analysed by MEME (http://meme-suite.org). The nucleotide sequence under the logo is conserved sequence that showed bit level more than 0.8 (bits > 0.8).

CesA4 pro	-358	AGAAATACATAATAACTTGAAAGCTACTCTAAGTTATA	-320
Polygalacturonase (PG) pro	-142	ATTTTATTGGCTTGGCTTTAAAGTAGATGAAGACAAGC	-179
XCP2 pro	-122	ATTCAGACTACTTTACTCTAAAGCAAAAAGAGCGACCT	-85
MYB46 (1) pro	-932	ACAATAATTAGATTTCTTCAAGTATACGTGTTGGTGCG	-895
MYB46 (2) pro	-604	TAATGTATACCTTGTGAATGAAGAAACTAATAGAAATG	-567
MYB46 (3) pro	-254	TATAATATAGTGTTGCTTTGTTTTAAAACATAAAAGAA	-291
MYB83 pro	-615	TTGATTGTGTCGTAAAATGGAAGTTACTTCAAAATAAG	-578
ATMC9 pro	-281	AGGTTTAGTTTCTTGCTTGAAAGCATTAATAAGTCAAG	-244

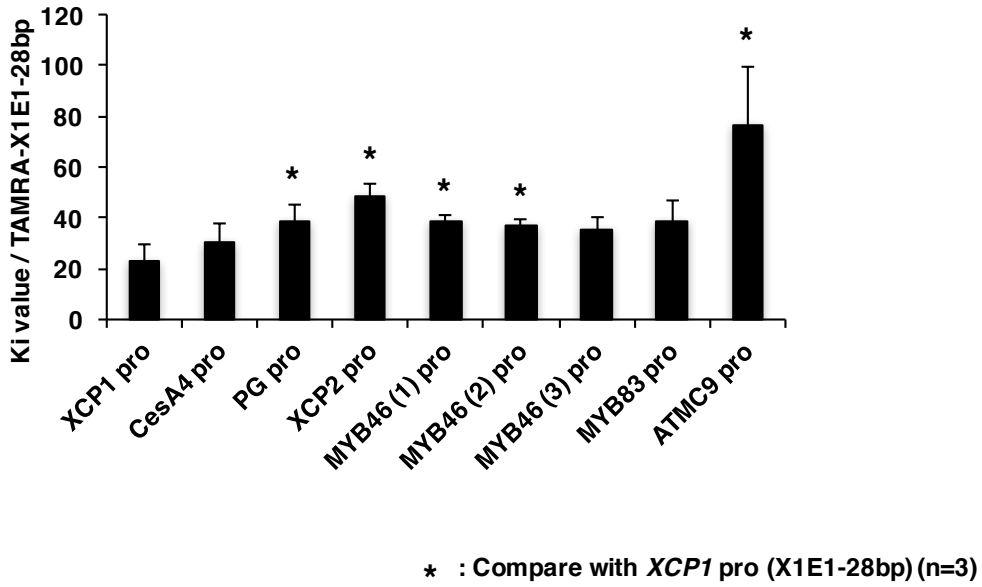

Figure 31.

Competitor binding assay by FCS using VND7 direct target gene promoter. Error bars are S.D. (n=3). Asterisks indicates statistically significant differences (Student and Welch's t-test; $p < 0.05$) compare with *XCP1* pro (X1E1-28bp).

Gene					Identity (%)	
Ideal core structure		C T T A A G A A G			X1E1-18bp	Ideal core
X1E1-18bp		C T T T G C T T C A A A G C C A A T				91.7
Pp1s49_32V6	-883	C T T T T T A T C A A A G A A G A T	-866	(+)	66.7	66.7
	-606	T T T C A A T A A A A A G C C A A A	-589	(+)	61.1	66.7
	-277	C T T T G C G T C C C A G A A C G T	-294	(-)	61.1	58.3
	-658	T T T T G C T C T G A A T C G T T C	-641	(+)	50.0	50.0
Pp1s315_40V6	-597	T T T A A A T G G A A A G C C G A G	-614	(-)	55.6	66.7
	-19	G C C T G C T T C G A T C C C T T C	-36	(-)	50.0	33.3
	-899	G C T T G C T A C A G A A T G A G C	-882	(+)	44.4	41.7
Pp1s52_60V6	-342	A T A T G C T T C T A C G C A C T T	-359	(-)	61.1	50.0
	-551	C T T T T C G T C C A C T T T C A A G	-534	(+)	61.1	75.0
	-222	T C A C A G T T A A A A G C C A A C	-205	(+)	55.6	58.3
Pp1s199_134V6	-397	C T T T G C T T C C T G A G C T C G	-414	(-)	55.6	58.3
	-133	C G A C C T T T C A T A G A A A A G	-150	(-)	50.0	66.7

Figure 32.

Comparison of the X1E1-18bp with *Physcomitrella XCP1* homologues gene promoters. Red fonts indicate the matched nucleotide sequence with X1E1-18bp. (+) and (-) are indicate sense and antisense strand, respectively. The sequence similarity to X1E1-18bp was displayed in left side of the chart.

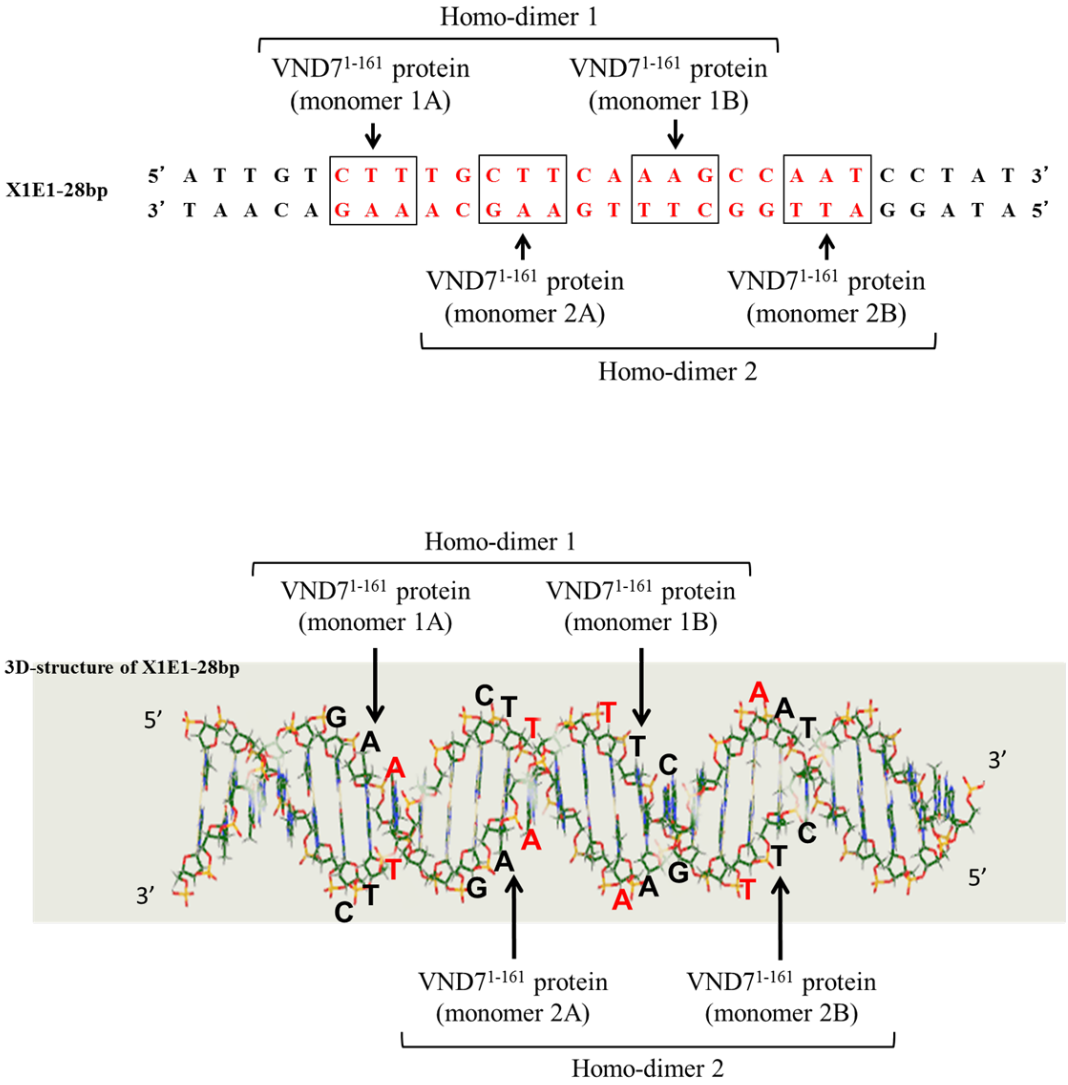

Figure 33.

Putative binding model between NAC domain of VND7 (VND7$^{1\text{-}161}$) and "*XCP1* X1E1 core structure" in X1E1-28bp. Two homo-dimerized VND7$^{1\text{-}161}$ proteins (monomer 1A and 1B, 2A and 2B) may bind to the two palindromic-like sequences that have a CTT (reverse complement: AAG)-like sequence as a binding site (CTTNNNNNNNAAG). Red sequence in X1E1-28bp: X1E1-18bp region, Box: "*XCP1* X1E1 core structure". The red nucleotides in 3D-structure of X1E1-28bp: core-nucleotides. The 3D-structure of DNA was made by using Abalone (http://www.biomolecular-modeling.com/Abalone/).

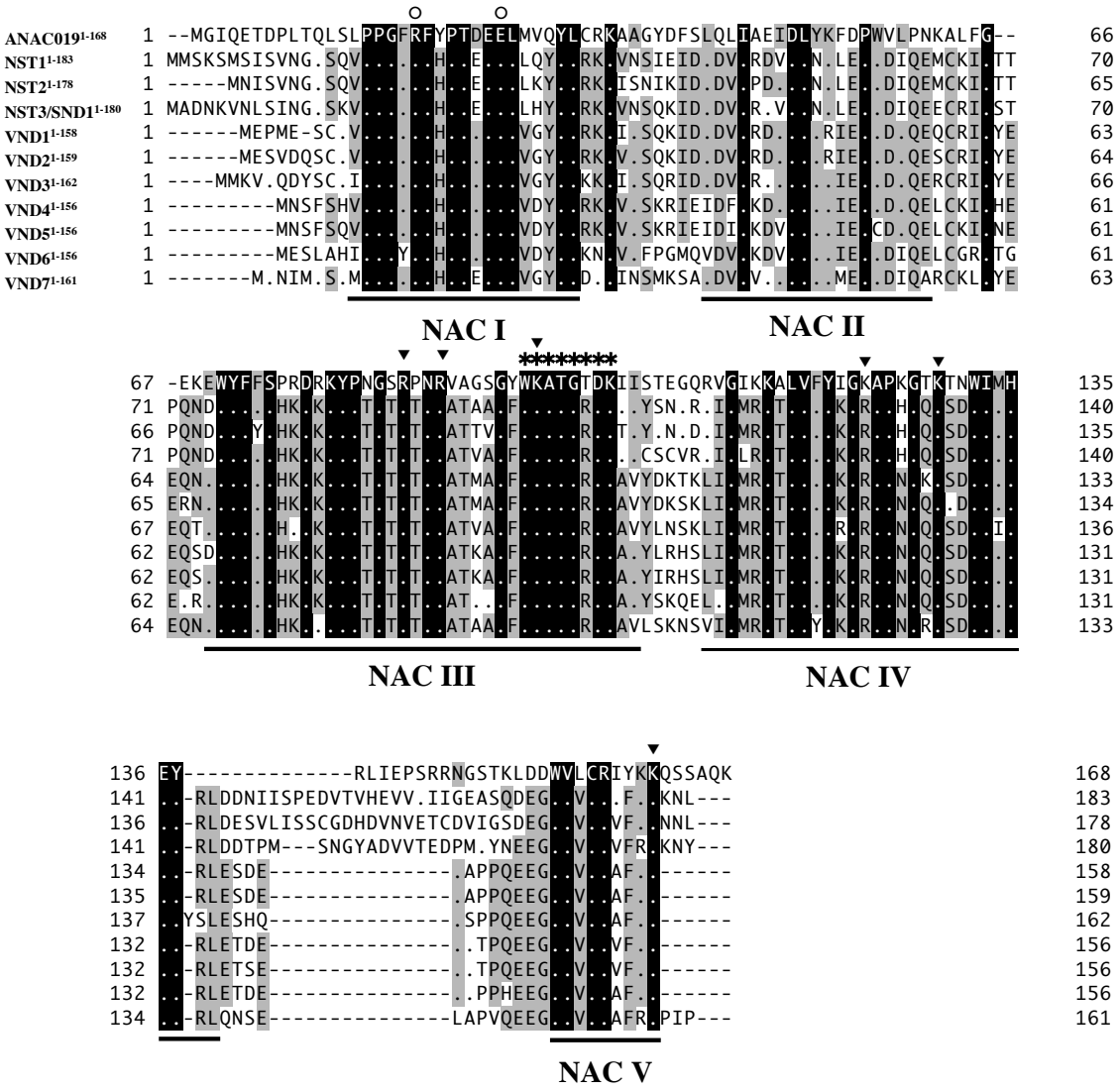

Figure 34.

Amino acid alignment among ANAC019, NST/SND, and VND NAC-domain proteins. Under bars indicate the NAC sub domain I to V (Kubo et al., 2005). Asterisks and triangles indicate amino acid residues that putatively interact with the DNA major groove region and the DNA backbone, respectively, based on the structure information on ANAC019. Circles indicate the amino acid residues that are involved in the dimer formation (Olsen et al., 2005; Welner et al., 2012).

Nucleotide sequence of X1E1-28bp		Ki value (S.D.)(nM)			
otide po		Adenine	Thymine	Guanine	Cytosine
A	-1	86.37 (± 1.25)	63.57 (± 2.88)	71.96 (± 8.19)	52.43 (± 5.31)
T	-2	69.54 (± 6.36)	79.77 (± 1.71)	57.83 (± 3.49)	51.18 (± 3.8)
T	-3	81.07 (± 12.67)	79.77 (± 1.71)	86.11 (± 24.81)	59.36 (± 10.28)
G	-4	62.18 (± 4.12)	50.99 (± 2.64)	72.27 (± 10.15)	49.15 (± 9.31)
T	-5	58.38 (± 4.1)	79.77 (± 1.71)	71.79 (± 12.88)	40.39 (± 5.83)
C	1	212.66 (± 4.28)	126.08 (± 11.63)	109.62 (± 19.83)	90.92 (± 7.13)
T	2	147.07 (± 7.59)	79.77 (± 1.71)	97.44 (± 20.31)	145.73 (± 28.69)
T	3	373.37 (± 31.71)	79.77 (± 1.71)	2493.48 (± 318.65)	5054.73 (± 857.12)
T	4	205.02 (± 28.33)	79.77 (± 1.71)	190.1 (± 36.16)	125.79 (± 4.41)
G	5	161.02 (± 18.48)	220.84 (± 21.49)	72.27 (± 10.15)	192.12 (± 32.3)
C	6	402.11 (± 53.28)	378.56 (± 100.39)	369.07 (± 34.42)	90.92 (± 7.13)
T	7	491.35 (± 45.69)	79.77 (± 1.71)	199.24 (± 41.2)	364.81 (± 91.68)
T	8	507.85 (± 51.19)	79.77 (± 1.71)	344.83 (± 82.48)	432.75 (± 129.1)
C	9	176.58 (± 22.03)	140.79 (± 28.66)	126.39 (± 17.93)	90.92 (± 7.13)
A	10	86.37 (± 1.25)	111.2 (± 23.55)	93.41 (± 15.28)	114.75 (± 47.6)
A	11	86.37 (± 1.25)	140.53 (± 21.38)	112.63 (± 21.89)	115.16 (± 51)
A	12	86.37 (± 1.25)	136.88 (± 28.21)	106.41 (± 44.26)	77.66 (± 42.8)
G	13	119.4 (± 14.56)	134.21 (± 21.61)	72.27 (± 10.15)	88.43 (± 46.99)
C	14	122.57 (± 7.46)	74.34 (± 13.91)	72.59 (± 27.4)	90.92 (± 7.13)
C	15	91.07 (± 3.87)	62.02 (± 11.56)	56.27 (± 7.74)	90.92 (± 7.13)
A	16	86.37 (± 1.25)	515.96 (± 95.69)	560.52 (± 118.1)	1423.2 (± 348.33)
A	17	86.37 (± 1.25)	196.21 (± 48.05)	125.85 (± 40.65)	51 (± 6.31)
T	18	122.98 (± 9.73)	79.77 (± 1.71)	39.23 (± 6.14)	89.86 (± 23.32)
C	+1	74.88 (± 24.62)	67.79 (± 10.38)	65.99 (± 10.34)	90.92 (± 7.13)
C	+2	47.09 (± 9.89)	56.94 (± 1.18)	61.46 (± 8.56)	90.92 (± 7.13)
T	+3	46.89 (± 5.8)	79.77 (± 1.71)	39.46 (± 8.25)	58.75 (± 10.7)
A	+4	86.37 (± 1.25)	58.4 (± 4.4)	39.79 (± 5.96)	36.47 (± 5.11)
T	+5	46.69 (± 7.07)	79.77 (± 1.71)	49.93 (± 6.26)	38.48 (± 6.82)

Table 1.

The calculated values of Ki for all the competitors with single substitutions on X1E1-28pb.

Selected VND7 binding sequences by SELEX.

Sample No.	Selected sequences
1	GGTGACGCGCGTGCCTTTTACAGCAATAC
2	CACTCAACGCTAAGGTTGCGTAGACT
3	ATCTTGCGGTGGGGTATTTTGTACGC
4	GAGAAAGCGTGTATGAGCAGTTTTGTC
5	CACTACATGCTTTGTCTAGGCTATTCTG
6	TGTCTCGCTTGGAGGTTGCGTAGAGT
7	TGGTAGCGTGTGTACGAAGAATCTGG
8	GCCAGTCGCTTTGTCCTTAAGGCATT
9	GAGCCTTTAAGCTCATTGTTGCTACT
10	ATCGGGTTTCGGCGTGCCCTGCACGG
11	GTTACCGTTCTACGTTACATCGCTCA
12	GATAGGGGGTACTTGCGTCACACGCT
13	GGCGTGCACATTACTCCATTCGTCTT
14	TCACGTAGTTATCTTCAACAATACGT
15	GTTTGGACTTTATGGTTAGCGTACAG
16	CCTCTTCAGTTTCTTCGTCGTCGATT
17	AGTGTACGCTATGCTCGGGGTAATG
18	CGTGTTATGTACGCCTAGTCATATAT
19	CTGTCGGGTGGGGCTATGTTGGTTGC
20	TACCTTACTTCTTACTTATTTCTTAC
21	ATAGCGTATCGGCGCCGCGTGTATCT
22	TGGGAGACTTAAACCTTGCGTAAGGT
23	CTTTGTACCTTGGTGATCAAGTTTGG
24	GACATATTTGCTTAGATCACACGCG
25	AATTGCCGGTCTCTTACGCCAAGTCTT
26	TTTGCGTCCGTATTAAGATTGGTGTT
27	ACATGGTCTTGGTTGCGTGTCGTACAG
28	TCCGGTTCTTTGCTTCGTGATGAGGT
29	TTTTCAGCTTGCTGTTCACGTTAACC
30	CTTTGCACTTACGGCTTTGGTGCCT
31	GCGTAAGATTTACGGTTGGCGTCGGGT
32	AAATAGGACGCTTGCGTTATTCACAA
33	GGCTGATGTTACGTGGGCTTCACGT
34	GTGTCGTGTTGTGGAAGTATTCTTGCC
35	CTTGGTGATCACGTTAATAGGTGTTA

Table 2.

Result of the SELEX analysis

	XCP1 pro (-148 bp to +9 bp)-GUS	
	Original	four-core mutation
Root		
Meristematic zone		
Protoxylem vessel pole	**24 / 39**	**0 / 52**
Root cap	**6 / 39**	**4 / 52**
Elongation / Differentiation zone		
Protoxylem vessel	**24 / 39**	**1 / 52**
Metaxylem vessel	**28 / 39**	**2 / 52**
Pericycle cell	**0 / 39**	**9 / 52**
Cotyledon		
Vein	**3 / 39**	**0 / 52**
Leave distal margin	**13 / 39**	**13 / 52**
Other cells*	**6 / 39**	**1 / 52**
True leaf		
Vein	**15 / 39**	**0 / 52**
Stomata	**0 / 39**	**1 / 52**
Other cells*	**4 / 39**	**6 / 52**

Number of positive T_1 plant / All T_1 plant
*** Epidermal cell and mesophyll cell**

Table 3.

Summary of localization pattern of GUS signal in *XCP1* promoter GUS constructs in *Arabidopsis*.

For deletion DNA binding assay using XCP1 promoter by FCS (X1E1 region).

Primer name	Primer sequences
Forward primer sequences (5′-3′)	
XCP1pro_for	agctgtatgttgaaaattgcacgcttagaacaaaaggcttaaccaaaaatgatccaaccgtgaagactcggagaccggcgtacttagtttttaaattaat cattgtctttgcttcaaagccaatcctatgagactttg
X1E1_for	agtttttaaattaatcattgtctttgcttcaaagccaatcctatgagactttg
X1E1-a_for	ttaaattaatcattgtctttgcttcaaagccaatcctatgagactttg
X1E1-b_for	ttaatcattgtctttgcttcaaagccaatcctatgagactttg
X1E1-c_for	cattgtctttgcttcaaagccaatcctatgagactttg
X1E1-d_for	ttgtctttgcttcaaagccaatcctatgagactttg
X1E1-e_for	gtctttgcttcaaagccaatcctatgagactttg
X1E1-f_for	ctttgcttcaaagccaatcctatgagactttg
X1E1-g_for	tttgcttcaaagccaatcctatgagactttg
X1E1-h_for	ttgcttcaaagccaatcctatgagactttg
X1E1-i_for	gcttcaaagccaatcctatgagactttg
X1E1-j_for	agtttttaaattaatcattgtctttgcttcaaagccaatcctatgaga
X1E1-k_for	agtttttaaattaatcattgtctttgcttcaaagccaatccta
X1E1-l_for	agtttttaaattaatcattgtctttgcttcaaagccaatcc
X1E1-m_for	agtttttaaattaatcattgtctttgcttcaaagccaat
X1E1-n_for	agtttttaaattaatcattgtctttgcttcaaagccaa
X1E1-o_for	agtttttaaattaatcattgtctttgcttcaaagcca
X1E1-p_for	agtttttaaattaatcattgtctttgcttcaaagcc
X1E1-q_for	agtttttaaattaatcattgtctttgcttcaaagc
X1E1-r_for	agtttttaaattaatcattgtctttgcttcaaa
X1E1-18bp_for	ctttgcttcaaagccaat
X1E1-20bp_for	tctttgcttcaaagccaatc
X1E1-22bp_for	gtctttgcttcaaagccaatcc
X1E1-24bp_for	tgtctttgcttcaaagccaatcct
X1E1-26bp_for	ttgtctttgcttcaaagccaatccta
X1E1-28bp_for	attgtctttgcttcaaagccaatcctat
Reverse primer sequences (5′-3′)	
XCP1pro_rev	caaagtctcataggattggctttgaagcaaagacaatgattaatttaaaaactaagtacgccggtctccgagtcttcacggttggatcatttttggttaagc ctttgttctaagcgtgcaattttcaacatacagct
X1E1_rev	caaagtctcataggattggctttgaagcaaagacaatgattaatttaaaaact
X1E1-a_rev	caaagtctcataggattggctttgaagcaaagacaatgattaatttaa
X1E1-b_rev	caaagtctcataggattggctttgaagcaaagacaatgattaa
X1E1-c_rev	caaagtctcataggattggctttgaagcaaagacaatg
X1E1-d_rev	caaagtctcataggattggctttgaagcaaagacaa
X1E1-e_rev	caaagtctcataggattggctttgaagcaaagac
X1E1-f_rev	caaagtctcataggattggctttgaagcaaag
X1E1-g_rev	caaagtctcataggattggctttgaagcaaa
X1E1-h_rev	caaagtctcataggattggctttgaagcaa
X1E1-i_rev	caaagtctcataggattggctttgaagc
X1E1-j_rev	tctcataggattggctttgaagcaaagacaatgattaatttaaaaact
X1E1-k_rev	taggattggctttgaagcaaagacaatgattaatttaaaaact
X1E1-l_rev	ggattggctttgaagcaaagacaatgattaatttaaaaact
X1E1-m_rev	attggctttgaagcaaagacaatgattaatttaaaaact
X1E1-n_rev	ttggctttgaagcaaagacaatgattaatttaaaaact
X1E1-o_rev	tggctttgaagcaaagacaatgattaatttaaaaact
X1E1-p_rev	ggctttgaagcaaagacaatgattaatttaaaaact
X1E1-q_rev	gctttgaagcaaagacaatgattaatttaaaaact
X1E1-r_rev	tttgaagcaaagacaatgattaatttaaaaact
X1E1-18bp_rev	attggctttgaagcaaag
X1E1-20bp_rev	gattggctttgaagcaaaga
X1E1-22bp_rev	ggattggctttgaagcaaagac
X1E1-24bp_rev	aggattggctttgaagcaaagaca
X1E1-26bp_rev	taggattggctttgaagcaaagacaa
X1E1-28bp_rev	taaggattggctttgaagcaaagacaat

Table 4.

Primer list in this study

For deletion DNA binding assay using VND7 direct target gene promoters by FCS (CesA4, Polygalacturonase: PG, XCP2, MYB46, MYB83 and ATMC9).

Primer name	Primer sequences
Forward primer sequences (5′-3′)	
CesA4 pro_for	agaaatacataataacttgaaagctactctaagttata
CesA4-1_for	tacataataacttgaaagctactctaagttata
CesA4-2_for	cataataacttgaaagctactctaag
CesA4-3_for	taataacttgaaagctactctaag
CesA4-4_for	aataacttgaaagctactctaag
CesA4-5_for	ataacttgaaagctactctaag
CesA4-6_for	agaaatacataataacttgaaagctactctaag
CesA4-7_for	agaaatacataataacttgaaagctactctaa
CesA4-8_for	agaaatacataataacttgaaagctactcta
PG pro_for	attttattggcttggctttaaagtagatgaagacaagc
PG-1_for	attggcttggctttaaagtagatgaagacaagc
PG-2_for	attttattggcttggctttaaagtagatgaaga
PG-3_for	tggcttggctttaaagtagatgaaga
PG-4_for	gcttggctttaaagtagatgaaga
PG-5_for	cttggctttaaagtagatgaagacaagc
PG-6_for	ttggctttaaagtagatgaaga
PG-7_for	attggcttggctttaaagtagatgaag
PG-8_for	attggcttggctttaaagtagatgaa
PG-9_for	attggcttggctttaaagtagatg
XCP2 pro_for	attcagactactttactctaaagcaaaaagagcgacct
XCP2-1_for	cagactactttactctaaagcaaaaagagcgacct
XCP2-2_for	agactactttactctaaagcaaaaagagcgacct
XCP2-3_for	gactactttactctaaagcaaaaagagcgacct
XCP2-4_for	actactttactctaaagcaaaaagagcgacct
XCP2-5_for	ctactttactctaaagcaaaaagagcgacct
XCP2-6_for	attcagactactttactctaaagcaaaaagagc
XCP2-7_for	attcagactactttactctaaagcaaaaa
XCP2-8_for	attcagactactttactctaaagcaaaa
XCP2-9_for	attcagactactttactctaaagcaaa
MYB46 (1) pro_for	acaataattagatttcttcaagtatacgtgttggtgcg
MYB46 (1)-1_for	attagatttcttcaagtatacgtgttggtgcg
MYB46 (1)-2_for	aattagatttcttcaagtatacgtgttggtgcg
MYB46 (1)-3_for	attagatttcttcaagtatacgtgttggtgcg
MYB46 (1)-4_for	ttagatttcttcaagtatacgtgttg
MYB46 (1)-5_for	aattagatttcttcaagtatacgtgt
MYB46 (1)-6_for	aattagatttcttcaagtatacgt
MYB46 (1)-7_for	acaataattagatttcttcaagtatacg
MYB46 (1)-8_for	aattagatttcttcaagtatac
MYB46 (2) pro_for	taatgtataccttgtgaatgaagaaactaatagaaatg
MYB46 (2)-1_for	tataccttgtgaatgaagaaactaatagaaatg
MYB46 (2)-2_for	taatgtataccttgtgaatgaagaaactaatag
MYB46 (2)-3_for	ataccttgtgaatgaagaaactaatagaaatg
MYB46 (2)-4_for	taccttgtgaatgaagaaactaatag
MYB46 (2)-5_for	tataccttgtgaatgaagaaactaat
MYB46 (2)-6_for	tataccttgtgaatgaagaaacta
MYB46 (2)-7_for	taatgtataccttgtgaatgaagaaact
MYB46 (2)-8_for	tataccttgtgaatgaagaaac
MYB46 (3) pro_for	tataatatagtgttgctttgttttaaaacataaaagaa
MYB46 (3)-1_for	tatagtgttgctttgttttaaaacataaaagaa
MYB46 (3)-2_for	tataatatagtgttgctttgttttaaaacataa
MYB46 (3)-3_for	tatagtgttgctttgttttaaaacataa
MYB46 (3)-4_for	atagtgttgctttgttttaaaacataaaagaa
MYB46 (3)-5_for	tagtgttgctttgttttaaaacataa
MYB46 (3)-6_for	tatagtgttgctttgttttaaaacat
MYB46 (3)-7_for	tatagtgttgctttgttttaaaac
MYB46 (3)-8_for	tataatatagtgttgctttgttttaaaa
MYB46 (3)-9_for	tatagtgttgctttgttttaaa
MYB83 pro_for	ttgattgtgtcgtaaaatggaagttacttcaaaataag
MYB83-1_for	tgtgtcgtaaaatggaagttacttcaaaataag
MYB83-2_for	gtgtcgtaaaatggaagttacttcaaaataag
MYB83-3_for	tgtcgtaaaatggaagttacttcaaa
MYB83-4_for	ttgattgtgtcgtaaaatggaagttacttcaaa
MYB83-5_for	tgtgtcgtaaaatggaagttacttca

Table 4.

Primer list in this study

For deletion DNA binding assay using VND7 direct target gene promoters by FCS (CesA4, Polygalacturonase: PG, XCP2, MYB46, MYB83 and ATMC9).

Primer name	Primer sequences
Forward primer sequences (5′-3′)	
MYB83-6_for	tgtgtcgtaaaatggaagttactt
MYB83-7_for	ttgattgtgtcgtaaaatggaagttact
MYB83-8_for	tgtgtcgtaaaatggaagttac
ATMC9 pro_for	aggtttagtttcttgcttgaaagcattaataagtcaag
ATMC9-1_for	tagtttcttgcttgaaagcattaataagtcaag
ATMC9-2_for	aggtttagtttcttgcttgaaagcattaataag
ATMC9-3_for	gtttcttgcttgaaagcattaataag
ATMC9-4_for	ttcttgcttgaaagcattaataag
ATMC9-5_for	tcttgcttgaaagcattaataag
ATMC9-6_for	cttgcttgaaagcattaataag
ATMC9-7_for	tagtttcttgcttgaaagcattaata
ATMC9-8_for	tagtttcttgcttgaaagcattaa
ATMC9-9_for	tagtttcttgcttgaaagcatta
Reverse primer sequences (5′-3′)	
CesA4 pro_rev	tataacttagagtagctttcaagttattatgtatttct
CesA4-1_rev	tataacttagagtagctttcaagttattatgta
CesA4-2_rev	cttagagtagctttcaagttattatg
CesA4-3_rev	cttagagtagctttcaagttatta
CesA4-4_rev	cttagagtagctttcaagttatt
CesA4-5_rev	cttagagtagctttcaagttat
CesA4-6_rev	cttagagtagctttcaagttattatgtatttct
CesA4-7_rev	ttagagtagctttcaagttattatgtatttct
CesA4-8_rev	tagagtagctttcaagttattatgtatttct
PG pro_rev	gcttgtcttcatctactttaaagccaagccaataaaat
PG-1_rev	gcttgtcttcatctactttaaagccaagccaat
PG-2_rev	tcttcatctactttaaagccaagccaataaaat
PG-3_rev	tcttcatctactttaaagccaagcca
PG-4_rev	tcttcatctactttaaagccaagc
PG-5_rev	gcttgtcttcatctactttaaagccaag
PG-6_rev	tcttcatctactttaaagccaa
PG-7_rev	cttcatctactttaaagccaag
PG-8_rev	ttcatctactttaaagccaag
PG-9_rev	catctactttaaagccaag
XCP2 pro_rev	aggtcgctctttttgctttagagtaaagtagtctgaat
XCP2-1_rev	aggtcgctctttttgctttagagtaaagtagtctg
XCP2-2_rev	aggtcgctctttttgctttagagtaaagtagtct
XCP2-3_rev	aggtcgctctttttgctttagagtaaagtagtc
XCP2-4_rev	aggtcgctctttttgctttagagtaaagtagt
XCP2-5_rev	aggtcgctctttttgctttagagtaaagtag
XCP2-6_rev	gctctttttgctttagagtaaagtagtctgaat
XCP2-7_rev	tttttgctttagagtaaagtagtctgaat
XCP2-8_rev	ttttgctttagagtaaagtagtctgaat
XCP2-9_rev	tttgctttagagtaaagtagtctgaat
MYB46 (1) pro_rev	cgcaccaacacgtatacttgaagaaatctaattattgt
MYB46 (1)-1_rev	cgcaccaacacgtatacttgaagaaatctaat
MYB46 (1)-2_rev	cgcaccaacacgtatacttgaagaaatctaatt
MYB46 (1)-3_rev	cgcaccaacacgtatacttgaagaaatctaat
MYB46 (1)-4_rev	caacacgtatacttgaagaaatctaa
MYB46 (1)-5_rev	acacgtatacttgaagaaatctaatt
MYB46 (1)-6_rev	acgtatacttgaagaaatctaatt
MYB46 (1)-7_rev	cgtatacttgaagaaatctaattattgt
MYB46 (1)-8_rev	gtatacttgaagaaatctaatt
MYB46 (2) pro_rev	catttctattagtttcttcattcacaaggtatacatta
MYB46 (2)-1_rev	catttctattagtttcttcattcacaaggtata
MYB46 (2)-2_rev	ctattagtttcttcattcacaaggtatacatta
MYB46 (2)-3_rev	catttctattagtttcttcattcacaaggtat
MYB46 (2)-4_rev	ctattagtttcttcattcacaaggta
MYB46 (2)-5_rev	attagtttcttcattcacaaggtata
MYB46 (2)-6_rev	tagtttcttcattcacaaggtata
MYB46 (2)-7_rev	agtttcttcattcacaaggtatacatta
MYB46 (2)-8_rev	gtttcttcattcacaaggtata

Table 4.

Primer list in this study

For deletion DNA binding assay using VND7 direct target gene promoters by FCS (CesA4, Polygalacturonase: PG, XCP2, MYB46, MYB83 and ATMC9).

Primer name	Primer sequences
Reverse primer sequences (5′-3′)	
MYB46 (3) pro_rev	ttcttttatgttttaaaacaaagcaacactatattata
MYB46 (3)-1_rev	ttatgttttaaaacaaagcaacactatattata
MYB46 (3)-2_rev	ttcttttatgttttaaaacaaagcaacactata
MYB46 (3)-3_rev	ttatgttttaaaacaaagcaacactata
MYB46 (3)-4_rev	ttcttttatgttttaaaacaaagcaacactat
MYB46 (3)-5_rev	ttatgttttaaaacaaagcaacacta
MYB46 (3)-6_rev	atgttttaaaacaaagcaacactata
MYB46 (3)-7_rev	gttttaaaacaaagcaacactata
MYB46 (3)-8_rev	ttttaaaacaaagcaacactatattata
MYB46 (3)-9_rev	tttaaaacaaagcaacactata
MYB83 pro_rev	cttattttgaagtaacttccattttacgacacaatcaa
MYB83-1_rev	cttattttgaagtaacttccattttacgacaca
MYB83-2_rev	cttattttgaagtaacttccattttacgacac
MYB83-3_rev	tttgaagtaacttccattttacgaca
MYB83-4_rev	tttgaagtaacttccattttacgacacaatcaa
MYB83-5_rev	tgaagtaacttccattttacgacaca
MYB83-6_rev	aagtaacttccattttacgacaca
MYB83-7_rev	agtaacttccattttacgacacaatcaa
MYB83-8_rev	gtaacttccattttacgacaca
ATMC9 pro_rev	cttgacttattaatgctttcaagcaagaaactaaacct
ATMC9-1_rev	cttgacttattaatgctttcaagcaagaaacta
ATMC9-2_rev	cttattaatgctttcaagcaagaaactaaacct
ATMC9-3_rev	cttattaatgctttcaagcaagaaac
ATMC9-4_rev	cttattaatgctttcaagcaagaa
ATMC9-5_rev	cttattaatgctttcaagcaaga
ATMC9-6_rev	cttattaatgctttcaagcaag
ATMC9-7_rev	tattaatgctttcaagcaagaaacta
ATMC9-8_rev	ttaatgctttcaagcaagaaacta
ATMC9-9_rev	taatgctttcaagcaagaaacta

Table 4.

Primer list in this study

For single-mutation DNA binding assay by FCS (linkerscan assay). Red: Nucleotide positions that were substituted by adenine, tymine, guanine and cytosine.

Primer name	Primer sequences
Forward primer sequences (5′-3′)	
X1E1-ls_1_for	aatgtctttgcttcaaagccaatcctat
X1E1-ls_2_for	atagtctttgcttcaaagccaatcctat
X1E1-ls_3_for	attatctttgcttcaaagccaatcctat
X1E1-ls_4_for	attgactttgcttcaaagccaatcctat
X1E1-ls_5_for	attgtatttgcttcaaagccaatcctat
X1E1-ls_6_for	attgtcattgcttcaaagccaatcctat
X1E1-ls_7_for	attgtctatgcttcaaagccaatcctat
X1E1-ls_8_for	attgtcttagcttcaaagccaatcctat
X1E1-ls_9_for	attgtctttacttcaaagccaatcctat
X1E1-ls_10_for	attgtctttgattcaaagccaatcctat
X1E1-ls_11_for	attgtctttgcatcaaagccaatcctat
X1E1-ls_12_for	attgtctttgctacaaagccaatcctat
X1E1-ls_13_for	attgtctttgcttaaaagccaatcctat
X1E1-ls_14_for	attgtctttgcttcaaaaccaatcctat
X1E1-ls_15_for	attgtctttgcttcaaagacaatcctat
X1E1-ls_16_for	attgtctttgcttcaaagcaaatcctat
X1E1-ls_17_for	attgtctttgcttcaaagccaaacctat
X1E1-ls_18_for	attgtctttgcttcaaagccaatactat
X1E1-ls_19_for	attgtctttgcttcaaagccaatcatat
X1E1-ls_20_for	attgtctttgcttcaaagccaatccaat
X1E1-ls_21_for	attgtctttgcttcaaagccaatcctaa
X1E1-ls_22_for	tttgtctttgcttcaaagccaatcctat
X1E1-ls_23_for	atttttctttgcttcaaagccaatcctat
X1E1-ls_24_for	attgttttgcttcaaagccaatcctat
X1E1-ls_25_for	attgtctttttcttcaaagccaatcctat
X1E1-ls_26_for	attgtctttgtttcaaagccaatcctat
X1E1-ls_27_for	attgtctttgctttaaagccaatcctat
X1E1-ls_28_for	attgtctttgcttctaagccaatcctat
X1E1-ls_29_for	attgtctttgcttcatagccaatcctat
X1E1-ls_30_for	attgtctttgcttcaatgccaatcctat
X1E1-ls_31_for	attgtctttgcttcaaatccaatcctat
X1E1-ls_32_for	attgtctttgcttcaaagtcaatcctat
X1E1-ls_33_for	attgtctttgcttcaaagctaatcctat
X1E1-ls_34_for	attgtctttgcttcaaagcctatcctat
X1E1-ls_35_for	attgtctttgcttcaaagccattcctat
X1E1-ls_36_for	attgtctttgcttcaaagccaattctat
X1E1-ls_37_for	attgtctttgcttcaaagccaatcttat
X1E1-ls_38_for	attgtctttgcttcaaagccaatcctta
X1E1-ls_39_for	gttgtctttgcttcaaagccaatcctat
X1E1-ls_40_for	agtgtctttgcttcaaagccaatcctat
X1E1-ls_41_for	atggtctttgcttcaaagccaatcctat
X1E1-ls_42_for	attggctttgcttcaaagccaatcctat
X1E1-ls_43_for	attgtgtttgcttcaaagccaatcctat
X1E1-ls_44_for	attgtcgttgcttcaaagccaatcctat
X1E1-ls_45_for	attgtctgtgcttcaaagccaatcctat
X1E1-ls_46_for	attgtcttggcttcaaagccaatcctat
X1E1-ls_47_for	attgtctttggttcaaagccaatcctat
X1E1-ls_48_for	attgtctttgcgtcaaagccaatcctat
X1E1-ls_49_for	attgtctttgctgcaaagccaatcctat
X1E1-ls_50_for	attgtctttgcttgaaagccaatcctat
X1E1-ls_51_for	attgtctttgcttcgaagccaatcctat
X1E1-ls_52_for	attgtctttgcttcagagccaatcctat
X1E1-ls_53_for	attgtctttgcttcaaggccaatcctat
X1E1-ls_54_for	attgtctttgcttcaaaggcaatcctat
X1E1-ls_55_for	attgtctttgcttcaaagcgaatcctat
X1E1-ls_56_for	attgtctttgcttcaaagccgatcctat
X1E1-ls_57_for	attgtctttgcttcaaagccagtcctat
X1E1-ls_58_for	attgtctttgcttcaaagccaagcctat
X1E1-ls_59_for	attgtctttgcttcaaagccaatgctat
X1E1-ls_60_for	attgtctttgcttcaaagccaatcgtat
X1E1-ls_61_for	attgtctttgcttcaaagccaatccgat
X1E1-ls_62_for	attgtctttgcttcaaagccaatcctgt
X1E1-ls_63_for	attgtctttgcttcaaagccaatcctag

Table 4.

Primer list in this study

For single-mutation DNA binding assay by FCS (linkerscan assay). Red: Nucleotide positions that were substituted by adenine, tymine, guanine and cytosine.

Primer name	Primer sequences
Forward primer sequences (5′ -3′)	
X1E1-ls_64_for	cttgtctttgcttcaaagccaatcctat
X1E1-ls_65_for	actgtctttgcttcaaagccaatcctat
X1E1-ls_66_for	atcgtctttgcttcaaagccaatcctat
X1E1-ls_67_for	attctctttgcttcaaagccaatcctat
X1E1-ls_68_for	attgcctttgcttcaaagccaatcctat
X1E1-ls_69_for	attgtccttgcttcaaagccaatcctat
X1E1-ls_70_for	attgtctctgcttcaaagccaatcctat
X1E1-ls_71_for	attgtcttcgcttcaaagccaatcctat
X1E1-ls_72_for	attgtctttccttcaaagccaatcctat
X1E1-ls_73_for	attgtctttgcctcaaagccaatcctat
X1E1-ls_74_for	attgtctttgctccaaagccaatcctat
X1E1-ls_75_for	attgtctttgcttccaagccaatcctat
X1E1-ls_76_for	attgtctttgcttcacagccaatcctat
X1E1-ls_77_for	attgtctttgcttcaacgccaatcctat
X1E1-ls_78_for	attgtctttgcttcaaacccaatcctat
X1E1-ls_79_for	attgtctttgcttcaaagcccatcctat
X1E1-ls_80_for	attgtctttgcttcaaagccactcctat
X1E1-ls_81_for	attgtctttgcttcaaagccaaccctat
X1E1-ls_82_for	attgtctttgcttcaaagccaatcccat
X1E1-ls_83_for	attgtctttgcttcaaagccaatcctct
X1E1-ls_84_for	attgtctttgcttcaaagccaatcctac
Reverse primer sequences (5′ -3′)	
X1E1_ls_1_rev	ataggattggctttgaagcaaagacatt
X1E1_ls_2_rev	ataggattggctttgaagcaaagactat
X1E1_ls_3_rev	ataggattggctttgaagcaaagataat
X1E1_ls_4_rev	ataggattggctttgaagcaaagtcaat
X1E1_ls_5_rev	ataggattggctttgaagcaaatacaat
X1E1_ls_6_rev	ataggattggctttgaagcaatgacaat
X1E1_ls_7_rev	ataggattggctttgaagcatagacaat
X1E1_ls_8_rev	ataggattggctttgaagctaagacaat
X1E1_ls_9_rev	ataggattggctttgaagtaaagacaat
X1E1_ls_10_rev	ataggattggctttgaatcaaagacaat
X1E1_ls_11_rev	ataggattggctttgatgcaaagacaat
X1E1_ls_12_rev	ataggattggctttgtagcaaagacaat
X1E1_ls_13_rev	ataggattggctttaagcaaagacaat
X1E1_ls_14_rev	ataggattggttttgaagcaaagacaat
X1E1_ls_15_rev	ataggattgtctttgaagcaaagacaat
X1E1_ls_16_rev	ataggatttgctttgaagcaaagacaat
X1E1_ls_17_rev	ataggtttggctttgaagcaaagacaat
X1E1_ls_18_rev	atagtattggctttgaagcaaagacaat
X1E1_ls_19_rev	atatgattggctttgaagcaaagacaat
X1E1_ls_20_rev	attggattggctttgaagcaaagacaat
X1E1_ls_21_rev	ttaggattggctttgaagcaaagacaat
X1E1_ls_22_rev	ataggattggctttgaagcaaagacaaa
X1E1_ls_23_rev	ataggattggctttgaagcaaagaaaat
X1E1_ls_24_rev	ataggattggctttgaagcaaaaacaat
X1E1_ls_25_rev	ataggattggctttgaagaaaagacaat
X1E1_ls_26_rev	ataggattggctttgaaacaaagacaat
X1E1_ls_27_rev	ataggattggctttaaagcaaagacaat
X1E1_ls_28_rev	ataggattggcttagaagcaaagacaat
X1E1_ls_29_rev	ataggattggctatgaagcaaagacaat
X1E1_ls_30_rev	ataggattggcattgaagcaaagacaat
X1E1_ls_31_rev	ataggattggatttgaagcaaagacaat
X1E1_ls_32_rev	ataggattgactttgaagcaaagacaat
X1E1_ls_33_rev	ataggattagctttgaagcaaagacaat
X1E1_ls_34_rev	ataggataggctttgaagcaaagacaat
X1E1_ls_35_rev	ataggaatggctttgaagcaaagacaat
X1E1_ls_36_rev	atagaattggctttgaagcaaagacaat
X1E1_ls_37_rev	ataagattggctttgaagcaaagacaat
X1E1_ls_38_rev	aaaggattggctttgaagcaaagacaat
X1E1_ls_39_rev	ataggattggctttgaagcaaagacaac
X1E1_ls_40_rev	ataggattggctttgaagcaaagacact
X1E1_ls_41_rev	ataggattggctttgaagcaaagaccat

Table 4.

Primer list in this study

For single-mutation DNA binding assay by FCS (linkerscan assay). Red: Nucleotide positions that were substituted by adenine, tymine, guanine and cytosine.

Primer name	Primer sequences
Reverse primer sequences (5′-3′)	
X1E1_ls_42_rev	ataggattggctttgaagcaaagccaat
X1E1_ls_43_rev	ataggattggctttgaagcaaacacaat
X1E1_ls_44_rev	ataggattggctttgaagcaacgacaat
X1E1_ls_45_rev	ataggattggctttgaagcacagacaat
X1E1_ls_46_rev	ataggattggctttgaagccaagacaat
X1E1_ls_47_rev	ataggattggctttgaaccaaagacaat
X1E1_ls_48_rev	ataggattggctttgacgcaaagacaat
X1E1_ls_49_rev	ataggattggctttgcagcaaagacaat
X1E1_ls_50_rev	ataggattggctttcaagcaaagacaat
X1E1_ls_51_rev	ataggattggcttcgaagcaaagacaat
X1E1_ls_52_rev	ataggattggctctgaagcaaagacaat
X1E1_ls_53_rev	ataggattggccttgaagcaaagacaat
X1E1_ls_54_rev	ataggattgcctttgaagcaaagacaat
X1E1_ls_55_rev	ataggattcgctttgaagcaaagacaat
X1E1_ls_56_rev	ataggatcggctttgaagcaaagacaat
X1E1_ls_57_rev	ataggactggctttgaagcaaagacaat
X1E1_ls_58_rev	ataggcttggctttgaagcaaagacaat
X1E1_ls_59_rev	atagcattggctttgaagcaaagacaat
X1E1_ls_60_rev	atacgattggctttgaagcaaagacaat
X1E1_ls_61_rev	atcggattggctttgaagcaaagacaat
X1E1_ls_62_rev	acaggattggctttgaagcaaagacaat
X1E1_ls_63_rev	ctaggattggctttgaagcaaagacaat
X1E1_ls_64_rev	ataggattggctttgaagcaaagacaag
X1E1_ls_65_rev	ataggattggctttgaagcaaagacagt
X1E1_ls_66_rev	ataggattggctttgaagcaaagacgat
X1E1_ls_67_rev	ataggattggctttgaagcaaagagaat
X1E1_ls_68_rev	ataggattggctttgaagcaaaggcaat
X1E1_ls_69_rev	ataggattggctttgaagcaaggacaat
X1E1_ls_70_rev	ataggattggctttgaagcagagacaat
X1E1_ls_71_rev	ataggattggctttgaagcgaagacaat
X1E1_ls_72_rev	ataggattggctttgaaggaaagacaat
X1E1_ls_73_rev	ataggattggctttgaggcaaagacaat
X1E1_ls_74_rev	ataggattggctttggagcaaagacaat
X1E1_ls_75_rev	ataggattggcttggaagcaaagacaat
X1E1_ls_76_rev	ataggattggctgtgaagcaaagacaat
X1E1_ls_77_rev	ataggattggcgttgaagcaaagacaat
X1E1_ls_78_rev	ataggattgggtttgaagcaaagacaat
X1E1_ls_79_rev	ataggatgggctttgaagcaaagacaat
X1E1_ls_80_rev	ataggagtggctttgaagcaaagacaat
X1E1_ls_81_rev	atagggttggctttgaagcaaagacaat
X1E1_ls_82_rev	atgggattggctttgaagcaaagacaat
X1E1_ls_83_rev	agaggattggctttgaagcaaagacaat
X1E1_ls_84_rev	gtaggattggctttgaagcaaagacaat

Table 4.

Primer list in this study

For guanine-based double-mutation DNA binding assay by FCS. Red: Nucleotide positions that were substituted by guanine or cytosine.

Primer name	Primer sequences
Forward primer sequences (5′-3′)	
X1E1-sm_gp.3_for	attgtctgtgcttcaaagccaatcctat
X1E1-dm_gp.1_for	attgtgtgtgcttcaaagccaatcctat
X1E1-dm_gp.2_for	attgtcggtgcttcaaagccaatcctat
X1E1-dm_gp.3_for	attgtctgggcttcaaagccaatcctat
X1E1-dm_gp.4_for	attgtctgtggttcaaagccaatcctat
X1E1-dm_gp.5_for	attgtctgtgcgtcaaagccaatcctat
X1E1-dm_gp.6_for	attgtctgtgctgcaaagccaatcctat
X1E1-dm_gp.7_for	attgtctgtgcttgaaagccaatcctat
X1E1-dm_gp.8_for	attgtctgtgcttcgaagccaatcctat
X1E1-dm_gp.9_for	attgtctgtgcttcagagccaatcctat
X1E1-dm_gp.10_for	attgtctgtgcttcaaggccaatcctat
X1E1-dm_gp.11_for	attgtctgtgcttcaaaggcaatcctat
X1E1-dm_gp.12_for	attgtctgtgcttcaaagcgaatcctat
X1E1-dm_gp.13_for	attgtctgtgcttcaaagccgatcctat
X1E1-dm_gp.14_for	attgtctgtgcttcaaagccagtcctat
X1E1-dm_gp.15_for	attgtctgtgcttcaaagccaagcctat
Reverse primer sequences (5′-3′)	
X1E1-sm_gp.3_rev	ataggattggctttgaagcacagacaat
X1E1-dm_gp.1_rev	ataggattggctttgaagcacacacaat
X1E1-dm_gp.2_rev	ataggattggctttgaagcaccgacaat
X1E1-dm_gp.3_rev	ataggattggctttgaagcccagacaat
X1E1-dm_gp.4_rev	ataggattggctttgaaccacagacaat
X1E1-dm_gp.5_rev	ataggattggctttgacgcacagacaat
X1E1-dm_gp.6_rev	ataggattggctttgcagcacagacaat
X1E1-dm_gp.7_rev	ataggattggctttcaagcacagacaat
X1E1-dm_gp.8_rev	ataggattggcttcgaagcacagacaat
X1E1-dm_gp.9_rev	ataggattggctctgaagcacagacaat
X1E1-dm_gp.10_rev	ataggattggccttgaagcacagacaat
X1E1-dm_gp.11_rev	ataggattgcctttgaagcacagacaat
X1E1-dm_gp.12_rev	ataggattcgctttgaagcacagacaat
X1E1-dm_gp.13_rev	ataggatcggctttgaagcacagacaat
X1E1-dm_gp.14_rev	ataggactggctttgaagcacagacaat
X1E1-dm_gp.15_rev	ataggcttggctttgaagcacagacaat

For core-mutation assay by FCS. Red: Nucleotide positions that were substituted by guanine or cytosine.

Primer name	Primer sequences
Forward primer sequences (5′-3′)	
X1E1-28bp (Original)_for	attgtctttgcttcaaagccaatcctat
X1E1-sm_gp.3_for	attgtctttgcttcaaagccaatcctat
X1E1-core-dm.1_for	attgtctgtgctgcaaagccaatcctat
X1E1-core-dm.2_for	attgtctgtgcttcagagccaatcctat
X1E1-core-dm.3_for	attgtctgtgcttcaaagccgatcctat
X1E1-core-dm.4_for	attgtctttgctgcaaagccgatcctat
X1E1-core-dm.5_for	attgtctttgcttcagagccgatcctat
X1E1-core-dm.6_for	attgtctttgctgcagagccaatcctat
X1E1 four-core-mu_for	attgtctgtgctgcagagccgatcctat
Reverse primer sequences (5′-3′)	
X1E1-28bp (Original)_rev	ataggattggctttgaagcaaagacaat
X1E1-sm_gp.3_rev	ataggattggctttgaagcacagacaat
X1E1-core-dm.1_rev	ataggattggctttgcagcacagacaat
X1E1-core-dm.2_rev	ataggattggctctgaagcacagacaat
X1E1-core-dm.3_rev	ataggatcggctttgaagcacagacaat
X1E1-core-dm.4_rev	ataggatcggctttgcagcaaagacaat
X1E1-core-dm.5_rev	ataggatcggctctgaagcaaagacaat
X1E1-core-dm.6_rev	ataggattggctctgcagcaaagacaat
X1E1 four-core-mu_rev	ataggatcggctctgcagcacagacaat

Table 4.

Primer list in this study

For FCS-based binding assay using XCP1 promoter (X1E1 region)
Forward primers are labelled TAMRA-labell at 5′ end.

Primer name	Primer sequences
Forward primer sequences (5′ -3′)	
TAMRA-XCP1pro_for	agctgtatgttgaaaattgcacgcttagaacaaaaggcttaaccaaaaatgatccaaccgtgaagactcggagaccggcgtacttagtttttaaattaatcattgtctttgcttcaaagcc aatcctatgagactttg
TAMRA-X1E1_for	agtttttaaattaatcattgtctttgcttcaaagccaatcctatgagactttg
TAMRA-X1E1-28bp_for	attgtctttgcttcaaagccaatcctat
Reverse primer sequences (5′ -3′)	
TAMRA-XCP1pro_rev	caaagtctcataggattggctttgaagcaaagacaatgattaatttaaaaactaagtacgccggtctccgagtcttcacggttggatcatttttggttaagccttttgttctaagcgtgcaatt ttcaacatacagct
TAMRA-X1E1_rev	caaagtctcataggattggctttgaagcaaagacaatgattaatttaaaaact
TAMRA-X1E1-28bp_rev	taaggattggctttgaagcaaagacaat

using VND7 direct target gene promoters (CesA4, Polygalacturonase: PG, XCP2, MYB46, MYB83 and ATMC9).
Forward primers are labelled TAMRA-labell at 5′ end. Red: Complementary sequence for forward primer.

Primer name	Primer sequences
Forward primer sequences (3′ -5′)	
TAMRA-VND7 target pro_for	ATTATGCTGAGTGAT
Reverse primer sequences (3′ -5′)	
TAMRA-CesA4 pro_rev	TATAACTTAGAGTAGCTTTCAAGTTATTATGTATTTCTATCACTCAGCATAAT
TAMRA-PG pro_rev	GCTTGTCTTCATCTACTTTAAAGCCAAGCCAATAAAATATCACTCAGCATAAT
TAMRA-XCP2 pro_rev	AGGTCGCTCTTTTTGCTTTAGAGTAAAGTAGTCTGAATATCACTCAGCATAAT
TAMRA-MYB46 (1) pro_rev	CGCACCAACACGTATACTTGAAGAAATCTAATTATTGTATCACTCAGCATAAT
TAMRA-MYB46 (2) pro_rev	CATTTCTATTAGTTTCTTCATTCACAAGGTATACATTAATCACTCAGCATAAT
TAMRA-MYB46 (3) pro_rev	TTCTTTTATGTTTTAAAACAAAGCAACACTATATTATAATCACTCAGCATAAT
TAMRA-MYB83 pro_rev	CTTATTTTGAAGTAACTTCCATTTTACGACACAATCAAATCACTCAGCATAAT
TAMRA-ATMC9 pro_rev	CTTGACTTATTAATGCTTTCAAGCAAGAAACTAAACCTATCACTCAGCATAAT

Table 4.

Primer list in this study

For transient assay	Red: Nucleotide positions that were substituted by guanine. Under bar: TOPO cloning site
Primer name	Primer sequences
Forward primer sequences (5′-3′)	
XCP1 pro_for	caccagtttttaaattaatcattgtctttgcttcaaagccaat
XCP1 pro-sm.1_for	caccagtttttaaattaatcattgtctgtgcttcaaagccaat
XCP1 pro-sm.2_for	caccagtttttaaattaatcattgtctttgctgcaaagccaat
XCP1 pro-sm.3_for	caccagtttttaaattaatcattgtctttgcttcagagccaat
XCP1 pro-sm.4_for	caccagtttttaaattaatcattgtctttgcttcaaagccgat
XCP1 pro-sm.5_for	caccagtttttaaattaatcattgtctttgcttcgaagccaat
XCP1 pro-sm.6_for	caccagtttttaaattaatcattgtctttgcttcaaaggcaat
XCP1 pro-dm.1_for	caccagtttttaaattaatcattgtctgtgctgcaaagccaat
XCP1 pro-dm.2_for	caccagtttttaaattaatcattgtctgtgcttcagagccaat
XCP1 pro-dm.3_for	caccagtttttaaattaatcattgtctgtgcttcaaagccgat
XCP1 pro-dm.4_for	caccagtttttaaattaatcattgtctttgctgcaaagccgat
XCP1 pro-dm.5_for	caccagtttttaaattaatcattgtctttgcttcagagccgat
XCP1 pro-dm.6_for	caccagtttttaaattaatcattgtctttgctgcagagccaat
XCP1 pro-core.mu_for	caccagtttttaaattaatcattgtctgtgctgcagagccgat
Reverse primer sequences (5′-3′)	
XCP1 pro_rev	aaaagccatagccaaatttgttcactgagagaagagg

For SELEX	N: Random nucleotide sequence region (26 bp).
Primer name	Primer sequences
SELEX template primer (5′-3′)	
SELEX 74bp	agcatcactgattcaagagcatagNNNNNNNNNNNNNNNNNNNNNNNNNttcaccttcagaactgatgtactc
Forward primer sequences (5′-3′)	
SELEX-for	agcatcactgattcaagagcatag
Reverse primer sequences (5′-3′)	
SELEX-rev	gagtacatcagttctgaaggtgaa

For GUS reporter expression assay	Red: Nucleotide positions that were substituted by guanine. Under bar: TOPO cloning site
Primer name	Primer sequences
Forward primer sequences (5′-3′)	
XCP1 pro (-148 bp to + 9 bp)-GUS-Original_for	caccagtttttaaattaatcattgtctttgcttcaaagccaat
XCP1 pro (-148 bp to + 9 bp)-GUS-four-core mutant_for	caccagtttttaaattaatcattgtctgtgctgcagagccgat
Reverse primer sequences (5′-3′)	
XCP1 pro_rev	aaaagccatagccaaatttgttcactgagagaagagg

Table 4.

Primer list in this study

5. Acknowledgements

I am deeply grateful to Prof. Taku Demura for the continuous support, guidance and critical discussion on my study. I deeply appreciate Associate Prof. Masatoshi Yamaguchi in Saitama University for guidance and continuous cooperation helped me a lot to accomplish research. I would like to express special thanks to Prof. Lacey Samuels, Assistant Prof. Misato Ohtani and Dr. Hitoshi Endo for fruitful discussions and manuscript writing. I would like to thanks Prof. Masataka Kinjo and Assistant Prof. Akira Kitamura in Hokkaido University for advice on the usage of FCS, and Assistant Prof. Yutaka Sato in Nagoya university for technical support with SELEX, and Associate Prof. Ko Kato, Assistant Prof. Arata Yoneda, Associate Prof. Minoru Kubo, Dr. Ryosuke Sano and Dr. Yoshimi Nakano in NAIST for fruitful discussions, and Mr. Atsunobu Suzuki for technical supports.

I also want to thank Prof. Toshiro Ito and Associate Prof. Mitsuhiro Aida for critical discussion on my research.

Lastly, I am grateful to all members in Demura Laboratory.

6. References

Anderson,B.J., Larkin,C., Guja,K. and Schildbach,J.F. (2008) Using fluorophore-labeled oligonucleotides to measure affinities of protein-DNA interactions. *Methods Enzymol.*, **450**, 253–272.

Avci,U., Petzold,H.E., Ismail,I.O., Beers,E.P. and Haigler,C.H. (2008) Cysteine proteases XCP1 and XCP2 aid micro-autolysis within the intact central vacuole during xylogenesis in Arabidopsis roots. *Plant J*, **56**, 303–315.

Axelos,M., Curie,C., Mazzolini,L., Bardet,C. and Lescure,B. (1992) A protocol for transient gene expression in Arabidopsis thaliana protoplasts isolated from cell suspension cultures. *Plant Physiol. Biochem.*, **30**, 123–128.

Boer,D.R., Freire-Rios,A., van den Berg,W.A., Saaki,T., Manfield,I.W., Kepinski,S., Lopez-Vidrieo,I., Franco-Zorrilla,J.M., de Vries,S.C., Solano,R. *et al.* (2014) Structural basis for DNA binding specificity by the auxin-dependent ARF transcription factors. *Cell*, **156**, 577–589.

Cheng,Y.C. and Prusoff,W.H. (1973) Relationship between the inhibition constant (Ki) and the concentration of inhibitor which causes 50 per cent inhibition (I50) of an enzymatic reaction. *Biochem. Pharmacol.*, **22**, 3099–3108.

Demura,T., Tashiro,G., Horiguchi,G., Kishimoto,N., Kubo,M., Matsuoka,N., Minami,A., Nagata-Hiwatashi,M., Nakamura,K., Okamura,Y., *et al.* (2002) Visualization by comprehensive microarray analysis of gene expression programs during transdifferentiation of mesophyll cells into xylem cells. *Proc. Natl. Acad. Sci. U.S.A.*, **99**, 15794–15799.

Dey,B., Thukral,S., Krishnan,S., Chakrobarty,M., Gupta,S., Manghani,C. and Rani,V. (2012) DNA–protein interactions: methods for detection and analysis. *Mol. Cell Biochem.*, **365**, 279–299.

Endo,H., Yamaguchi,M., Tamura,T., Nakano,Y., Nishikubo,N., Yoneda,A., Kato,K., Kubo,M., Kajita,S., Katayama,Y., *et al*. (2015) Multiple classes of transcription factors regulate the expression of VASCULAR-RELATED NAC-DOMAIN7, a master switch of xylem vessel differentiation. *Plant Cell Physiol*., **56**, 242–254.

Ernst,H.A., Olsen,A.N., Larsen,S. and Lo Leggio,L. (2004) Structure of the conserved domain of ANAC, a member of the NAC family of transcription factors. *EMBO Rep*., **5**, 297–303.

Fukuda,H. (2004) Signals that control plant vascular cell differentiation. *Nat. Rev. Mol. Cell Biol*., **5**, 379–391.

Funk,V., Kositsup,B., Zhao,C. and Beers,E.P. (2002) The Arabidopsis xylem peptidase XCP1 is a tracheary element vacuolar protein that may be a papain ortholog. *Plant Physiol*., **128**, 84–94.

Furey,W.S., Joyce,C.M., Osborne,M.A., Klenerman,D., Peliska,J.A. and Balasubramanian,S. (1998) Use of Fluorescence Resonance Energy Transfer To Investigate the Conformation of DNA Substrates Bound to the Klenow Fragment. *Biochemistry*, **37**, 2979–2990.

Gonzalez-Barrios,M., Fierro-Gonzalez,J.C., Krpelanova,E., Mora-Lorca,J.A., Pedrajas,J.R., Penate,X., Chavez,S., Swoboda,P., Jansen,G. and Miranda-Vizuete,A. (2015) Cis- and trans-regulatory mechanisms of gene expression in the ASJ sensory neuron of *Caenorhabditis elegans*. *Genetics*, **200**, 123–134.

Harada,K., Mikuni,S., Beppu,H., Niimi,H., Abe,S., Hano,N., Yamagata,K., Kinjo,M. and Kitajima,I. (2013) A rapid and high-throughput quantitation assay of the nuclear factor κB activity using fluorescence correlation spectroscopy in the setting of clinical laboratories. *PLoS One*, **8**, e75579.

Helwa,R. and Hoheisel,J. (2010) Analysis of DNA–protein interactions: from nitrocellulose filter binding assays to microarray studies. *Anal. Bioanal. Chem*., **398**, 2551–2561.

Hill,A.V. (1910) The possible effects of the aggregation of the molecules of haemonglobin on its dissociation curves. *J. Physiol. (Lond)*, **40**, iv–vii.

Hill,A.V. (1913) The combinations of hemoglobin with oxygen and with carbon monoxide. *Biochem. J.*, **7**, 471–480.

Horvath,C.M. (2000) STAT proteins and transcriptional responses to extracellular signals. *Trends Biochem. Sci*, **25**, 496–502.

Hussey,S.G., Mizrachi,E., Creux,N.M. and Myburg,A.A. (2013) Navigatingthe transcriptional roadmap regulating plant secondary cell wall deposition. *Front. Plant Sci.*, **4**, 325.

Jensen,M.K., Kjaersgaard,T., Nielsen,M.M., Galberg,P., Petersen,K., O'Shea,C. and Skriver,K. (2010) The Arabidopsis thaliana NAC transcription factor family: structure-function relationships and determinants of ANAC019 stress signalling. *Biochem. J.*, **2**, 183–196.

Kim,W.C., Ko,J.H. and Han,K.H. (2012) Identification of a cis-acting regulatory motif recognized by MYB46, a master transcriptional regulator of secondary wall biosynthesis. *Plant Mol. Biol.*, **78**, 489–501.

Kim,W.C., Kim,J.Y., Ko,J.H., Kim,J. and Han,K.H. (2013) Transcription factor MYB46 is an obligate component of the transcriptional regulatory complex for functional expression of secondary wall-associated cellulose synthases in Arabidopsis thaliana. *Plant Physiol.*, **170**, 1374–1378.

Kinjo,M. and Rigler,R. (1995) Ultrasensitivehybridizationanalysisusing fluorescence correlation spectroscopy. *Nucleic Acids Res.*, **23**, 1795–1799.

Ko,J.H., Kim,W.C. and Han,K.H. (2009) Ectopic expression of MYB46 identifies transcriptional regulatory genes involved in secondary wall biosynthesis in Arabidopsis. *Plant J.*, **60**, 649–665.

Kobayashi,T., Okamoto,N., Sawasaki,T. and Endo,Y. (2004) Detection of protein-DNA interactions in crude cellular extracts by fluorescence correlation spectroscopy. *Anal. Biochem.*, **332**, 58–66.

Kovtun,Y., Chiu,W.L., Tena,G. and Sheen,J. (2000) Functional analysis of oxidative stress-activated mitogen-activated protein kinase cascade in plants. *Proc. Natl. Acad. Sci. U.S.A.*, **97**, 2940–2945.

Kubo,M., Udagawa,M., Nishikubo,N., Horiguchi,G., Yamaguchi,M., Ito,J., Mimura,T., Fukuda,H. and Demura,T. (2005) Transcription switches for protoxylem and metaxylem vessel formation. *Genes Dev.*, **19**, 1855–1860.

Lindemose,S., Jensen,M.K., Velde,J.V., O'Shea,C., Heyndrickx,K.S., Workman,C.T., Vandepoele,K., Skriver,K. and De Masi,F.D. (2014) A DNA-binding-site landscape and regulatory network analysis for NAC transcription factors in Arabidopsis thaliana. *Nucleic Acids Res.*, **42**, 7681–7693.

McCarthy,R.L., Zhong,R. and Ye,Z.H. (2011) Secondary wall NAC binding element (SNBE), a key cis-acting element required for target gene activation by secondary wall NAC master switches. *Plant Signal. Behav.*, **6**, 1282–1285.

Mitsuda,N., Hisabori,T., Takeyasu,K. and Sato,M.H. (2004) VOZ; isolation and characterization of novel vascular plant transcription factors with a one-zinc finger from Arabidopsis thaliana. *Plant Cell Physiol.*, **7**, 845–854.

Mitsuda,N., Seki,M., Shinozaki,K. and Ohme-Takagi,M. (2005) The NAC transcriptional factors NST1 and NST2 of Arabidopsis regulate secondary wall thickenings and required for anther dehiscence. *Plant Cell*, **17**, 2993–3006.

Mitsuda,N., Iwase,A., Yamamoto,H., Yoshida,M., Seki,M., Shinozaki,K. and Ohme-Takagi, M. (2007) NAC Transcription Factors, NST1 and NST3, Are Key Regulators of the Formation of Secondary Walls in Woody Tissues of *Arabidopsis*. *Plant Cell*, **19**, 270–280.

Nakano,Y., Yamaguchi,M., Endo,H., Rejab,N.A. and Ohtani,M. (2015)

NAC-MYB-based transcriptional regulation of secondary cell wall biosynthesis in land plants. *Front. Plant Sci.*, **6**, 288.

Octobre,G., Lemercier,C., Khochbin,S., Robert-Nicoud,M. and Souchier,C. (2005) Monitoring the interaction between DNA and a transcription factor (MEF2A) using fluorescence correlation spectroscopy. *C. R. Biol.*, **328**, 1033–1040.

Oh,S., Park,S. and Han,K.H. (2003) Transcriptional regulation of secondary growth in Arabidopsis thaliana. *J. Exp. Bot.*, **54**, 2709–2722.

Ohashi-Ito,K., Oda,Y. and Fukuda,H. (2010) Arabidopsis VASCULAR- RELATED NAC-DOMAIN6 directly regulates the genes that govern programmed cell death and secondary wall formation during xylem differentiation. *Plant Cell*, **22**, 3461–3473.

Ohta,M., Ohme-Takagi,M. and Shinshi,H. (2000) Three ethylene-responsive transcription factors in tobacco with distinct transactivation functions. *Plant J.*, **22**, 29–38.

Olsen,A.N., Ernst,H.A., Leggio,L.L. and Skriver,K. (2005) DNA-binding specificity and molecular functions of NAC transcription factors. *Plant Sci.*, **169**, 785–797.

O'Malley,R.C., Huang,S.S., Song,L., Lewsey,M.G., Bartlett,A., Nery,J.R., Galli,M., Gallavotti,A. and Ecker,J.R. (2016) Cistrome and Epicistrome Features Shape the Regulatory DNA Landscape. *Cell*, **165**, 1280–1292.

Pyo,H., Demura,T. and Fukuda,H. (2004) Spatial and temporal tracing of vessel differentiation in young Arabidopsis seedlings by the expression of an immature tracheary element-specific promoter. *Plant Cell Physiol.*, **45**, 1529–1536.

Pyo,H., Demura,T. and Fukuda,H. (2007) TERE; a novel cis-element responsible for a coordinated expression of genes related to programmed cell death and secondary wall formation during differentiation of tracheary elements. *Plant J.*, **51**, 955–965.

Rohs,R., West,SM., Sosinsky,A., Liu,P., Mann,RS. and Honig,B. (2009a) The role of DNA shape in protein–DNA recognition. *Nature*, **461**, 1248–1253.

Rohs,R., West,SM., Liu,P. and Honig,B. (2009b) Nuance in the double-helix and its role in protein-DNA recognition. *Curr. Opin. Struct. Biol.*, **19**, 171–177.

Rohs,R., Jin,X., West,S.M., Joshi,R., Honig,B. and Mann,R.S. (2010) Origins of specificity in protein-DNA recognition. *Annu. Rev. Biochem.*, **79**, 233–269.

Sato,Y., Demura,T., Yamawaki,K., Inoue,Y., Sato,S., Sugiyama,M. and Fukuda,H. (2006) Isolation and characterization of a novel peroxidase gene ZPO-C whose expression and function are closely associated with lignification during tracheary element differentiation. *Plant Cell Physiol.*, **47**, 493–503.

Sawa,S., Demura,T., Horiguchi,G., Kubo,M. and Fukuda,H. (2005) The ATE genes are responsible for the repression of the transdifferentiation into xylem cells in Arabidopsis. *Plant Physiol.*, **137**, 141–148.

Schuetz,M., Smith,R. and Ellis,B. (2013) Xylem tissue specification, patterning, and differentiation mechanisms. *J. Exp. Bot.*, **64**, 11–31.

Shimada,T., Fujita,N., Maeda,M. and Ishihama,A. (2005) Systematic search for the Cra-binding promoters using genomic SELEX system. *Genes Cells*, **10**, 907–918.

Slattery,M., Riley,T., Liu,P., Abe,N., Gomez-Alcala,P., Dror,I., Zhou,T., Rohs,R., Honig,B., Bussemaker,H.J. *et al.* (2011) Cofactor binding evokes latent differences in DNA binding specificity between hox proteins. *Cell*, **147**, 1270–1282.

Tran,L.S.P., Nakashima,K., Sakuma,Y., Simpson,S.D., Fujita,Y., Maruyama,K., Fujita,M., Seki,M., Shinozaki,K. and Yamaguchi-Shinozaki,K. (2004) Functional analysis of Arabidopsis NAC transcription factors controlling expression of erd1 gene under drought stress. *Plant Cell*, **16**, 2482–2498.

Tsutsumi,M., Muto,H., Myoba,S., Kimoto,M., Kitamura,A., Kamiya,M., Kikukawa,T., Takiya,S., Demura,M., Kawano,K. *et al.* (2016) In vivo fluorescence correlation spectroscopy analyses of FMBP-1, a silkworm transcription factor. *FEBS Open Bio.*, **6**, 106–125.

Tuerk,C. and Gold,L. (1990) Systematic evolution of ligands by exponential enrichment: RNA ligands to bacteriophage T4 DNA polymerase. *Science*, **249**, 505–510.

Turner,S., Gallois,P. and Brown,D. (2007) Tracheary element differentiation. *Annu. Rev. Plant Biol.*, **58**, 407–433.

Vinkemeier,U., Cohen,S.L., Moarefi,I., Chait,B.T., Kuriyan,J. and Darnell,J.E.Jr. (1996) DNA binding of in vitro activated Stat1a, Stat1b, and truncated Stat1: interaction between NH2 terminal domains stabilizes binding of two dimers to tandem DNA sites. *EMBO J.*, **15**, 5616–5626.

Weirauch,M.T., Yang,A., Albu,M., Cote,A., Montenegro-Montero,A., Drewe,P., Najafabadi,H., Lambert,S., Mann,I., Cook,K. *et al.* (2014) Determination and inference of eukaryotic transcription factor sequence specificity. *Cell*, **158**, 1431–1443.

Welner,D.H., Lindemose,S., Grossmann,J.G., Møllegaard,N.E., Olsen,A.N., Helgstrand,C., Skriver,K. and Lo Leggio,L. (2012) DNA binding by the plant-specific NAC transcription factors in crystal and solution: A firm link to WRKY and GCM transcription factors. *Biochem. J.*, **444**, 395–404.

White,M.D., Angiolini,J.F., Alvarez,Y.D., Kaur,G., Zhao,Z.W., Mocskos,E., Bruno,L., Bissiere,S., Levi,V. and Plachta,N. (2016) Long-Lived Binding of Sox2 to DNA Predicts Cell Fate in the Four-Cell Mouse Embryo. *Cell*, **165**, 75-87.

Wohland,T., Friedrich,K., Hovius,R. and Vogel,H. (1999) Study of ligand- receptor interactions by fluorescence correlation spectroscopy with different fluorophores: evidence that the homopentameric 5-hydroxytryptamine type 3As receptor binds only one ligand. *Biochemistry*, **38**, 8671 – 8681.

Wölcke,J., Reimann,M., Klumpp,M., Göhler,T., Kim,E. and Deppert,W. (2003) Analysis of p53 "latency" and "activation" by fluorescence correlation spectroscopy. Evidence for different modes of high affinity DNA binding. *J. Biol. Chem.*, **35**,

32587–32595.

Xu,B., Ohtani,M., Yamaguchi,M., Toyooka,K., Wakazaki,M., Sato,M., Kubo,M., Nakano,Y., Sano,R., Hiwatashi,Y. *et al*. (2014) Contribution of NAC transcription factors to plant adaptation to land. *Science*, **343**, 1505–1508.

Xue,G.P. (2005) A CELD-fusion method for rapid determination of the DNA-binding sequence specificity of novel plant DNA-binding proteins. *Plant J*., **41**, 638–649.

Yamamoto,R., Demura,T. and Fukuda,H. (1997) Brassinosteroids induce entry into the final stage of tracheary element differentiation in cultured *Zinnia* cells. *Plant Cell Physiol*., **38**, 980–983.

Yamaguchi,M., Kubo,M., Fukuda,H. and Demura,T. (2008) VASCULAR-RELATED NAC-DOMAIN7 is involved in the differentiation of all types of xylem vessels in Arabidopsis roots and shoots. *Plant J*., **55**, 652–664.

Yamaguchi,M. and Demura,T. (2010) Transcriptional regulation of secondary wall formation controlled by NAC domain proteins. *Plant Biotechnol*., **27**, 237–242.

Yamaguchi,M., Goué,N., Igarashi,H., Ohtani,M., Nakano,Y., Mortimer,J.C., Nishikubo,N., Kubo,M., Katayama,Y., Kakegawa,K. *et al*. (2010) VASCULAR-RELATED NAC-DOMAIN6 and VASCULAR-RELATED NAC-DOMAIN7 effectively induce transdifferentiation into xylem vessel elements under control of an induction system. *Plant Physiol*., **153**, 906–914.

Yamaguchi,M., Mitsuda,N., Ohtani,M., Ohme-Takagi,M., Kato,K. and Demura,T. (2011) VASCULAR-RELATED NAC-DOMAIN7 directly regulates the expression of a broad range of genes for xylem vessel formation. *Plant J*., **66**, 579–590.

Zhao,C., Johnson,B.J., Kositsup,B. and Beers,E.P. (2000) Exploiting secondary growth in Arabidopsis: construction of xylem and bark cDNA libraries and cloning of three xylem endopeptidases. *Plant Physiol*., **123**, 1185–1196.

Zhong,R., Demura,T. and Ye,Z.H. (2006) SND1, a NAC domain transcription factor, is a key regulator of secondary wall synthesis in fibers of Arabidopsis. *Plant Cell*, **18**, 3158–3170.

Zhong,R., Richardson,E.A. and Ye,Z.H. (2007) Two NAC domain transcription factors, SND1 and NST1, function redundantly in regulation of secondary wall synthesis in fibers of Arabidopsis. *Planta*, **225**, 1603–1611.

Zhong,R., Lee,C. and Ye,Z.H. (2010) Global analysis of direct targets of secondary wall NAC master switches in Arabidopsis. *Mol. Plant*, **3**, 1087–1103.

Zhou,J., Zhong,R. and Ye,Z.H. (2014) Arabidopsis NAC Domain Proteins, VND1 to VND5, Are Transcriptional Regulators of Secondary Wall Biosynthesis in Vessels. *PLoS One*, **9**, e105726.